UNIVERSITÀ DEGLI STUDI DI TRIESTE
UNIVERSITÀ DEGLI STUDI DI UDINE

XXXIII CICLO DEL DOTTORATO DI RICERCA IN AMBIENTE E VITA

SEISMOTECTONIC CHARACTERIZATION OF THE SOUTHERN ALPS – DINARIDES JUNCTION AREA (NE ITALY)

Settore scientifico-disciplinare: **GEO/03 GEOLOGIA STRUTTURALE**

Dottoranda/Ph.D. Student

Dott.ssa Giulia Patricelli

Coordinatore/Ph.D. Program Coordinator

Prof. Giorgio Alberti

Supervisore di Tesi/Thesis Supervisor

Prof.ssa Maria Eliana Poli

ANNO ACCADEMICO 2019/2020

Contents

ABSTRACT

The recent tectonic activity of eastern Friuli was investigated through a multidisciplinary approach. The study area, which comprises eastern Friuli Plain and the Julian prealpine border, represents the junction zone between the SSE verging front of the Southalpine Chain and the NW-SE trending strike slip structures of the eastern Friuli-western Slovenia domain. At present, both seismological and GPS data show that the 2-3 mm/yr accumulating deformation is released through the interaction among reverse, transpressive and strike-slip faults. Regarding seismicity, the distribution of earthquakes shows that most of the events are mostly located along the prealpine and alpine arcuate belt and at least two Mw > 6.0 events are documented: the 1511 Mw 6.3 earthquake and the 1976-77 sequence (Mw ≤ 6.4). In more recent times, the activation of the Raune strike-slip fault in western Slovenia caused the occurrence of two seismic sequences, in 1998 (Mw 5.6) and 2004 (Mw 5.2). With the aim to further explore the involvement of the active faults of eastern Friuli during the strongest seismic events occurred in the area, this work is focused on the recent activity of the tectonic structures. Following a multidisciplinary approach, the deep 3D-geometry of 4 main fault-systems were reconstructed by combining ENI seismic lines interpretation and hypocentral distribution analysis. Successively, a morphotectonic survey was conducted along the Julian prealpine border with the aim to detect the surficial anomalies related to tectonic activity. The collected morphotectonic hints allowed to define a NW-SE elongated zone of surficial deformation, highlighting the recent activity of the Colle Villano-N Thrust (CV-N) and the Colle Villano-Borgo Faris-Cividale trasnpressive Fault-System (CV-BFC). Based on the morphostructural results, two palaeoseismological trenches were dug: the Fraelacco trench across the CV-N Thrust and the Campeglio trench across the CV Thrust. At Campeglio site, the excavated trench revealed the presence of palaeoliquefaction features, thus suggesting that the area experienced seismic shaking. Differently, at Fraelacco site, the displacement of the Canodusso Subsynthem (21- 23 kyr cal BP)

allowed to identify two deformative episodes in the last 21 kyr, with the latest likely occurred in historical times.

INTRODUCTION

The seismotectonic characterization of an area represents a key aspect within seismic hazard studies. Particularly, the detailed analysis of active faults and their association to seismic events play a fundamental role in the identification of the seismogenic structures and the definition of their seismicity rates (slip per event and recurrence time interval) and seismic potential (maximum expected magnitude).

Referring to the national territory, the Eastern Southalpine area is characterized by seismic hazard values among the highest of Italy. Located at the northeasternmost tip of the Adria microplate, Friuli region represents the interaction area between the inherited NW-SE oriented fronts of the External Dinarides and the SSE-verging Southalpine fronts. Moreover, starting from the transition Miocene-Pliocene, the indentation and counterclockwise rotation caused the development of NW-SE strike-slip fault systems in western Slovenia. They propagate NW-ward up to eastern Friuli region, affecting the elder structures. At present, the deformation is released through the interplay between reverse and strike-slip fault systems, but the way in which this interaction occurs is still not completely understood. As a matter of fact, eastern Friuli region represents the transition zone between the western-central Friuli dominant compressional deformational area and the dominant strike-slip strain domain of western Slovenia. Despite the low-to-medium strain rates (2 -3 mm7yr, Serpelloni et al., 2016), many strongest earthquakes (M > 6) affected this area since historical times. Therefore, a detailed seismotectonic study could help to better define the active faults which drive deformation and consequently, to characterize the seismogenic structures of the area able to release strong earthquakes.

In this regard, many distinct disciplines can provide useful information for a detailed characterization of the active tectonic structures, independently from one another. Each discipline,

(from neotectonics, to palaeoseismicity, to historical and instrumental seismicity) covers a different time interval and contributes to investigate the tectonic structure from a certain point of view (top view, section view, 3D view) (Caputo and Hally, 2008). All the results obtained are to be considered complementary and their integration certainly leads to a more comprehensive characterization. Therefore, the use of the multidisciplinary methodology certainly represents the added value in seismotectonic studies.

In this work, following a multilayer approach, the recent activity of the Quaternary fault systems of the area and their possible involvement during strong earthquakes was investigated. Particularly, the study is articulated in six parts.

The first part illustrates the regional geological and seismotectonic setting. Based on bibliographic data, the stratigraphic and structural evolution of eastern Friuli is described. Historical and instrumental seismic catalogues were useful to depict the seismicity of the study area, while the knowledge regarding the strain pattern of eastern Friuli derives from the integration of seismological and satellite data analysis available from the literature.

The second part deals with the reconstruction of the 3D structural model through the interpretation of ENI seismic lines. Particularly, the interpolation of eight elaborated geological cross sections via 3D Move software allowed the reconstruction of the 3D-geometry of the active fault systems of eastern Friuli, up to a depth of 5 km.

In the third part, the seismogenic volume thickness was investigated through the hypocentral distribution analysis of the seismic events registered between 1978 and 2019. The projection of the earthquakes on the structural model reconstructed in this study allowed to investigate the deep geometry of the tectonic structures, while the seismically released strain pattern was outlined

through the analysis of the available focal mechanisms. Subsequently, the distribution of 1976-1977 Friuli sequence was also analysed and compared to the post 1977 seismicity.

The fourth part illustrates the results of the morphotectonic survey carried out along the Julian prealpine area. Particularly, the analysis of remote sensing data covering the eastern Friuli region allowed to detect the surficial anomalies of the study area. The collected morphotectonic hints, validated through field survey, highlighted the recent tectonic activity of the investigated tectonic structures (Colle Villano-N Thrust and Colle Villano-Borgo Faris – Cividale transpressive Fault System), and revealed useful to outline the deformation zone of the active fault systems.

The fifth part deals with the palaeoseismology study. Following preliminary geophysical survey, the recent activity of the active fault systems marked by the most pronounced surficial evidence was investigated through the realization of two palaeoseismological trenches. Particularly, the interpretation of the excavated wall allowed the identification of the deformative episodes associated to the investigated tectonic structure.

Finally, the interpretations of the previous sections results are integrated and further analysed in a comprehensive and conclusive discussion.

CHAPTER 1: REGIONAL GEOLOGICAL AND SEISMOTECTONIC SETTING

The study area belongs to the eastern Southalpine domain, in NE Italy. The Eastern Southalpine Chain (ESA) is a S-vergent fold-and-thrust belt and represents a back-verging chain compared to the Alps (Figs. 1.1 and 1.2). ESA is separated to the North from the N-verging Austroalpine domain by the Periadriatic Lineament (PL) and is bordered to the West by the sinistral Trento-Cles, Calisio e Schio-Vicenza Fault-System (Giudicarie System). Towards the East, the ESA extends up to the Italian-Slovenian border area, where it interacts with the dextral Fella Sava (FS) and Idrija-Ampezzo (IA) Fault-Systems (Fig. 1.3). To the South, the external front involves the Upper Pleistocene-Holocene Veneto-Friuli piedmont plain.
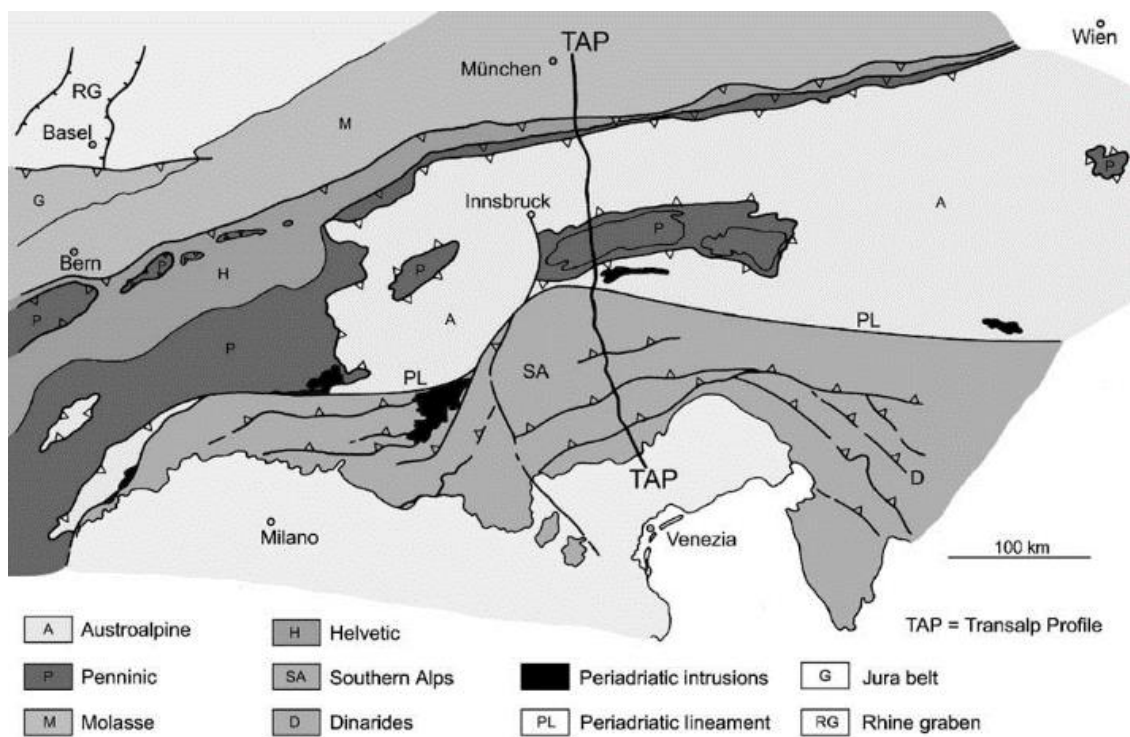

Fig. 1.1 – Structural sketch of the Alps and location of the TRANSALP profile (TAP) (from Castellarin et al., 2006).
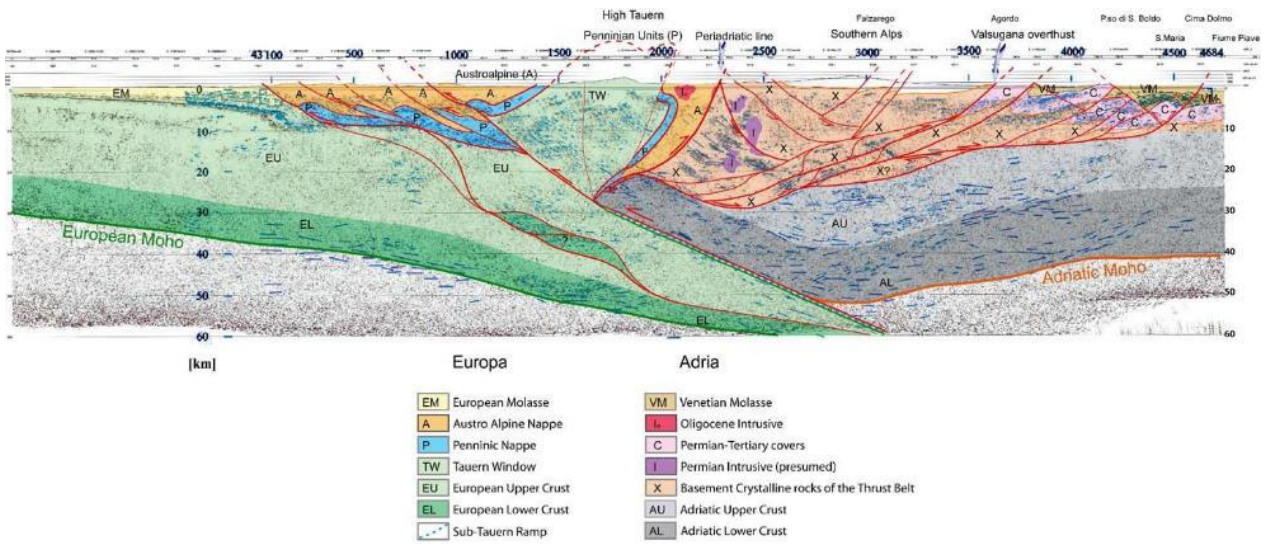
Fig. 1.2 – Interpretation of TRANSALP profile (from Castellarin et al., 2006), showing the subduction of European plate and the indentation of Adria microplate which caused the development of the S-vergent Southalpine Chain.

Fig. 1.3 – Structural sketch of the northeastern Adria-Europe collision zone (Vrabec and Fodor, 2006).

Both Austroalpine and Southalpine domains derive from the continental passive margin of Adria microplate, which represents the northernmost portion of the African plate (D'Argenio et al., 1980).

Starting from Early Permian – Middle Triassic, the break-up of the Pangea led to the development of the Tethys Ocean separating the African and European plates. The extensional tectonic phase guiding the spreading of the Tethyan realm continued up to the late Early Creta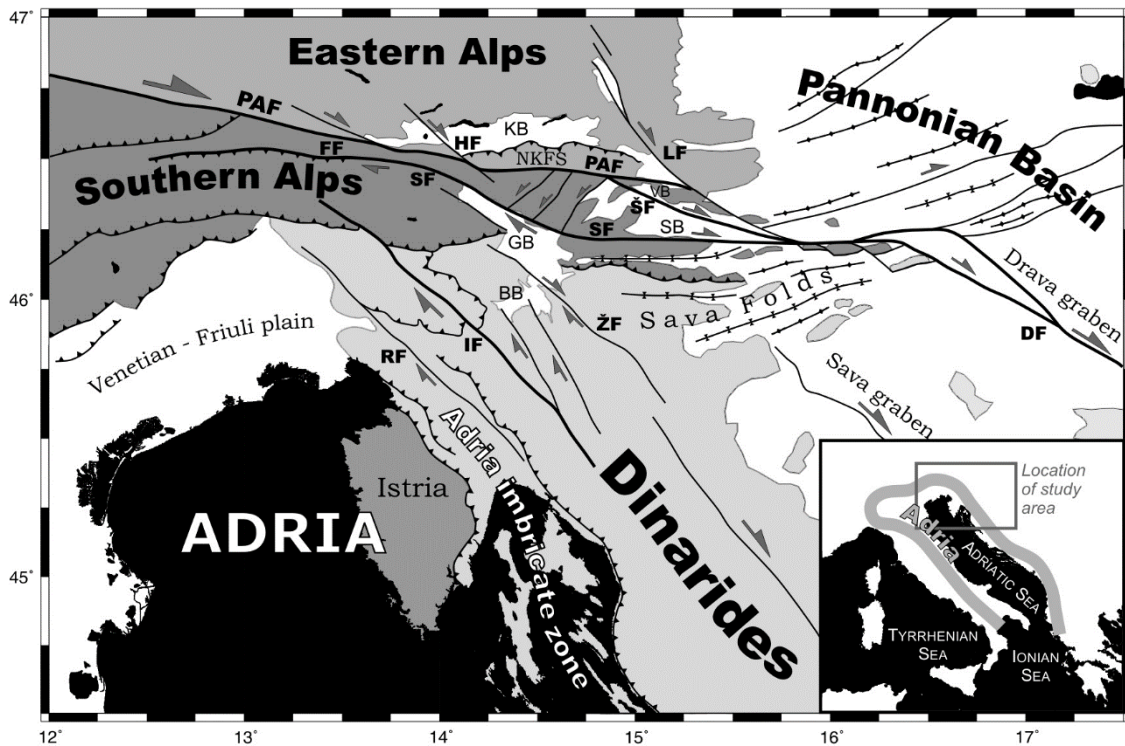ceous, when a basic change in the plate kinematics produced the Africa-Europe continental margin convergence (Castellarin et al., 2006). The tectonic inversion caused the onset of the S-verging subduction of the European plate and the development of the Austroalpine and the Southalpine domains. Particularly, the evolution of the Southern Alps is the results of a polyphasic compressional tectonics (Doglioni and Bosellini, 1987; Castellarin et al., 1992; Caputo, 1996; Castellarin and Cantelli, 2000; Caputo et al., 2010). From the late Upper Cretaceous to the Eocene, the Eoalpine deformation affected only the central and western parts of the Southern Alps (Doglioni and Bosellini, 1987). At the same time, the development of the External Dinaric Chain in the eastern domain affected the study area. Because of the intense tectonic deformation related to the ongoing collision, the SW-ward propagation of the External Dinaric Chain persisted until Oligocene (Doglioni and Bosellini, 1987). Starting from Chattian, the indentation of Adria microplate below the Austroalpine domain caused remarkable uplift of the Alpine Chain s.s. (Castellarin et al., 2006) and was responsible of the development of the S-SSE verging Eastern Southalpine Chain since middle Miocene (Neoalpine phase) (Doglioni and Bosellini, 1987; Castellarin and Cantelli, 2000). As a consequence of the ongoing compression, combined to the anticlockwise rotation of Adria microplate (Márton et al., 2003), the activation of dextral strike-slip fault systems affected the eastern Southalpine domain since Miocene – Pliocene transition (Fella-Sava and Idrija-Ampezzo Fault-Systems) (Vrabec and Fodor, 2006).

1.1 STRUCTURAL SETTING AND EVOLUTION OF FRIULI AREA

Focusing on the study area, the present structural framework of eastern Friuli reflects its articulated tectonic evolution.

1.1.1 MESOZOIC EVOLUTION

Since late Triassic the eastern Friuli region was part of the African passive margin of the Tethyan extensional domain. During the rifting phase, deformation was accommodated by NW-SE oriented normal faults and NE-SW striking transcurrent/transtensive faults. Following the collapse of the carbonate platform, the middle Jurassic palaeogeography dealt with a structural high on which the middle-late Mesozoic Friuli Carbonate Platform developed and three distinct basinal domains all around (Fig. 1.4): the Slovenian Basin in the NE (Buser, 1989), the Carnian Basin in the N (Podda and Ponton, 1997) and the Belluno Basin in the W (Bosellini et al., 1981; Masetti et al., 2012).

Fig. 1.4 – Palaeogeographich setting of central-eastern Southern Alps during middle Jurassic (Zanferrari et al., 2013). LP: Periadriatic Lineament, LG: Giudicarie-S and Val Trompia Faults; VS: Valsugana Fault; FS: Fella-Sava Fault.

1.1.2 LATE CRETACEOUS-PALEOGENE EVOLUTION

In response to the instauration of an about N60° compressional regime (Doglioni and Bosellini, 1987; Castellarin et al., 1992; Caputo, 1996), the SW-ward propagation of the External Dinarides affected the Carnian-Slovenian Basin starting from Coniacian – Santonian. The SW-ward migration of the chain-foredeep system continued until Eocene, causing the diachronous E to W drowning of the Friuli Carbonate Platform. The pre-existing NW-SE Mesozoic normal faults were usually inverted to reverse faults and the development of new NW-SE oriented normal faults lead to the dismembering of the NE border of the Friuli platform, which was completely drowned during Lutetian (Sartorio et al., 1997; Venturini, 2002; Placer et al., 2010). The Paleocene – late Eocene palaeogeography dealt with the External Dinaric outer fronts separating the piggy-back basinal domain to the NE from the foreland domain to the SW. In late Eocene the compressional Dinaric forces ceased, and the area remained under subaerial exposure until the end of the Oligocene.

1.1.3 NEOGENE-QUATERNARY EVOLUTION

The new contractional event affected the present Friuli region starting from latest Oligocene. In response to a variable NNE-SSW to NNW-SSE oriented compressional regime the S(SE)-verging Eastern Southalpine Chain developed, superimposing on the pre-existing tectonic lineaments. The older Dinaric structures were folded, displaced, and locally re-activated depending on their orientation with respect to the sigma1 (Zanferrari et al., 2013).

Particularly, during the Neogene – Quaternary, many different tectonic events can be recognized.

- The Chattian – Burdigalian event (also known as "Insubric event") caused the uplifting of the Alpine Chain *s.s.* under a N20°-30° oriented maximum compressional axis (Castellarin and Cantelli, 2000). During this phase, the present Friuli region was only slightly affected by

tectonic activity since it represented the alpine foreland basin. The Aquitanian – Langhian terrigenous – carbonate sequence (Cavanella Group, *sensu* ENI), filling the gently N-dipping foreland basin, is characterized by a SSE-thinning geometry. Moreover, the petrographic composition of the sequence, consistent with the Austroalpine units of Alpine Chain *s.s.* (Stefani, 1987, Fantoni et al., 2002; Monegato et al., 2010), testifies the northern provenance of the sediments.

- The Serravallian – Present event (also known as "Neoalpine event") (Massari et al., 1986, Zanferrari et al., 2008a) led to the main evolution of the Eastern Southalpine fold and thrust belt. During the Serravallian-Messinian time interval, in response to the NNW oriented compressional regime (Castellarin and Cantelli, 2000; Caputo et al., 2010), the exhumation and rapid uplift of the Eastern Southalpine Chain caused the formation of new S- verging, ENE-WSW thrust fronts (Zanferrari et al., 2013) and the development in the present Friuli region of a strongly subsiding slightly N-tilted foredeep basin (Fantoni et al., 2002; Toscani et al., 2016). The NNW-thickening of the clastic wedge testifies that the source area was represented by the Austroalpine domain, located to the North (Fantoni et al., 2002).

Since Mio-Pliocene transition a variation of the regional stress field occurred: the onset of the counterclockwise rotation of Adria microplate (Márton et al., 2003) combined with its northward motion, resulted in an oblique convergence. As a consequence of this new geodynamic arrangement, dextral strike-slip faulting activated in western Slovenia (Vrabec and Fodor, 2006; Kastelic et al., 2008). The newly developing NW-SE trending steep fault system (Ravne, Idrija, Predjama and Raša faults) displaced both the Dinaric and the Southalpine structures (Vrabec and Fodor, 2006; Kastelic et al., 2008; Moulin et al., 2014 and 2016). Meanwhile in central Friuli, the S-(SE)-ward propagation of the Southalpine fold and thrust belt (Castellarin and Cantelli, 2000) occurred through the activation of (W)SW-(E)NE

striking frontal segments and fault splay, together with the segmentation and reactivation of pre-existing favorably oriented tectonic lineaments (Galadini et al., 2005; Zanferrari et al., 2008, 2013).

Since late Miocene, continental conditions established in the Veneto – Friuli Prealpine area (Massari et al., 1986; Zanferrari et al., 2008b) and a deep incision of the fluvial valleys developed as a consequence of the Messinian Salinity Crisis. The following Pliocene marine ingression (Ghielmi et al, 2010) caused the infill of the Messinian palaeovalleys and extended north up to the present pre-alpine border (Monegato and Stefani, 2011; Zanferrari et al, 2013). However, despite the S(SE)-ward propagation of Southalpine fronts, in the Veneto-Friuli plain the accommodation space was inhibited by the NE-propagation of the Northern Apennines (Caputo et al., 2010). As a matter of fact, while the source area for sediments was still the Southalpine Chain (Stefani, 1987; Monegato and Stefani, 2011), the thin continental Plio-Pleistocene sequence is characterized by a prominent thickening towards the Apennine Chain (Fantoni et al., 2002; Caputo et al., 2010; Toscani et al., 2016).

Starting from late Calabrian, the advance and retreat phases of the Tagliamento glacier strongly controlled the sedimentation of the area (Zanferrari et al., 2008a; Fontana et al., 2010). Particularly, during the last glacial maximum (LGM) the evolution of the Tagliamento glacier was articulated in two phases of glacial culminations (Monegato et al., 2007) (Fig. 1.5).

The first and most extensive glacial advance occurred between 26.5 and 23 cal kyr BP and was responsible of the formation of the most continuous external end-moraine belt: the Santa Margherita advance. A fast aggradation in the distal areas of the sandur continued until just before the 23.5 cal kyr BP interphase (Arcano phase) when the glacier withdrew, terraces formed in the amphitheater but in the distal sandur the fluvioglacial aggradation continued.
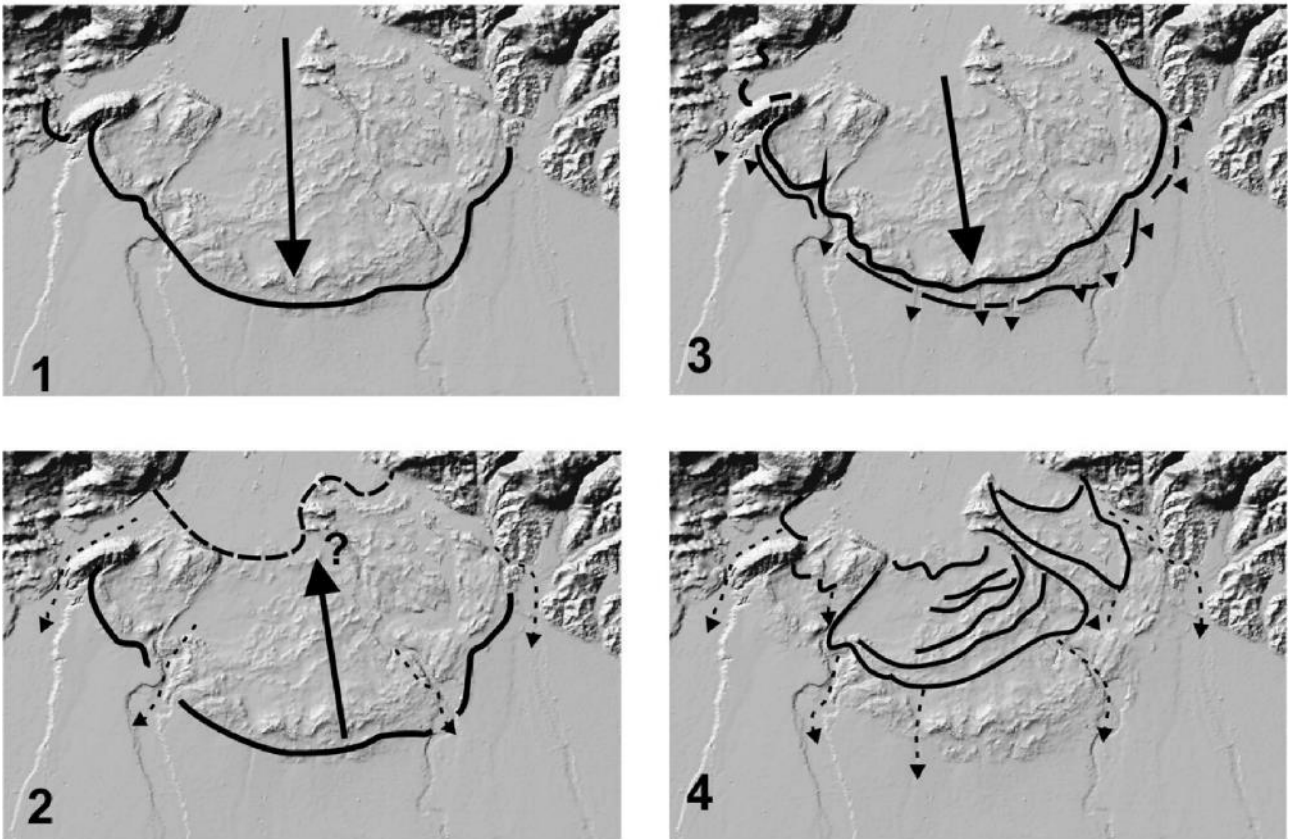
Fig. 1.5 – The evolution of the Tagliamento glacier during the last glacial maximum: 1: Santa Margherita maximum advance; 2: Arcano phase; 3: Canodusso maximum advance; 4: Remanzacco recessional phase (from Monegato, 2007).

The subsequent re-advance, the Canodusso maximum advance, occurred between 23 and 21 cal kyr BP. The glacier almost reached the previous culmination position, but it didn't override the S. Margherita deposits, causing only a reshaping of the elder moraine ridges. Finally, during the youngest advance (Remanzacco phase Fig. 1.5), occurred between the end of the Canodusso maximum advance (21 cal kyr BP) and the deglaciation of Ragogna Lake (20.3-18.8 cal kyr BP) (Monegato, 2007), the glacier underwent several fluctuations, but it remained in the inner part of the amphitheater and was articulated in different sub-lobes. About 19 cal kyr BP the glacier withdrew from the amphitheater and vegetation spread across the basin.

1.2 STRATIGRAPHY

Starting from the upper Carnian Travenanzes Formation, the simplified stratigraphic model of Friuli region, functional to the interpretation of seismic lines, is composed of five units (Mancin et al., 2016; Toscani et al., 2016).

- The Mesozoic platform succession includes the Dolomia Principale and the Friulian-Dinaric Platform (Zanferrari et al., 2013), which developed from late Triassic to late Cretaceous. It deals with an about 3000 m thick sequence of mostly inner platform facies, with locally transgressive and emersion episodes (Cousin, 1981; Sartorio et al., 1987; Cati et al., 1987; Tentor et al., 1994; Venturini S., 2002).

- The Upper Cretaceous-upper Eocene turbiditic sequence: it represents the filling of the foredeep of the SW-verging External Dinaric Chain. The complete westward thinning sequence up to 4000 m (Sartorio et al., 1997; Venturini, 2002; Fantoni et al., 2002) is characterized by siliciclastic turbiditic sequence (Maastrichtian flysch), carbonatic megabeds (*seismoturbidites*, Tunis and Venturini, 1992) (Grivò Flysch, Thanetian *p.p.* – Ypresian *p.p.*) and calciclastic and siliciclastic turbidites in the upper part (Savorgnano Marls and Cormons Flysch, lower-middle Eocene).

- The lower-middle Miocene sequence: it is commonly referred to as "Cavanella Group" and is composed of shallow water marine sediments. In the context of seismic lines interpretation Cavanella Group represents an important regional-scale seismo-stratigraphic group of reflectors, showing an overall tabular geometry and a SW-ward thinning with thicknesses spanning from tens to hundreds of meters (Toscani et al., 2016).

- The middle-upper -Miocene Molasse sequence: it represents the foredeep deposition of the SE-ward verging Southalpine Chain. In the High Friuli Plain, at the outer border of the prealpine relieves, the upper portion of the sequence consists of very thick fan delta and

alluvial deposits dated back to latest Tortonian-early Messinian (Montello Conglomerate, Massari et al., 1986; Zanferrari et al., 2008a), testifying the transition from terrigenous platform to continental facies (Zanferrari et al., 2013).

- The Plio-Quaternary sequence: it develops on top of the Messinian Unconformity, and it is composed of thick conglomeratic channel bodies filling the narrow Messinian canyons since the successive transgression episode (Friuli Superunit, Fontana et al., 2019). The sea ingression extended in the Tagliamento palaeovalley area, north up to Osoppo, where coarse grained Gilbert-type deltaic bodies are preserved: the Osoppo Conglomerate, dated back to Zanclean (Monegato, 2006; Monegato and Vezzoli, 2011). The middle-to-late Pleistocene sequence covering the erosional plain surface deals with alluvial and glacial facies (Fontana et al., 2019) (see the attached Morphostructural Map). The pre-LGM deposition comprises the Tagliamento glacial and fluvioglacial Plaino Unit (PLI) and the Natisone alluvial/fluvioglacial Buttrio (BUT) and Poggiobello (PGB) Units. The LGM succession includes the Tagliamento alluvial and glacial deposits (Spilimbergo Unit - SPB) and the alluvial and fluvioglacial deposits of the Isonzo basin and Isonzo-Natisone-Torre River System (Gorizia Unit - GOR), while the contemporary alluvial fan deposits of the Natisone stream are represented by the Cividale Unit (CIV). The post-LGM alluvial, lagoonal, onshore and offshore coastal deposits covering the Friuli Plain are grouped in the Grado Unit (GRA) (Fontana et al., 2019).

1.3 SEISMOTECTONIC SETTING

Concerning the seismicity of the NE Italy and surroundings, the distribution of earthquakes, registered by the OGS seismometric network (http://rts.crs.inogs.it), depicts an arcuate belt

coinciding with the alpine and pre-alpine border region of Friuli Venezia Giulia and western Slovenia (Fig. 1.6). Particularly, regarding the historical seismicity of the prealpine Julian Prealps, the Parametric Catalogue of Italian Earthquakes (CPTI15 v3.0, Rovida et al., 2021) documents two destructive seismic events (Mw > 6.0) since the year 1000.
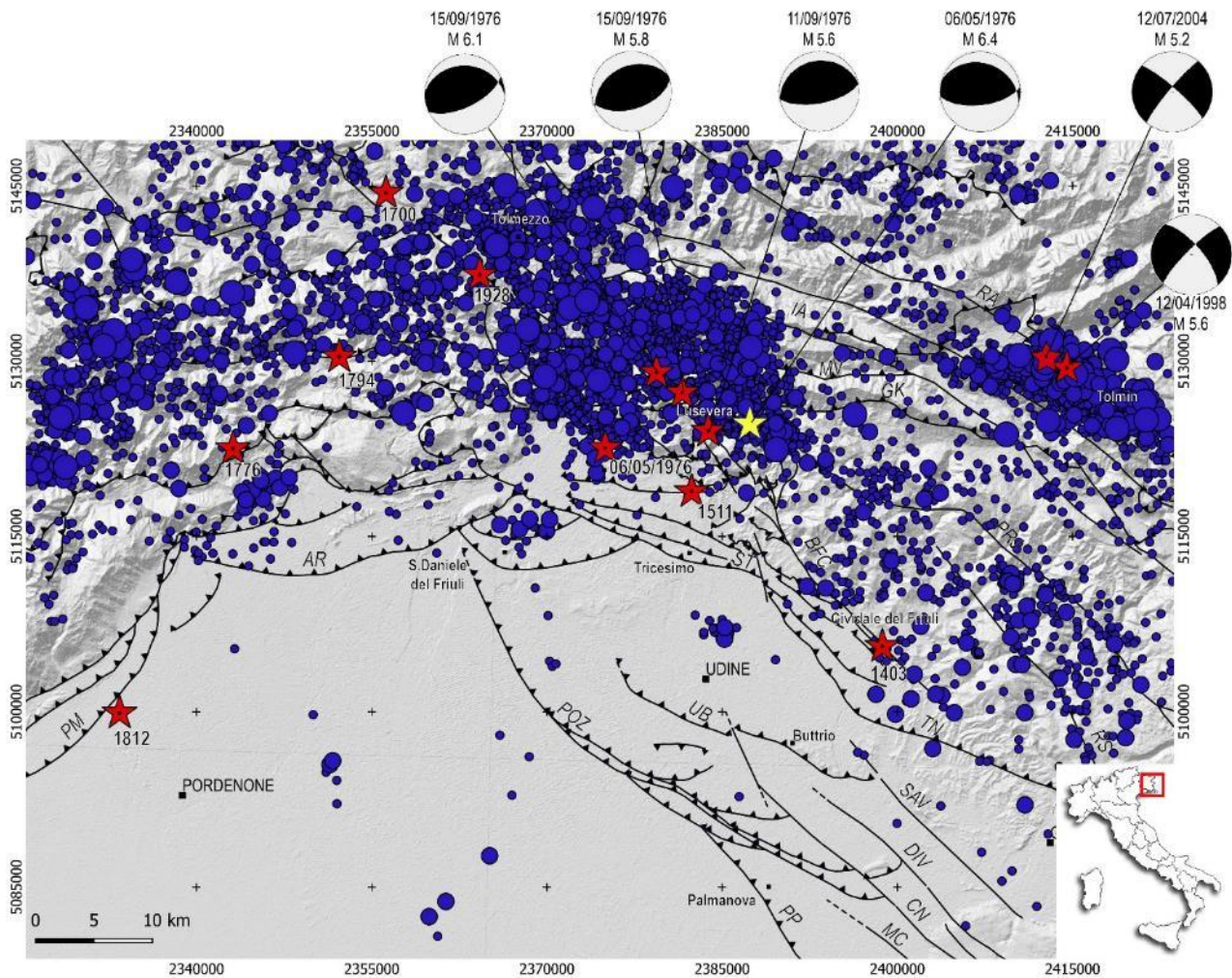

Fig. 1.6 – Seismicity of the eastern Friuli. Red stars: Mw ≥ 5.5 historical events from CPTI15 v3.0 (Rovida et al., 2021); yellow star: instrumental epicenter of the May mainshock from Rebez et al. (2018), blue circles: instrumental earthquakes extracted from Friuli Venezia Giulia Seismometric Network Bulletin (http://www.crs.inogs.it/bollettino/RSFVG/RSFVG.en.html). Focal mechanisms from Saraò et al., (2021). Fault's acronyms: AR: Arba-Ragogna Th.; BFC: Borgo Faris-Cividale Ft; CN: Colle Nero Ft.; DIV: Divača Ft.; GK: Gemona-Kobarid Th.; IA: Idrija-Ampezzo Ft.; MC: Monte Cosici Ft.; MV: Musi-Verzegnis Th.; PM: Polcenigo-Maniago Th.; POZ: Pozzuolo Th.; PP: Palmanova-Panzano Th.; PRJ: Predjama Ft.; RA: Raune Ft.; RS: Raša Ft.; SAV: Savogna Ft.; ST: Susans-Tricesimo Th.; TN: Trnovo Th.; UB: Udine-Buttrio Th.

On March the 26th, 1511 a strong earthquake (Mw 6.3) affected a wide area extending from Friuli to western Slovenia (Fig. 1.7). Based on macroseismic data inversion, Fitzko et al. (2005) proposed an earthquake-model scenario consistent with a Mw 6.9 event which activated the 50 km long SE portion of the Idrija strike-slip fault. An updated macroseismic field was elaborated by Camassi et al. (2011) by considering the political and cultural situation of that time, characterized by popular uprisings and epidemic outbursts. The revised epicenter of 1511 event is located near Tarcento, where intensity value Imax of 9 MSC was estimated. Regarding the possible source responsible of the 1511 event, Camassi et al. (2011) concluded that the earthquake involved both Alpine and Dinaric structures.
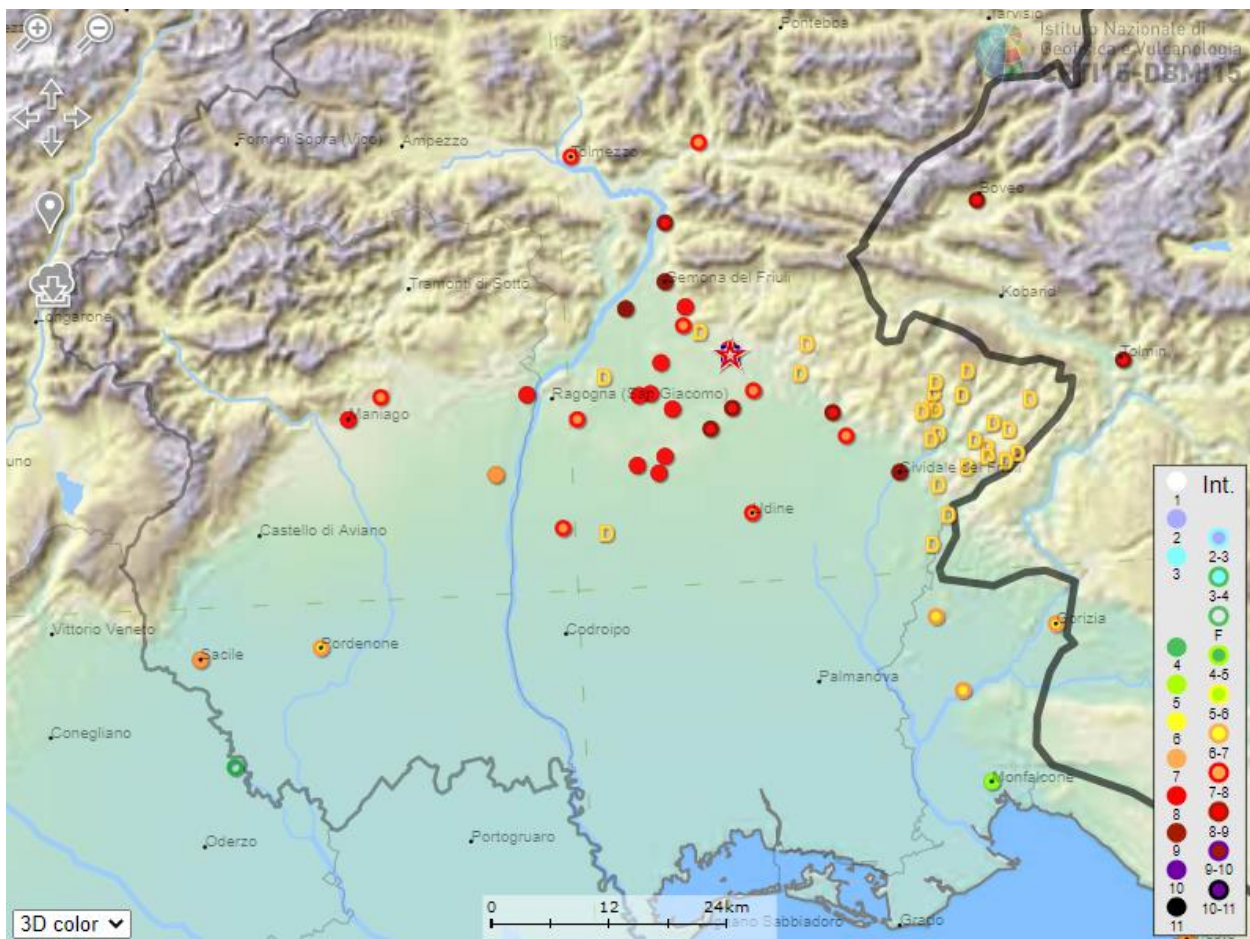

Fig. 1.7 – Damage distribution of 1511 event (https://emidius.mi.ingv.it/CPTI15-DBMI15/event/15110326_1440_000).

Recent palaeoseismological analysis revealed Holocene surface rupturing referable to the 1511 event across the Colle Villano – Borgo Faris-Cividale fault system (Falcucci et al., 2018), across the Idrija (Bavec et al., 2013; Grützner et al., 2021) and Predjama Faults (Grützner et al., 2021).

Concernig the 1976 Friuli earthquakes, Slejko (2018) deeply described and analyzed the sequence on the basis of a large amount of bibliography. Preceded by a Ml 4.5 foreshock, on May the 6th, a destructive earthquake (Ml 6.45) struck central-eastern Friuli, where Imax 9-10 MSC were recorded (Fig. 1.8). After the strong Ml 5.3 aftershock on May the 9th, the seismic activity slowly decreased until September.
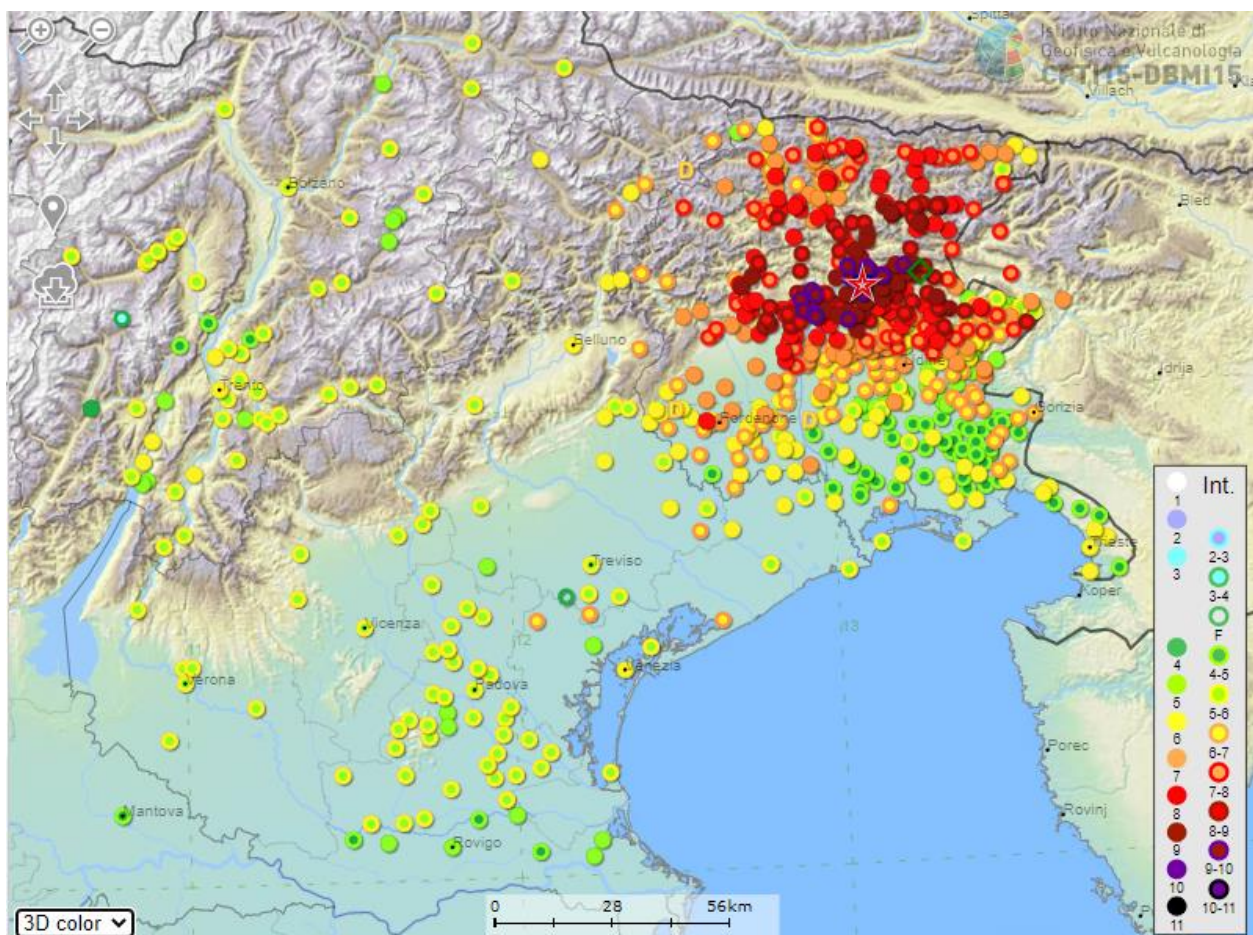

Fig. 1.8 – Damage distribution of the 06/05/1976 event (https://emidius.mi.ingv.it/CPTI15-DBMI15/event/19760506_2000_000). Red star: macroseismic epicenter; green diamond: instrumental epicenter (Slejko et al., 1999).

Two quakes on September the 11th (Ml 5.1 and 5.6, respectively) and two others on September the 15th (Ml 5.8 and 6.1, respectively) caused further damage (Figs. 1.9 and 1.10). One year later, on September the 16th 1977, another seismic event with Ml 5.2 occurred and was followed by its aftershock series which lasted more than one month. The only data interpreted as coseismic deformation (Steinhauser and Lenhardt, 1986) come from GPS levelling measurements done in 1952 and 1977, which allowed to estimate 25 cm of maximum deformation between Venzone (+ 18 cm) and Carnia (-7 cm) (Talamo et al., 1978). Regarding the Mw 6.45 mainshock, the macroseismic epicenter is located between Buia and Gemona del Friuli (DBMI15) (Fig. 1.6), while the instrumental hypocentral location of the event (Slejko, 2018) is placed near Lusevera, about 12 km ENE, in a sector of the pre-Alpine foothills where no major settlements are found.
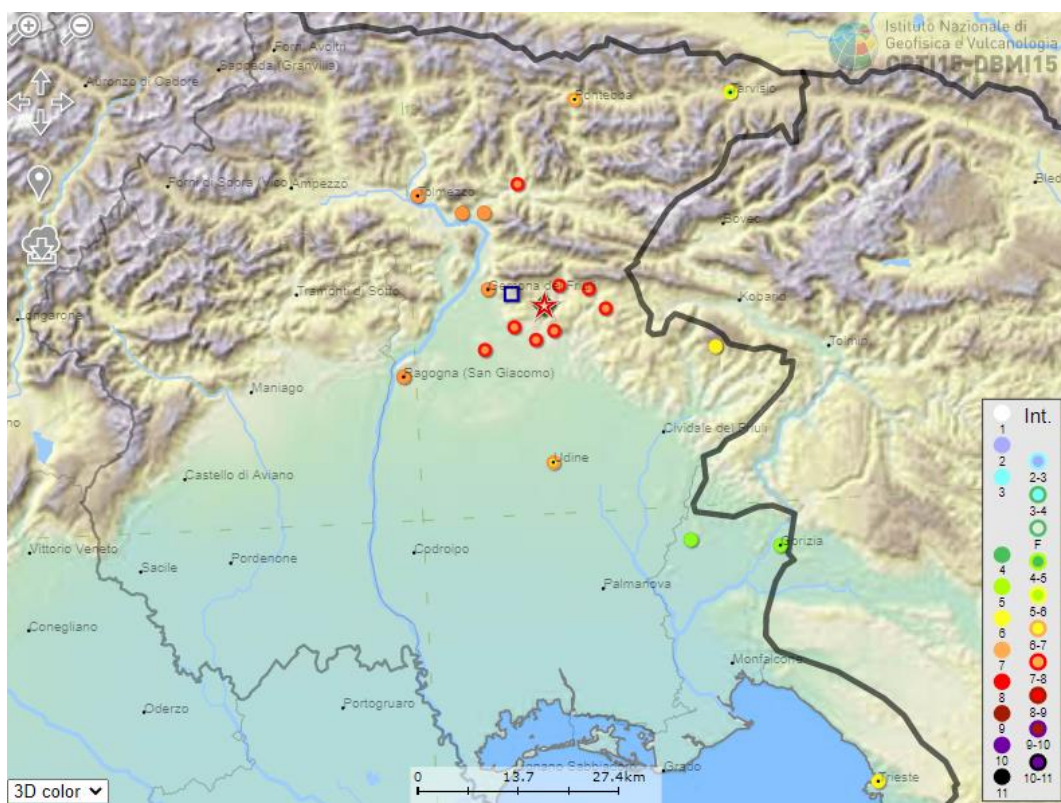

Fig. 1.9 – Damage distribution of the 11/09/1976 event (https://emidius.mi.ingv.it/CPTI15-DBMI15/event/19760911_1635_000).
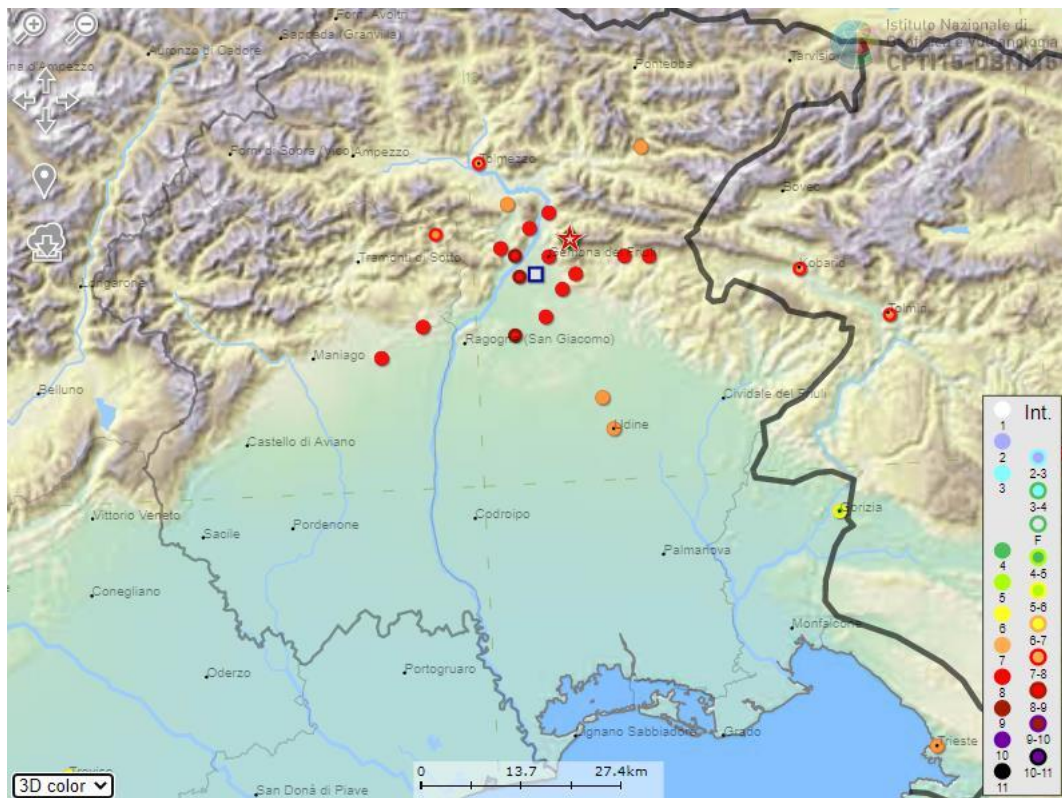
Fig. 1.10 – Damage distribution of the 15/09/1976 event (https://emidius.mi.ingv.it/CPTI15-DBMI15/event/19760915_0921_000).

The elaboration of focal mechanisms shows that most of the main events in the sequence are of reverse type on a low angle plane dipping towards the N-NW, similar to the main shock mechanism, with a small strike-slip component (Slejko et al., 1999; Aoudia et al., 2000; Pondrelli et al., 2001; Poli et al., 2002; Slejko et al, 2018, Saraò et al., 2021). Regarding the possible source, most of the interpretations agree with the activation of two different structures: Amato et al. (1976) and Aoudia et al. (2000) proposed the activation of the Buja-Tricesimo Fault for the May event and the involvement of the Periadriatic Thrust during September. Poli et al. (2002) and Galadini et al. (2005) agree for the interpretation of the May event, but the Authors assessed the activation of a deeper structure during the event of September. The activation of a single source for the entire sequence, whose surficial expression is compatible with the Buia-Tricesimo Thrust, was proposed by Cheloni et al., (2012) based on geodetic data. Conversely, Pondrelli et al. (2001) attributed most of the

events to the Periadriatic Thrust and only two aftershocks of May to the Dinaric structures. Recently, Poli and Zanferrari (2018) proposed the Susans-Tricesimo Thrust as the responsible source of the May event, based on the evidence of Quaternary deformation both on the surface and in seismic profiles. Nevertheless, a possible activation of the Buia Thrust is not excluded.

Following 1976-1977 sequence, the instrumental seismicity recorded two other more recent sequences in 1998 and 2004 (Fig. 1.6). The April 1998 sequence had a Mwmax of 5.6 (Bajc et al., 2001), while a Mwmax 5.2 event was registered during the July 2004 sequence (Živčić et al., 2006; Zupancîč et al., 2001). Both sequences are associated to the NW-SE dextral strike-slip Raune Fault, which is actively propagating through interaction of individual right-stepping fault segments and breaching of local transtensional step-over zones (Kastelic et al., 2008).

The analysis of instrumental seismic events, together with the stress and strain tensor inversion from focal mechanisms, depicts the strain pattern of NE Friuli - western Slovenia area. Two different deformational sectors can be recognized:

i)   central Friuli. This area is characterized by a medium to high seismicity concentrated between 5-12 km depth (Peruzza et al., 2002). Middle-to-low angle E-W and WNW-ESE reverse faults accommodate compressive stress regime. In this sector, where the 1976 main shock is located, the maximum compressional axis is about N-S (Slejko et al., 1999).

ii)   NE Friuli - W Slovenia. This area is characterized by deeper events (1998, Mw 5.6 Bovec and 2004 Mw 5.1 Tolmin) and shows a more complex deformational field, dominated by strike-slip tectonics (Bernardis et al., 2000; Kastelic et al., 2008; Moulin et al., 2014; Grützner et al., 2021) with transtensional (Poli and Renner, 2004) and/or transpressional features (Falcucci et al., 2018).

The orientation of the P-T axes obtained from the analysis of focal mechanisms (Bressan et al., 2018) are in good agreement with the orientation of the principal strain-rate axes estimated from GPS velocities (ca. NW-SE in the western area and ca. NNE-SSW in the eastern area) (Serpelloni et al., 2016). The study area corresponds to a relatively high strain-rate patch of the Alpine Chain, characterized by maximum values of $0.36*10^{-7}yr^{-1}$ in the Montello-Cansiglio region and decreasing rates towards the east, up to western Slovenia (Serpelloni et al., 2016). The Friuli crustal velocity field illustrates the NNW moving of northern Adria with respect to the stable Alps (Bechtold et al., 2009), with velocity values spanning from 0.8-1.1 mm/yr for the southalpine area, to 2.5-3.5 mm/yr for the plain and prealpine area. These values suggest an about 2 mm/yr NNW-shortening (D'Agostino et al., 2005; Bechtold et al., 2009; Devoti et al., 2011). GPS velocities profiles across Eastern Southern Alps (ESA) and Dinaric-Slovenian deformation belt define an about 1 mm/yr shortening accommodating across the ESA front partitioned between a major dip-slip and a minor strike-slip component. Even though the GPS coverage is poor, an about 1mm/yr shortening and a maximum 1.2 mm/yr right-lateral motion rate are estimated for the Dinaric strike-slip faults (Cheloni et al., 2012; Serpelloni et al., 2016).

CHAPTER 2: 3D-STRUCTURAL MODEL OF EASTERN FRIULI

In the framework of the regional project "Faglie Attive FVG", in cooperation with the University of Trieste and the Istituto Nazionale di Oceanografia e Geofisica Sperimentale, the Geological Survey of the Friuli Venezia Giulia Region enabled an agreement with ENI for the consulting of their exclusive data. Therefore, ENI industrial seismic lines covering an area of more than one thousand square kilometers were examined with the aim to reconstruct the buried setting of the Friuli plain and to detect the main active faults of the study area. In addition, focusing on the Quaternary activity of the detected tectonic structures, the Plio-Quaternary base surface was reconstructed from geognostic data, both available from the literature and supplied by Friuli Venezia Giulia Region.

2.1 METHODS

2.1.1 PLIO-QUATERNARY BASE SURFACE RECONSTRUCTION

Regarding the reconstruction of the Plio-Quaternary deposition base surface, the database of wells supplied by Friuli Venezia Giulia Region was integrated with the geoelectrical surveys by Vecchia and De Wrachien (1968). The depth value of pre-Plio-Quaternary bedrock (in terms of turbidites or Molasse) was extracted from every well log, normalized for the datum plane and interpolated through Ordinary Kriging mode of 3D Move software. However, the elaborated gridding surface didn't properly represent the Plio-Quaternary bottom since it didn't fit with the numerous well exceeding the 60 m drilling depth that don't cut through the pre-Plio-Quaternary bedrock. Therefore, in order to better constrain the interpolated surface, the bottom well depth values of the latter were considered as minimum values of the base-Plio-Quaternary surface depth, then included within the interpolation phase. Furthermore, the NE border of the reconstructed surface

was constrained with the outcropping bedrock limit, included in the interpolation process as minimum elevation points of the top of the pre-Plio-Quaternary bedrock.

The interpolation process used, the Ordinary Kriging, is a method based on a generalized least squares regression algorithm, which interpolates values by minimizing the error variance of the estimate. The spatial distribution of data is automatically analyzed by 3D Move by calculating the Omnidirectional Sample Variogram. Moreover, a Variogram Surface is elaborated in order to analyze the anisotropy of the variance (supplementary material of Patricelli and Poli, 2020). The parametric variogram function adopted by the software in the interpolation procedure is the exponential variogram function, since it best fits the Omnidirectional Variogram calculated. Regarding the anisotropy of the variance, it was not considered in the interpolation process. Nevertheless, the variogram surface elaborated (supplementary material of Patricelli and Poli, 2020) clearly shows a central NW-SE elongated well defined region, which corresponds to the area where most of the bedrock wells are located. Conversely moving southwestwards, where the Plio-Quaternary bottom reaches -300 masl depths, the interpolation is less constrained, both because fewer data are present and because it mostly deals with no-bedrock wells exceeding the 60 m depth.

2.1.2 SEISMIC LINES INTERPRETATION

The 3D geometry of the active fault systems characterizing the eastern Friuli plain was reconstructed though the interpretation of ENI seismic profiles via 3D-Move™ Software by Petroleum Experts. Seismic sections were calibrated with ENI exploration well logs (Buttrio, Cargnacco1, Lavariano1 and Terenzano1), and the top of the main stratigraphic horizons were detected and then digitalized in the 2D-sections. The deepest interpretable and well recognizable horizons are the Carnian Unconformity, located between the Carnian dolomitic and evaporitic unit (Raibl Formation, now

Travenanzes Formation, Neri et al., 2007) and the above Carnian-Norian carbonate platform of the Dolomia Principale (DPR). Even though the Dolomia Principale is not well detectable on seismic lines, it was distinguished from the carbonate platform in order to better constrain the velocity model. Based on Cargnacco 1 stratigraphy, the top of DPR was mapped by considering a constant thickness of 875 m above the Carnian Unconformity.

Moving upward, the mapped horizons are: the top of the Jurassic-Cretaceous-Paleocene carbonate platforms, the bottom and top of Cavanella Group (early middle Miocene), coinciding with the top of the turbiditic upper Paleocene-Eocene succession and the bottom of the middle to upper Miocene "Molassa", respectively. The base of the Plio-Quaternary succession is marked by the Messinian unconformity, eroding increasingly older and uplifted units towards the NE (from upper Miocene Molasse to lower Eocene turbiditic units). To map the Messinian Unconformity, the analyzed seismic profiles were calibrated with the interpolated Plio-Quaternary base surface.

For the 2D time to depth sections conversion a simplified seismostratigraphic model was elaborated (Table 2.1) and uploaded in the 3D Move Software. The model was obtained by integrating the stratigraphic framework of the study area with the velocity logs of some ENI exploratory wells and velocity values extracted from bibliography.

SEISMOSTRATIGRAPHIC UNIT		VELOCITY [m/s]
Plio-Quaternary Units		2000
Upper Molasse		2600-3000
Cavanella Group		4000
Eocene turbiditic Units		3600
Carbonatic platform Units		6100
Dolomia Principale		7000
Travenanzes Formation		6000

Table 2.1. – Velocity model adopted for the 2D depth conversion. Velocity values derive from ENI well logs and from bibliography (Zanferrari et al., 2008a and b; Toscani et al., 2016).

Particularly, velocity values of the lower stratigraphic units (late Triassic Travenanzes Formation and Dolomia Principale, Jurassic-Cretaceous platform carbonates, late Paleogene - early Eocene turbidites) were derived from the comparison between Cargnacco 1 and Amanda 1 wells; the middle – late Miocene Molasse velocity was derived from Gemona 1 well, while the early - middle Miocene Cavanella Group and Plio-Quaternary succession velocity values were extracted from bibliography (Zanferrari et al., 2013; Toscani et al., 2016). It is worth noting that the comparison between the Amanda 1 bis (A1) located in the undeformed foreland and the Cargnacco1 (C1) velocity logs (Fig. 2.1) testifies that stratigraphic units involved in the deformation are generally characterized by higher velocities with respect to the same units in undeformed areas (Amanda 1Bis well). Cargnacco1 (C1) well shows two tectonic repetitions of the stratigraphic series at 2575 m and 2945 m depth, respectively. These two tectonic reverse structures are interpreted by Venturini S. (2002) as the evidence of the compressive events connected to Paleogene (Dinaric) tectonic phase. Since the study area corresponds to the active deforming front, higher velocity values have been adopted in the velocity model. A distinction needs to be made regarding the middle – late Miocene Molasse velocity adopted in the northern and southern portion of the study area, respectively. Particularly, for the northern portion (Sections E, F, G, H) the middle – late Miocene Molasse velocity value was derived from Gemona 1 well. Differently in the southern piedmont plain no conglomerate Molasse body exists, then a lower value of 2600 m/s extracted from bibliography (Zanferrari et al., 2013; Toscani et al., 2016) was adopted.
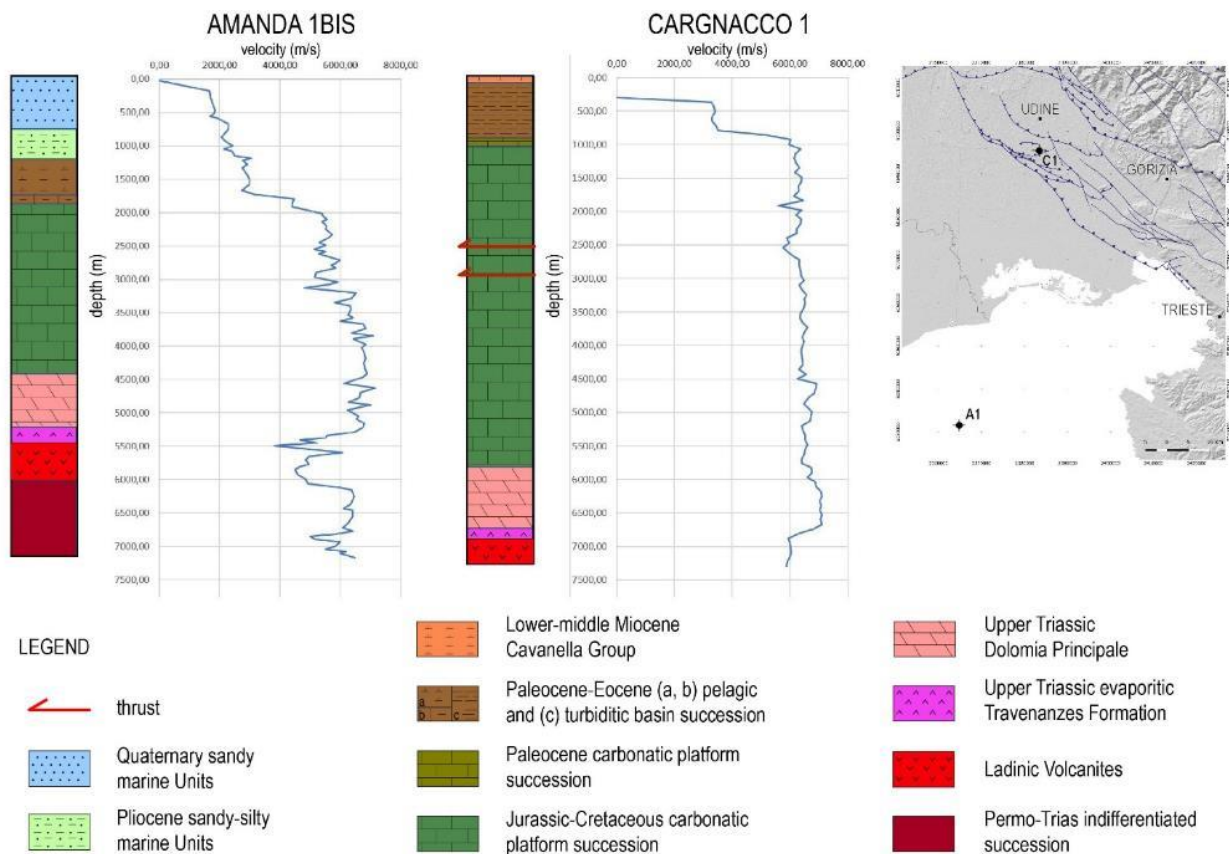
Fig. 2.1. – Comparison between ENI velocity logs and stratigraphic columns of Amanda 1 bis and Cargnacco 1 wells (Nicolich et al., 2004). The top right map shows the wells locations (Patricelli and Poli, 2020).

Once digitalized, each section was converted from time to depth through the Database Method of 2D Conversion tool, which considers the velocity values settled in the stratigraphic model and compute the conversion procedure as the incremental sum of the thicknesses of equal velocity (Move 2019.1 KnowledgeBase). Starting from the 2D geological sections obtained from the interpretation of seismic lines, the 3D surface of the main tectonic structure was constructed through the interpolation procedure of the *Create new fault* within the *Create Surface with Boundaries* tool. The *Control Points for Kriging* option was ticked in order to create a surface from points that is geostatistically valid (Move 2019.1 KnowledgeBase).

2.2 RESULTS

2.2.1 PLIO-QUATERNARY BASE SURFACE

The reconstructed structural model of the study area well depicts the eastern Friuli active fault systems, mainly buried under the LGM Friuli Plain surface. The interpolated Quaternary base surface (Fig. 2.2) shows that the Plio-Quaternary succession in NE Friuli gets thicker from the pre-alpine border, where the bedrock crops out, moving towards S-SW where it exceeds the -300 m asl depth (Fig. 2.2).

It is worth noting that abrupt deepening of the Plio-Quaternary bottom is present at the footwall of the main reverse structures, testifying that tectonic activity strongly controlled deposition during Quaternary. Regarding the stratigraphic thickness a distinction should be made.

Out of the front of the Southalpine Chain, he Plio-Quaternary succession includes both Pliocene marine sediments and Quaternary continental deposits (Mancin et al., 2016; Toscani et al, 2016), while in the north-easternmost portion of the Friuli Plain the exploratory wells didn't record Pliocene sedimentation. Nevertheless, near Osoppo a continental conglomerate dated back to late Zanclean (Monegato and Stefani, 2010) is present. Similarly, we cannot exclude the presence of Pliocene continental deposits filling the carved Messinian canyons even at the northeastern border of Friuli Plain. Therefore, even knowing that locally the Quaternary deposits directly overly the pre-Plio-Quaternary bedrock, the erosional top of the pre-Plio-Quaternary surface here reconstructed will be uniformly considered as Plio-Quaternary surface.

The interpolated Plio-Quaternary base surface was useful to calibrate the bottom of the Quaternary deposition in seismic lines and accordingly, to detect and locally to quantify the Quaternary vertical displacement of the tectonic structures recognized on seismic profiles. Particularly, among all the analyzed seismic profiles covering the entire Friuli Plain, eight geological cross sections intersecting

the investigated tectonic structures of Eastern Friuli were elaborated (A, B, C, D, E, F, G and H, traces in Fig. 2.3). Sections A to D are located in the southern portion of the study area (Friuli Plain), while sections E to H are placed in the northern corner of the plain (High Friuli Plain/Julian Prealps).
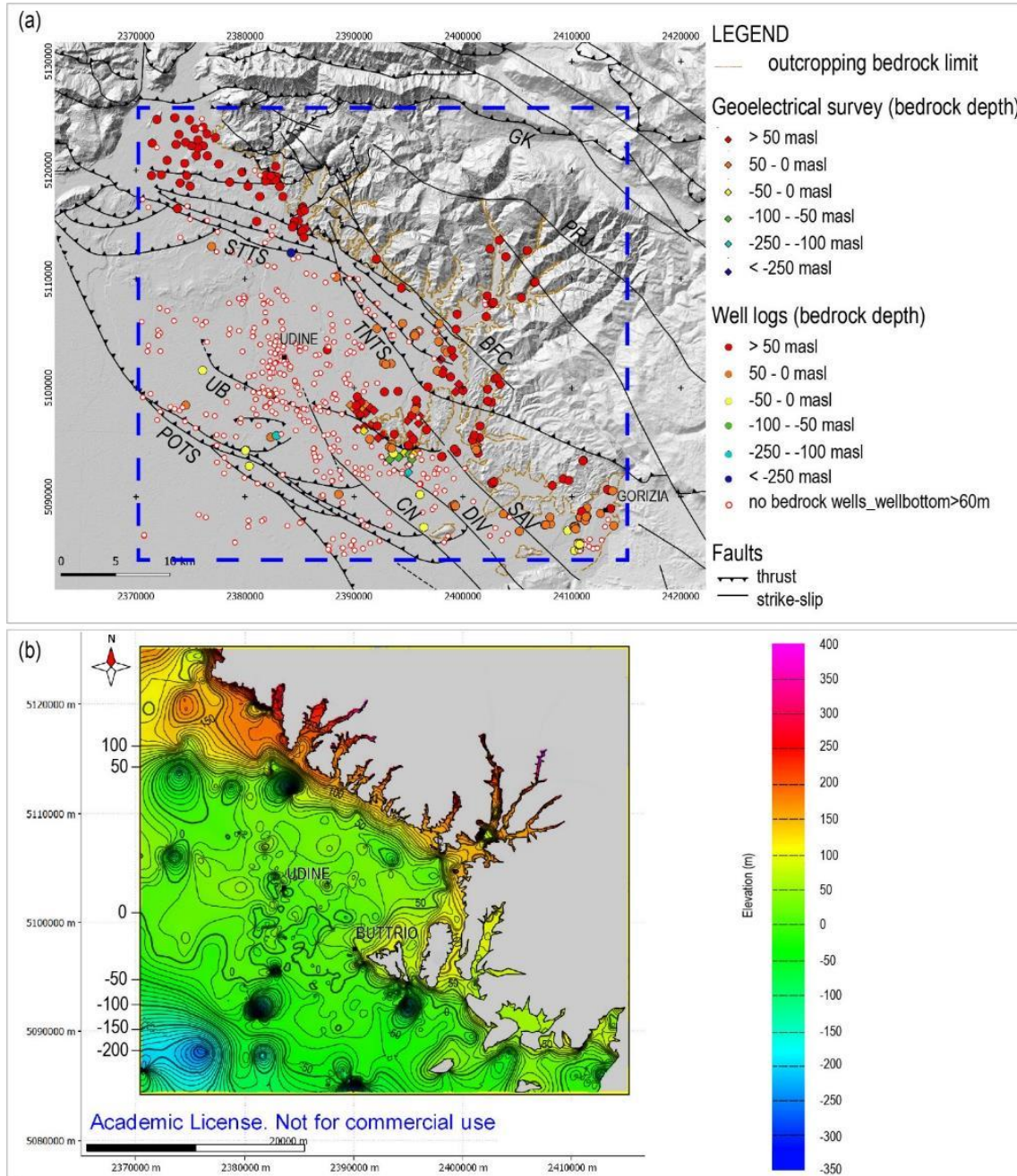

Fig. 2.2 - (a) Distribution of geophysical surveys and geological data used for the reconstruction of the Plio-Quaternary base surface. Fault's acronyms: BFC: Borgo Faris-Cividale Ft; CN: Colle Nero Ft.; DIV: Divača Ft.; GK: Gemona-Kobarid Th.; POTS: Pozzuolo Th. System; PRJ: Predjama Ft; SAV: Savogna Ft.; STTS: Susans-Tricesimo Th. System; TNTS: Trnovo Th. System; UB: Udine-Buttrio Th.; (b) Plio-Quaternary base surface computed from the interpolation of geophysical and geological data (Patricelli and Poli, 2020).

2.2.2 – QUATERNARY ACTIVE FAULT SYSTEMS OF EASTERN FRIULI

The piedmont Friuli Plain included between Tricesimo and Pozzuolo del Friuli is characterized by the presence of 4 fault-systems: the Pozzuolo Thrust System (POTS), the Trnovo Thrust System (TNTS), the Colle Villano-Borgo Faris-Cividale transpressive Fault-System and the Susans-Tricesimo Thrust System (STTS) (Fig. 2.3).

Starting from the southern portion of the study area, sections A, B, C and D intersect three main NW-SE trending thrust systems: the Pozzuolo (POTS), the Trnovo (Placer et al., 2010) Thrust Systems (TNTS) and the Colle Villano - Borgo Faris-Cividale Fault System (CV-BFC) (Fig. 2.3).

POZZUOLO THRUST SYSTEM

The NW-SE striking Pozzuolo Thrust System (POTS) extends for about 35 km from San Daniele del Friuli to Medea (Fig. 2.3). Detaching from the Carnian Unconformity (at a depth of about 7 km, Fig. 2.4 a, b, c) it cuts through the entire succession causing a wide ramp anticline in the carbonates. Lower Eocene turbiditic sequence onlaps the anticline and locally, the overlying Cavanella Group directly lies on top of the carbonate succession (Venturini, 1987; 2002; Fantoni et al., 2002; Merlini et al., 2002; Nicolich et al., 2004). However, both turbiditic units and Cavanella Group were affected by the neoalpine reactivation of POTS. Geometric complexity of the thrust-system increases toward the SE (Fig. 2.4 a, b, c): in its northern portion (Section A, Fig. 2.4 a), POTS shows a single thrust fault (POZ1) which gives rise to a wide Paleogene Dinaric anticline in the carbonates and strongly displaces the top of carbonate platform. The Dinaric anticline is sealed by the Cavanella Group, but POZ1 displaces Cavanella Group and affects also Neogene-Quaternary deposits.
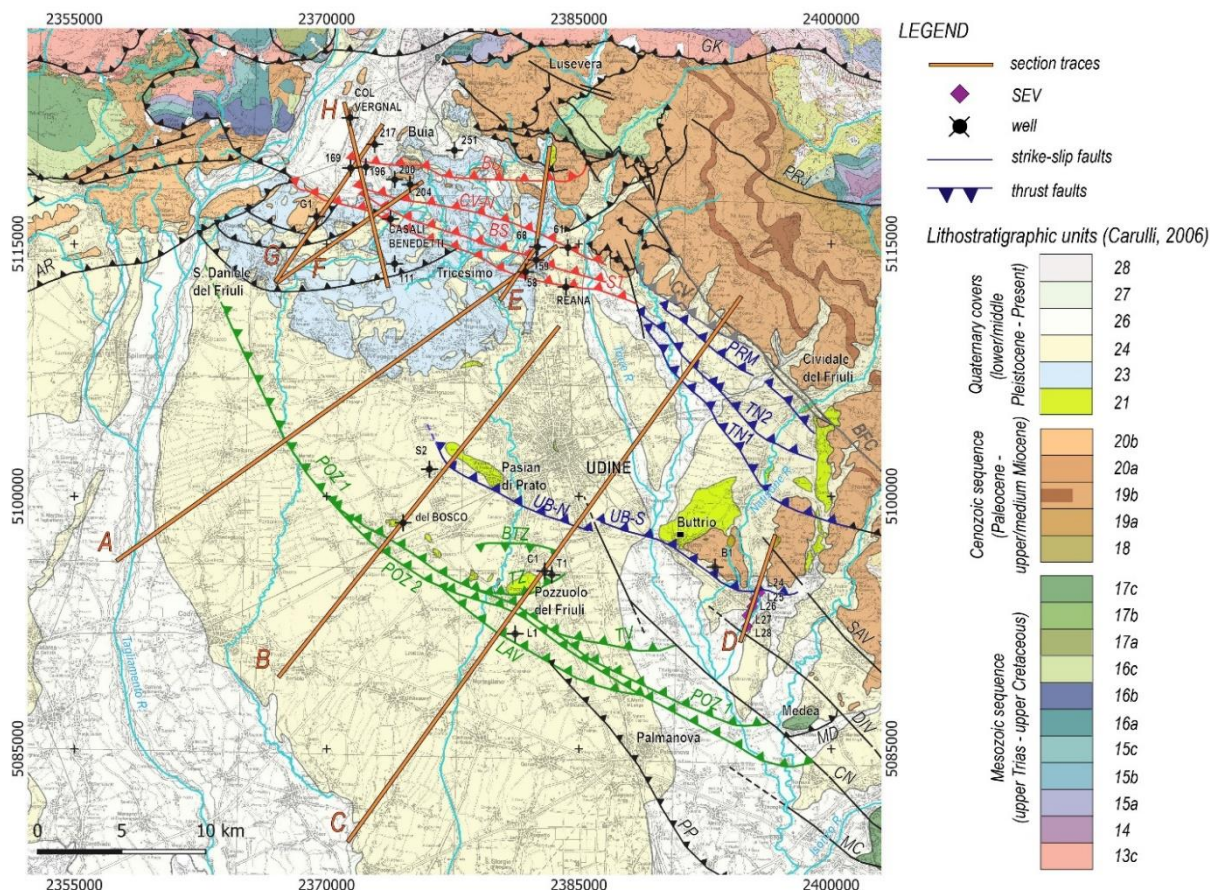
Fig. 2.3. - Structural map of NE Friuli Plain. Legend: A, B, C, D, E, F, G, H, Q: geological cross sections from seismic interpretation (ENI). B1: Buttrio well; C1: Cargnacco well; G1: Gemona well; L1: Lavariano well. Green thrusts: Pozzuolo Thrust System (POTS); blue thrusts: Trnovo Thrust System (TNTS); red thrusts: Susans-Tricesimo Thrust System, (STTS); grey faults: Colle Villano-Borgo Faris-Cividale Fault System (CV-BFC) as reconstructed in this study. Black faults: faults derived from bibliography. AR: Arba-Ragogna Th; BFC: Borgo Faris-Cividale Ft, BS: Borgo Soima Th, BTZ: Terenzano Backth, BU: Buia Th, CN: Colle Nero Ft, CV-N: Colle Villano-North Th, CV: Colle Villano Thrust; LAV: Lavariano Th, DIV: Divača Ft, GK: Gemona-Kobarid Th, MC: Monte Cosici Ft, MD: Medea Th, POZ1-2: Pozzuolo 1 and Pozzuolo 2 Ths, PP: Palmanova-Panzano Th, PRJ: Predjama Ft, PRM: Premariacco Th, SAV: Savogna Ft, ST: Susans-Tricesimo Th, TN1-2: Trnovo 1 and Trnovo 2 Ths, TV: Trivignano Th, TZ: Terenzano Th, UB-N and UB-S: Udine-Buttrio Th northern and southern segments.
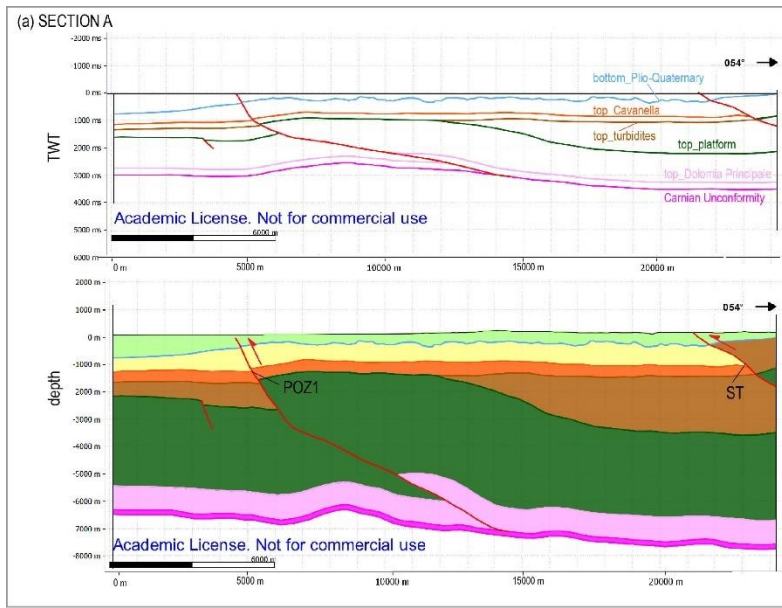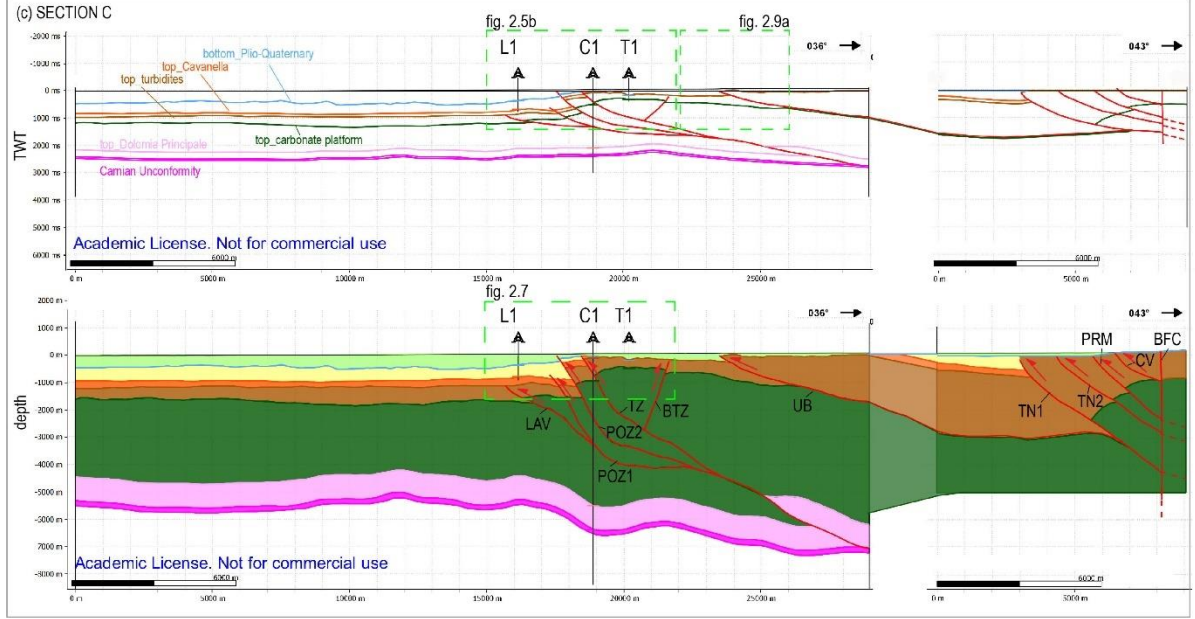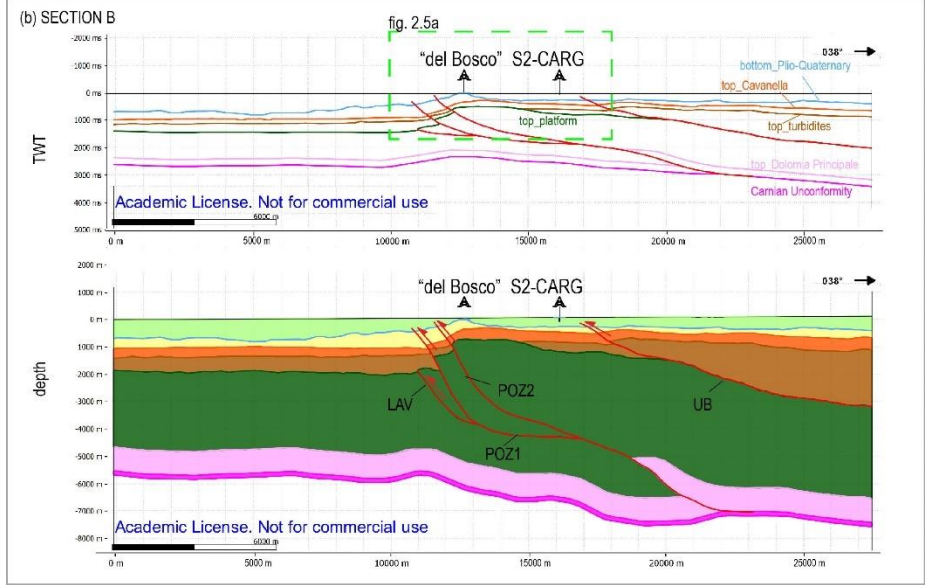
Fig. 2.4. - Seismic interpretation of the main seismo-stratigraphic horizon and related geological cross sections A (a), B (b) and C (c) representing the buried setting of the NE Friuli Plain. Section traces and acronyms are reported in Fig. 2.3 (Patricelli and Poli, 2020).

LEGEND

Plio-Quaternary deposits

Molasse (Upper Miocene)

Cavanella Group (Lower-Middle Miocene)

Turbidite Units (Upper Paleocene-Lower Eocene)

Carbonate Platform (Jurassic-Cretaceous-Paleocene)

Dolomia Principale (Upper Triassic)

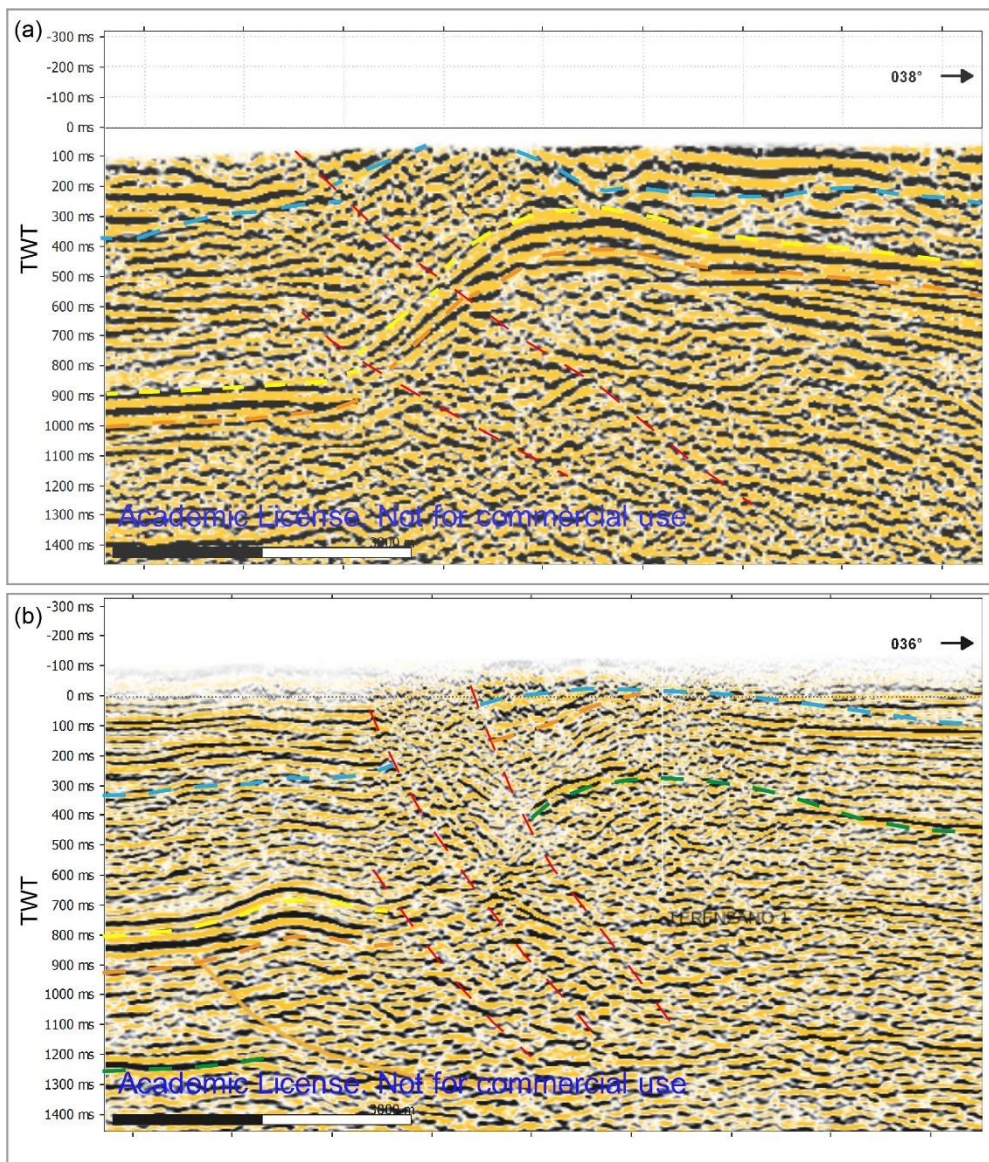Travenanzes Formation (Upper Triassic)

36

Fig. 2.5 - Clippings of seismic lines of sections B(a) and C (b) across Pozzuolo Thrust System with a 3X vertical exaggeration of the z scale.

In the central sector (Section B, Fig. 2.4 b) POTS is split into two fault strands: POZ1 and POZ2. The anticline in the carbonates is evident, but in this sector, the compressional deformation strongly involves Cavanella Group, Molasse and the Plio-Quaternary deposits. In the hanging-wall of the POZ1 Thrust, the Plio-Quaternary unconformity partially eroded the Molasse anticline, drilled by "del Bosco" well (Fig. 2.5 a). Here the deformation of the Plio-Quaternary surface is clear: the "del Bosco" well, located near Variano (UD), drilled the Molasse pronounced anticline at 26.74 masl (Venturini, 1987). Conversely, the S2-CARG-FVG well (Zanferrari et al., 2008a) located at Colloredo di Prato (UD), about 4 km NE from the first one, cut through 157 m of Quaternary deposits from

37

datum plane, reaching a depth of -44.7 m asl and then highlighting the SW-verging anticline geometry.

Moving SE, in the most deformed area (Section C, Fig.2.4 c), strain is accommodated by at least three more reverse structures: POZ1, POZ2 and a frontal buried thrust (Lavariano Thrust: LAV), which displaces carbonates and slightly deforms Cavanella Group (Fig. 2.5 b). In the hanging-wall of POZ1, Terenzano Thrust (TZ) with its Backthrust (BTZ) and Trivignano Thrust (TV) develop, cutting through the entire stratigraphic succession up to the Quaternary units (Fig. 2.4 c).

The along length profile (Fig. 2.6) reveals a complex tectonic history of POTS: it records an inherited Paleogene tectonic phase as external SW-verging thrust of the External Dinarides with about 1000 m vertical displacement on the Jurassic-Cretaceous-Paleocene carbonate platform. Nevertheless, it shows also a clear Neogene activity involving both the Cavanella Group and the Plio-Quaternary bottom.
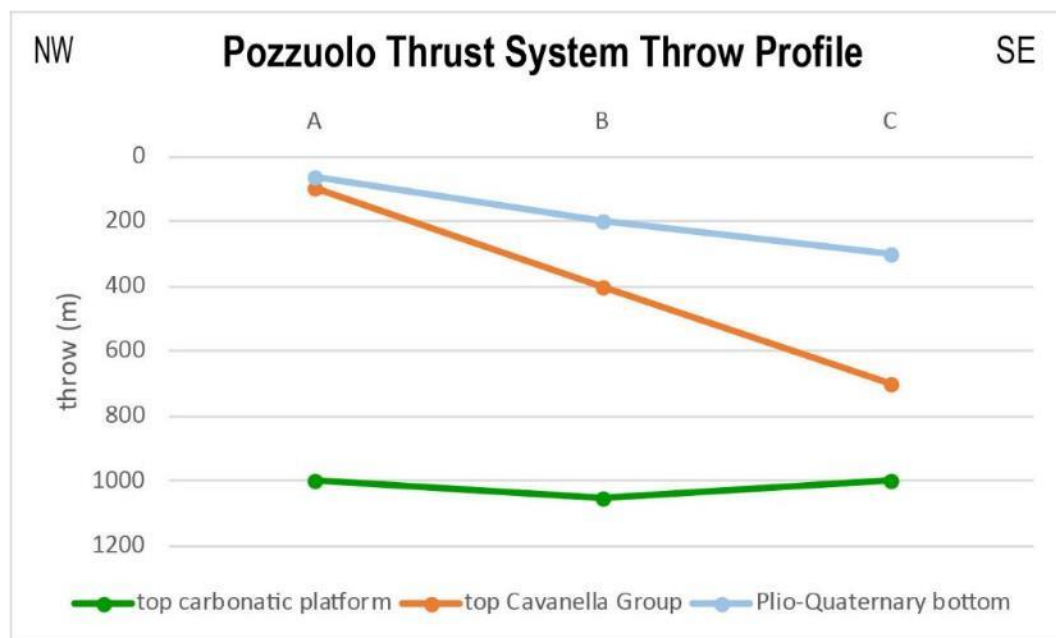

Fig. 2.6 - Along length throw profile of Pozzuolo Thrust System, elaborated by collecting for each section A, B and C the vertical displacement of the top carbonatic platform, top Cavanella Group and Plio-Quaternary bottom horizons (Patricelli and Poli, 2020).

The graph highlights a strong displacement of the Friuli Carbonate Platform during the Dinaric tectonic phase and the SE-ward increasing of throw values on the Neogene-Quaternary stratigraphic units, thus suggesting a SE-ward greater activity during the Neoalpine tectonic phase, probably linked to the reactivation of a NE-SW trending lateral ramp of the Dinaric thrust-system as frontal one (Terenzano Thrust). Neogene-Quaternary tectonics is partitioned along POZ between a strike-slip component (on the NW-SE striking portion) and a dip-slip component (on the WSW-ENE striking Terenzano and Trivignano frontal ramp) as suggested by Venturini S. (1987). Seismic sections provided by ENI, implemented with well logs and geologic field data, show that POTS cuts the succession in the lower stratigraphic units (carbonate platforms, turbiditic succession and Cavanella Group) by means of a well recognizable fault plane. Conversely, upward, the more recent and shallow units (Molasse and Plio-Quaternary deposits) are characterized by a pervasive deformation, which appears to be spread in a wider dipping zone (Fig. 2.5).

By correlating the stratigraphic logs of ENI exploratory wells Lavariano 1 (L1) and Cargnacco 1 (C1) (Fig. 2.7), located on the most deforming portion of POTS, a throw of 318 m affecting the Plio-Quaternary base was calculated for the Pozzuolo 1 Thrust (POZ1). The Quaternary units directly lie on the pre-Quaternary bedrock in both stratigraphies (Cavanella Group in C1 and Molasse in L1 wells, according to Nicolich at al., 2004), but any better constrains regarding the age of the oldest Quaternary units are not available. Then a maximum Quaternary age can be inferred for the vertical displacement, estimating a 0.12 mm/yr minimum Quaternary vertical deformation rate. By correcting the vertical displacement for the dip value of 65° of the shallow ramp fault of the Pozzuolo1 Thrust, a slip rate value of 0.14 mm/yr can be estimated.
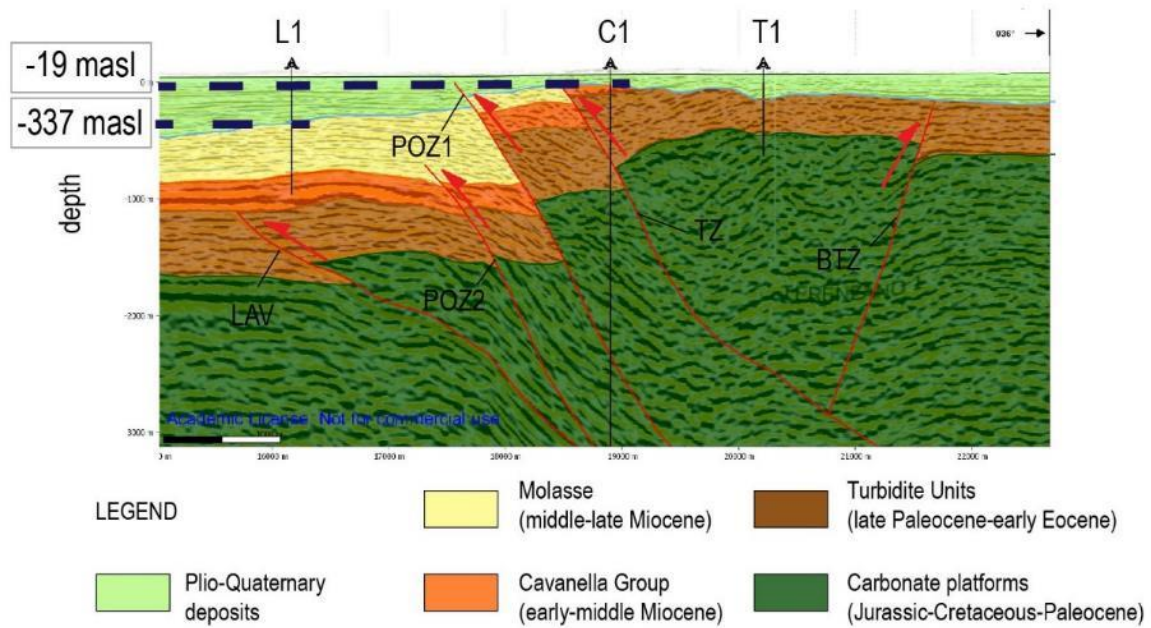
Fig. 2.7 - Detail of Section C showing the displacement of the bottom of the Plio-Quaternary succession (see Fig. 2.4 c for location) (Patricelli and Poli, 2020).

The morphological evidence of the Pozzuolo Thrust System activity, which are represented by surficial anomalies in the LGM Friuli plain south of Udine (Comel 1947; Zanferrari et al., 2008a; Fontana et al., 2014a, b), are collected in the Morphotectonic Map. Particularly, along the Pozzuolo thrust many isolated relieves are present: the Variano, Orgnano and Pozzuolo highs. These relieves, cropping out on the LGM surface, are made of pre-LGM Friuli Superunit (FS, Fontana et al., 2019). Particularly, in the proximity of Pozzuolo del Friuli locality, the pre-LGM conglomerates lie over the pre-Quaternary Cavanella Group (Comel, 1955; Fontana et al., 2004, 2014a and 2014b; Zanferrari et al., 2008a). In this area, the Cormor stream is confined between terrace slopes, up to 10 m high, until the Hill of Pozzuolo, which is interpreted as a structural high (Galadini et al., 2005). During the LGM this relief acted as an obstacle, forcing the outwash streams to pass around it and forming two fans on each side of the uplifted terrace (Fontana et al., 2014a). On top of the hill the presence of well-evolved polycyclic soils developing since middle Pleistocene is documented (Feruglio, 1925c; Fontana, 1999; Fontana et al., 2014a). Near Pozzuolo del Friuli, Fontana (1999) measured an about

4 m scarp carved on pre-LGM Friuli Superunit. At the base of the scarp the pre LGM units are in contact with the Remanzacco subsynthem, dated at 22.0 – 19.5 kyr cal BP (Fontana et al., 2014a). Thus, a minimum late Quaternary slip rate of 0.2 - 0.22 mm/yr can be estimated for the Pozzuolo 1 Thrust (POZ1).

TRNOVO THRUST SYSTEM

The second recognized tectonic structure is the Trnovo Thrust System (TNTS), which is composed of three main thrust faults: Udine-Buttrio (UB), Trnovo (TN) and Premariacco (PRM) Thrusts; (Fig. 2.3). TNTS probably originates deeply on Permo-Trias detachment levels, not detectable on seismic lines because of the elevated depth, and is responsible of the SW overlapping of the carbonate platform and turbiditic units on the Cavanella and Molasse (Fig 2.4 c). Placer et al. (2010) identify the Trnovo Thrust as the outer front of the External Dinarides, but more recently Falcucci et al., (2018) segmented it in two portions: the Susans Tricesimo Thrust (ST) and the Trnovo Thrust (TN) (Fig. 2.3). In detail, within the TNTS, PRM likely only slightly deforms the Plio-Quaternary bottom surface, and local outcropping of lower Eocene turbiditic sequence are documented along the Natisone riverbed (Fig.2.3 and Morphotectonic Map) (GeoCGT, 2008). Within the TNTS, the Udine-Buttrio Thrust (UB) extends for a total length of about 25 km under Udine plain and it is segmented in two distinct portions (UB-NW and UB-SE, Fig. 2.3) by the NNW-SSE oriented dextral Paparotti Fault (PF).

The NW segment (UB-NW) runs as a flat on the top of the carbonate platform rising with a frontal ramp causing a ramp-anticline. It deforms Paleocene-Eocene turbidites, Cavanella Group and Molasse, involving the Plio-Quaternary deposition, as shown in section B (Fig 2.4 b). Many morphotectonic elements are associated to the Udine-Buttrio Thrust (Morphotectonic Map). Particularly, along the UB NW-segment, the presence of Udine and Pasian di Prato highs is

documented, where pre-LGM Friuli Superunit outcrops (Fontana et al., 2019). The Udine high is a conglomeratic relief, on top of which a monumental burial (the "Sant'Osvaldo Tumulus") dated back to the Bronze Age (about 2000 BC) is present, and the burial location was chosen just because of the elevated position (Càssola Guida and Calosi, 2002). The Pasian di Prato high, which crops out from late LGM Canodusso subsynthem (Zanferrari et al., 2008a), is bordered towards the SW by a 4 m high scarp carved on pre-LGM deposits. Knowing that an age of 23–21 kyr cal BP was estimated for the Canodusso subsynthem (Monegato et al., 2007), a throw rate of 0.17 – 0.19 mm/yr can be calculated, which gives a slip rate of the order of 0.35 – 0.38 mm/yr for the UB-NW.

Differently, the southern segment of the Udine-Buttrio Thrust (UB-SE) probably runs in a flat along the Cretaceous-Paleocene platform interface, rupturing the Paleocene thin succession and rising with a final ramp in Eocene turbidites (sections C and D, Figs. 2.4 c and 2.8). In the proximity of the surface UB-SE heavily displaces the Quaternary deposition (Fig. 2.9 a, b).
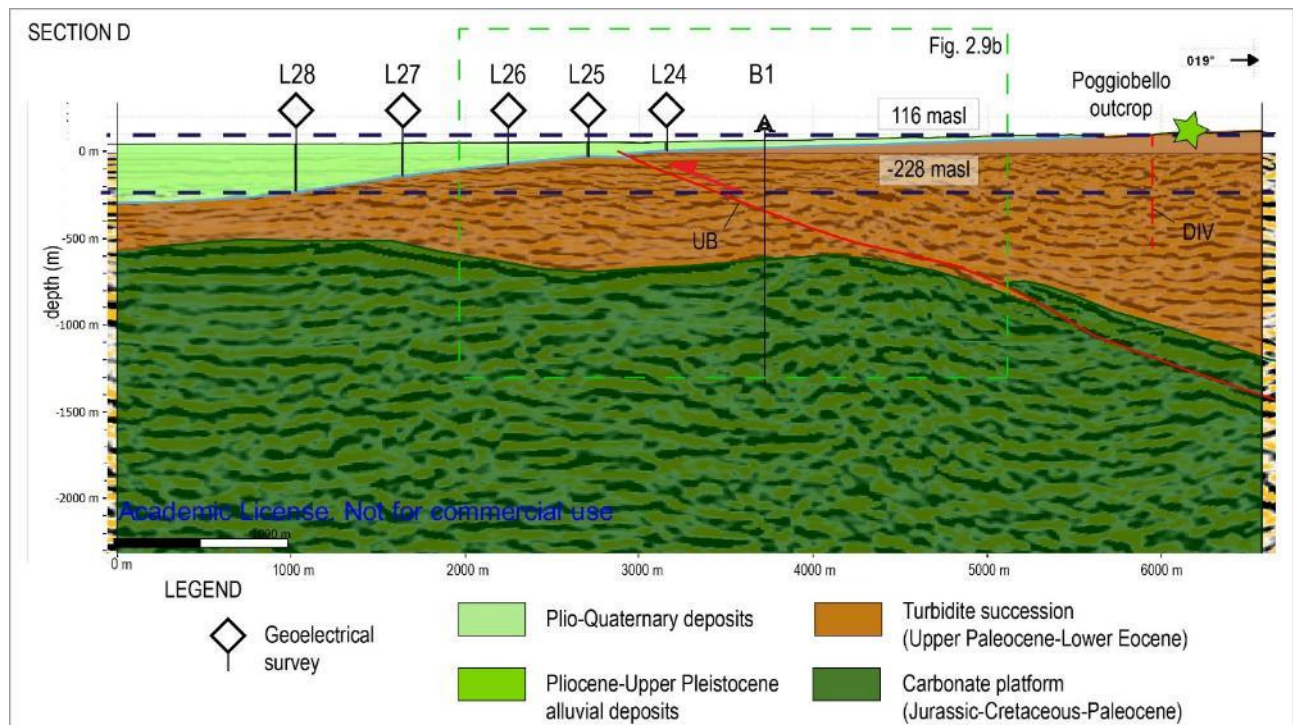

Fig. 2.8 - Geological cross section D (see Fig 3.2 for location), showing the displacement of the Quaternary units along the southern segment of the Udine-Buttrio Thrust (Patricelli and Poli, 2020).
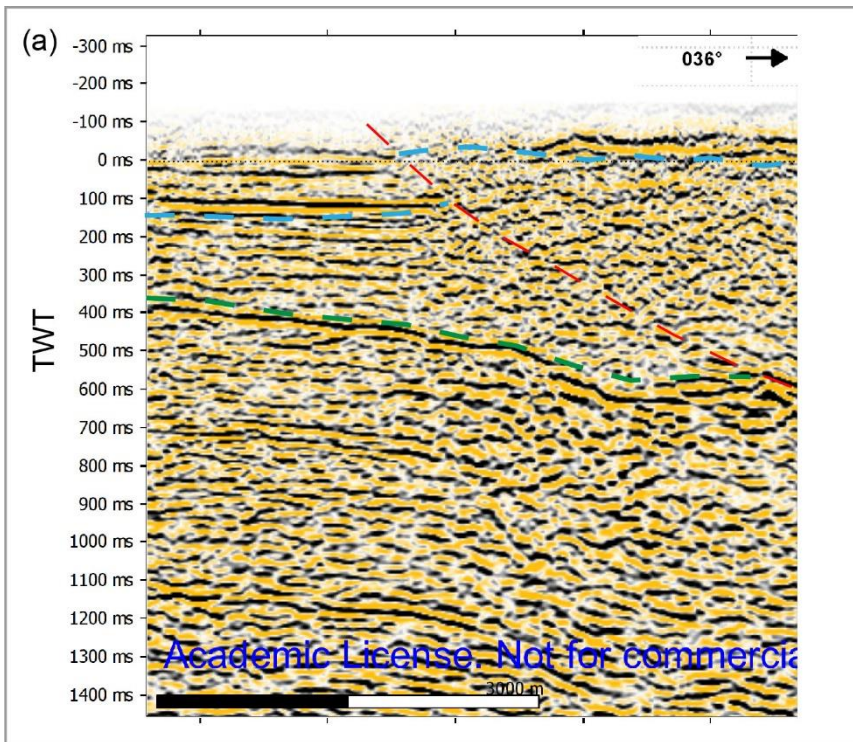
Fig. 2.9 - Clippings of seismic lines of sections C (a) and D (b) across Udine-Buttrio Thrust with a 3X vertical exaggeration of the z scale.
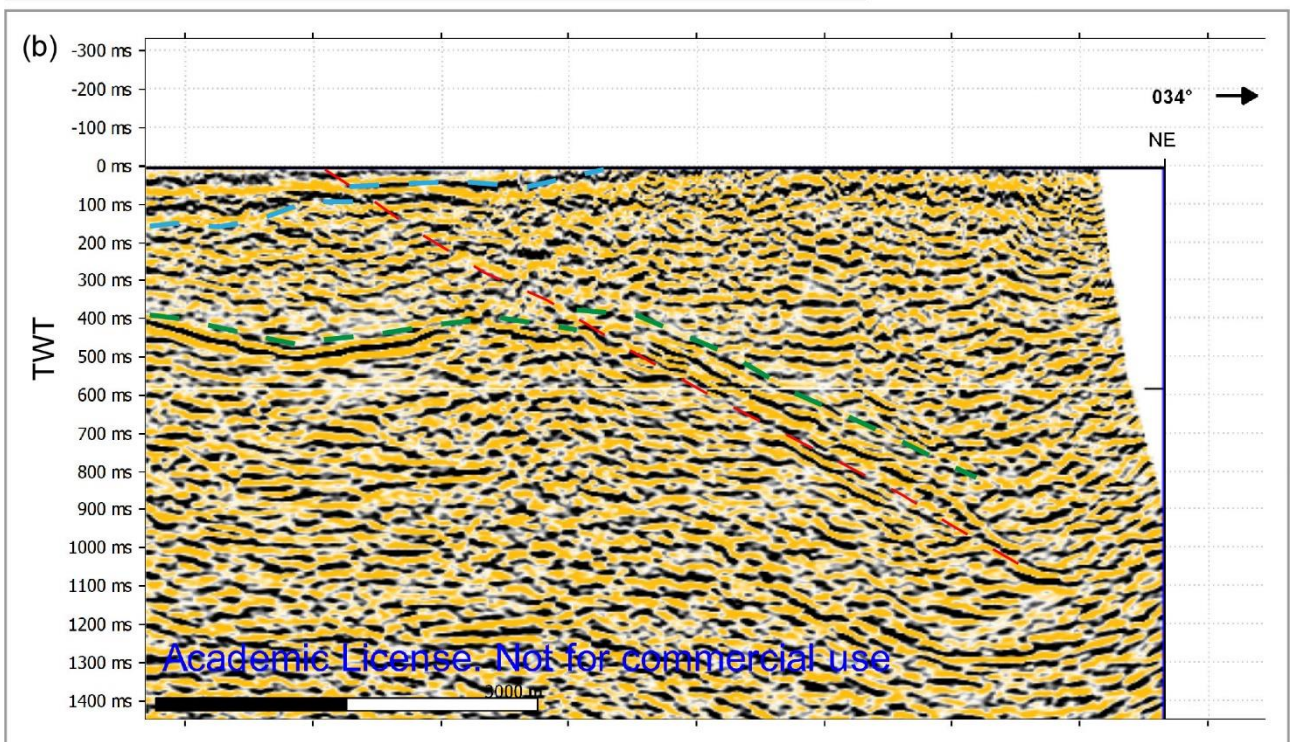
Near Buttrio and Collio hills, UB-SE is responsible of the outcropping of Eocene turbiditic (Morphotectonic Map) units and the reconstructed Plio-Quaternary base surface highlights the presence of a NW-SE trending about 300 m deepening of the Quaternary cover SW of the outcropping Eocene turbiditic units. On top of the hills (i.e. in its hanging-wall), at altitudes between

100 and 130 m asl, a late-to-middle Pleistocene unit crops out: the Poggiobello Unit (PGB). It is characterized by intensely altered and partly cemented coarse gravels, with abundant sandy-silty matrix, partly related to weathering processes. On top of these deposits, a very well evolved soil characterized by a 5 YR 5/8 color is preserved. By correlating the bottom of PGB with the Plio-Quaternary base surface interpolated from geophysical data (Fig. 2.9) a vertical displacement of 344 m and throw rate of 0.13 mm/yr can be estimated for UB-SE, thus revealing a minimum Quaternary slip rate of 0.27 mm/yr.

Recently, Viscolani et al. (2020) identify a WNW-ESE trending tectonic scarp west of Manzano village, on the left Natisone bank (Morphotectonic Map). Following a morphotectonic survey and geophysical prospections, the Authors interpret the morphological element as the surficial expression of a splay associated to the Udine-Buttrio blind Thrust and estimate a post-glacial vertical rate of 0.08-0.17 mm/yr. Actually, it is worth noting that any Poggiobello outcrops are not documented south of this scarp (Morphotectonic Map).

COLLE-VILLANO - BORGO FARIS-CIVIDALE TRANSPRESSIVE SYSTEM

At the hanging wall of the TNTS, the Colle Villano – Borgo Faris-Cividale transpressive Fault-System is present. Seismic lines show a possible connection at depth of the frontal reverse Colle Villano splay to the high-angle Borgo Faris-Cividale Fault (Fig. 2.4 c).

The Borgo Faris-Cividale Fault is a NW-SE trending dextral strike-slip fault and represents the NW-ward extension of the Raša fault (Moulin et al., 2016). Its surficial trace can be followed from Attimis towards Cividale del Friuli thanks the documented numerous well exposed surficial evidence, both structural and morphological (Morphotectonic Map). BFC displaces the Dinaric macroanticline characterizing the Paleogenic turbidtic units of the Grivò and Savorgnano Marls and Sandstones of

the eastern prealpine area (Zanferrari et al., 2008a). Moreover, recent field and palaeoseismological investigations suggest a combined activity for both Colle Villano and Borgo Faris-Cividale (BFC) NW-SE strike-slip Fault System (Falcucci et al., 2018). Many morphostructural evidence associated to the BFC activity are documented in the area extending from Savorgnano del Torre to Togliano di Faedis, such as anomalies of the drainage pattern of the waterstreams flowing SW from the prealpine relieves and the presence of suspended Quaternary glacis in the Malina and in the Poiana drainage basins. In addition, the portion area comprised between the high angle BFC strike-slip Fault and the Colle Villano frontal splay is characterized by an impeded drainage, with many stagnation zones and back tilted surfaces which force the waterstreams to assume a meandering pattern, thus testifying the combined activity of CV and BFC. Further morphotectonic evidence of the BFC are documented even in the southeastern portion of the study area, where a depressed 100 m wide morphological corridor marks the fault trace (Moulin et al., 2016). Across the fault, the dextral deflection of the SW flowing waterstreams and the discontinuity of ridgecrests are documented (Morphotectonic Map). Particularly, a lateral offset of 175 m and 330 m were estimated by Moulin et al. (2016) at Campeglio di Faedis and Fornalis sites, respectively.

Moving to the northernmost portion of the study area, E, F, G and H geologic cross sections (Fig. 2.10) allowed to reconstruct the subsurface geometry of the High Friuli Plain. The main active fault system which affects the study area is the Susans-Tricesimo Thrust System (STTS). STTS is composed of four reverse fault planes: the Susans-Tricesimo (ST), Borgo Soima (BS), Colle Villano (CV) and Buia (BU) WNW-ESE oriented reverse faults. Two additional thrust-faults were detected at the footwall of the Susans-Tricesimo Thrust (the Majano MAJ and San Tomaso STOM Thrusts), which seem to affect only slightly the Quaternary deposition in this area. Conversely, a Quaternary activity can be assessed for ST, BS, CV and BU Thrusts.

In this regard, it is important to specify that, despite the same name, the Colle Villano Thrust do not necessarily represent a unique structure. As a matter of fact, a set of NNW-SSE oriented dextral strike-slip faults is mapped between Povoletto and Savorgnano del Torre (Zanferrari et al., 2008a). These structures, which are interpreted as the faults responsible for the segmentation of the Trnovo thrust system (Placer et al., 2010), presently separate the STTS to the NW from the TNTS to the SE. However, while in the NW area the CV Thrust is interpreted as the inner thrust of the Susans-Tricesimo Thrust System, Falcucci et al. (2018) recently interpreted the Colle Villano Thrust SE of Savorgnano del Torre like the frontal reverse splay of the Borgo Faris-Cividale strike-slip fault. In this work the original names are kept but with the aim to prevent confusion the Colle Villano-N (CV-N) will refer to the northwestern strand of CV, while the simple Colle Villano (CV) name will be used for the southeastern transpressive strand.

SUSANS-TRICESIMO THRUST SYSTEM

The Susans-Tricesimo Thrust (ST) is a medium angle reverse fault which brings the Eocene turbiditic units on top of the middle – late Miocene Molasse: ST is responsible of an about 1.2 s displacement on the top of the carbonatic platform and clearly propagates within the Eocene turbidites and Plio-Quaternary succession (sections E and F, Fig. 2.10 a and b). Moving North, in section G (Fig. 2.10 c), ST displaces the Molasse (Montello Unit, Zanferrari et al., 2013). At the foot wall of ST, a Molasse anticline representing the Susans Hill is very well recognizable on seismic profile. The anticlinal structure is generated by the San Tomaso (STOM) Thrust and its frontal splay (Majano Thrust, MAJ). They both propagate within the Eocene turbidites, Cavanella Group and upper Molasse and, from seismic lines, the involvement of the Plio-Quaternary cover is evident (Fig. 2.11). In section E (Fig. 2.10 a) the projected Reana well finds the top Molasse at a depth of-260 masl, covered by an about 330 m thick conglomeratic unit and a 78 m thick gravel deposition. Conversely, about 5 km NW the

61 well testifies the presence of 40 m thick gravel deposition directly above the turbiditic units (encountered at about 140 masl). Therefore, the involvement of the Plio-Quaternary units suggests a recent tectonic activity for the Susans-Tricesimo Thrust. Recently, Moulin and Benedetti (2018) conducted a morphotectonic survey in the Tricesimo area and interpreted the 8-12 m high SSW facing scarp on the east and west banks of Soima stream like the result of the Tricesimo thrust activity (Morphotectonic Map).

At the hanging wall of ST two other high-to-middle angle thrust faults are present: Borgo Soima (BS) and Colle Villano-N (CV-N) Thrusts. They slightly displace the top of the carbonatic platform and can be traced up to the 0 masl. Particularly in section E (Fig. 2.10 a), BS propagates within a deep Plio-Quaternary palaeochannel, probably causing the deformation of the channel itself (Fig. 2.11 a). In section E a third reverse structure (Nimis Thrust, NI) was detected at the hanging wall of Colle Villano-N. The most internal structure detected is the Buia Thrust (BU), a low angle thrust fault which slightly displaces the top of the carbonatic platform. In section E (Fig. 2.10 a) BU is constrained at surface by the tectonic contact between Cavanella Group and Eocene turbidites cropping out near Tarcento (Zanferrari et al., 2013).
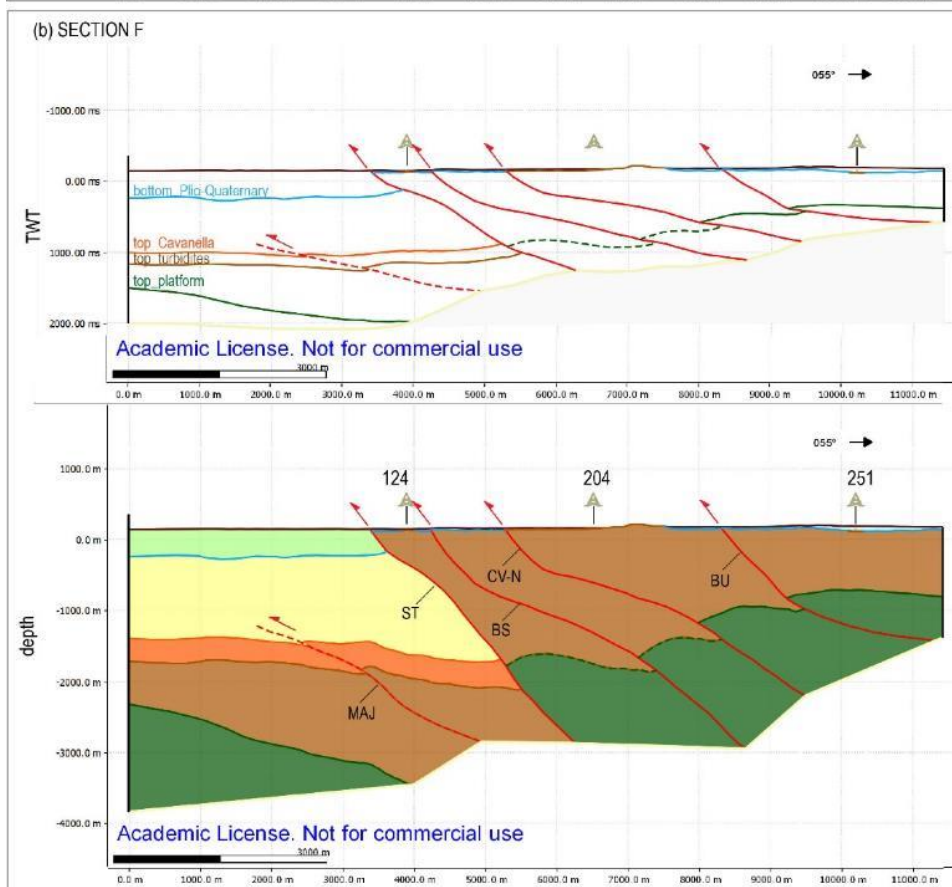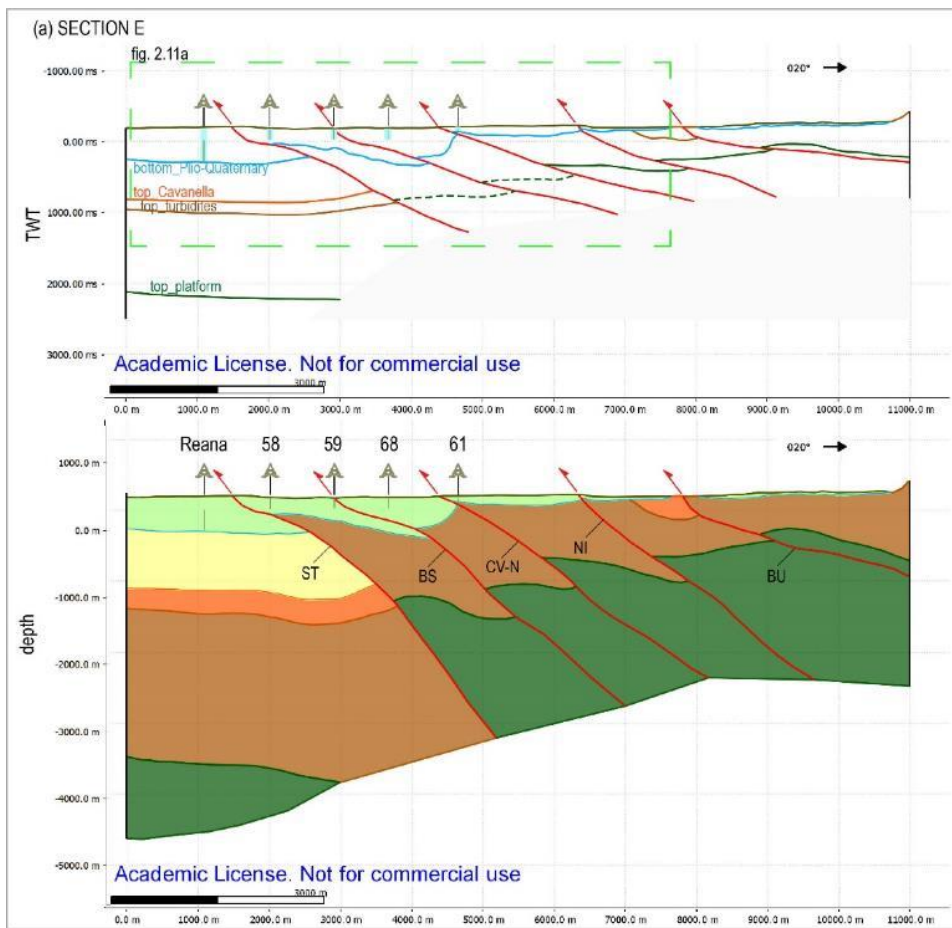
Fig.2.10 - Seismic interpretation of the main seismo-stratigraphic horizon and related geological cross sections E (a), F (b), G (c) and H (d) representing the buried setting of the High Friuli Plain. Section traces and acronyms are reported in Fig. 2.3.

Fig.2.10 - continued

(c) SECTION G

(d) SECTION H

LEGEND

- Plio-Quaternary deposits
- Molasse (middle-late Miocene)
- Cavanella Group (early-middle Miocene)
- Turbidite Units (late Paleocene-early Eocene)
- Carbonate Platforms (Jurassic-Cretaceous-Paleocene)
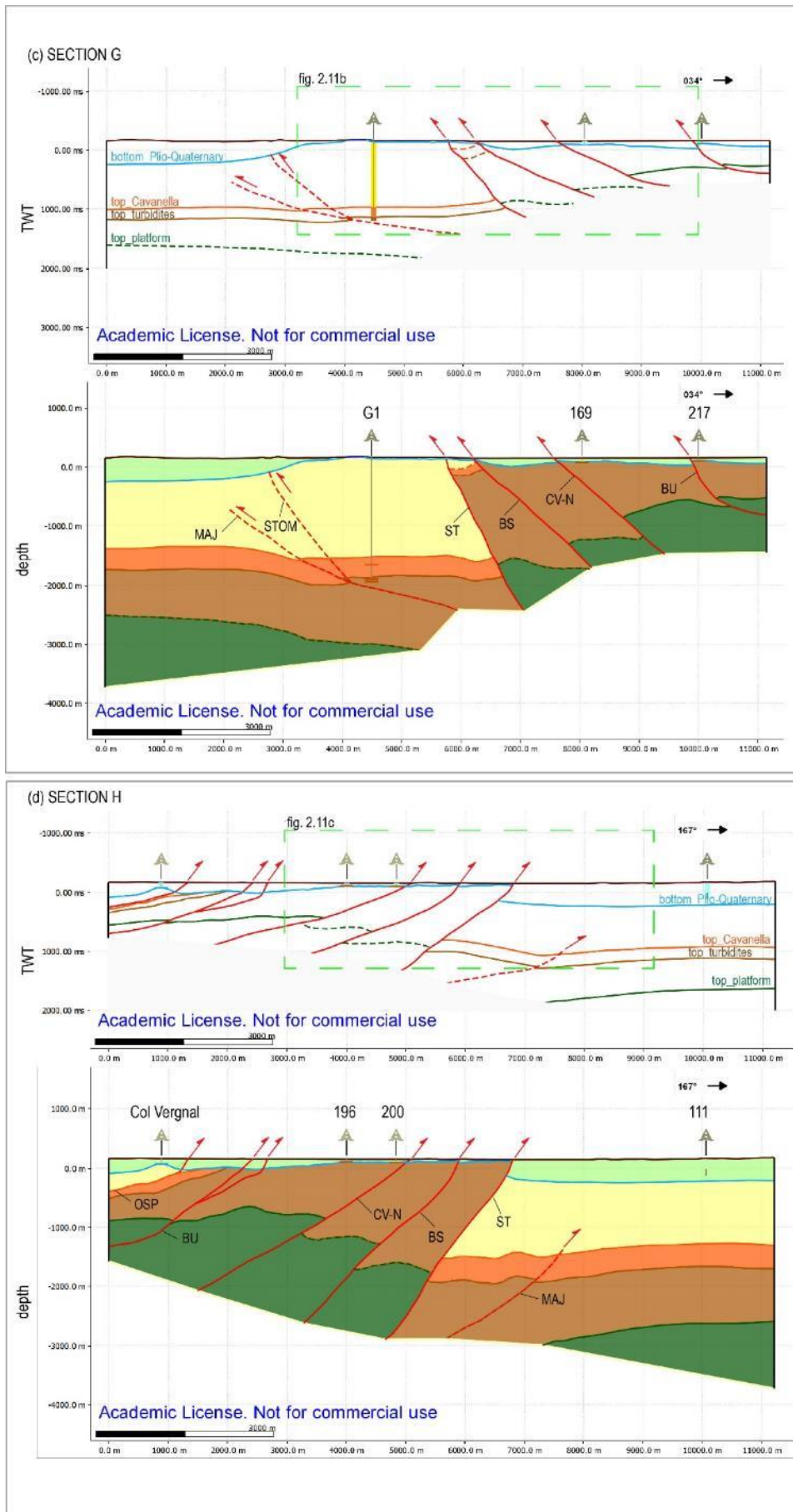
Fig. 2.11 - Clippings of seismic lines of sections E (a), G (b) and H (c) across Susans-Tricesimo Thrust System with a 3X vertical exaggeration of the z scale.

Legend:
- thrust fault (red)
- Messinian Unconformity (blue)
- top Cavanella Group (yellow)
- bottom Cavanella Group (orange)
- top carbonate platform (green)

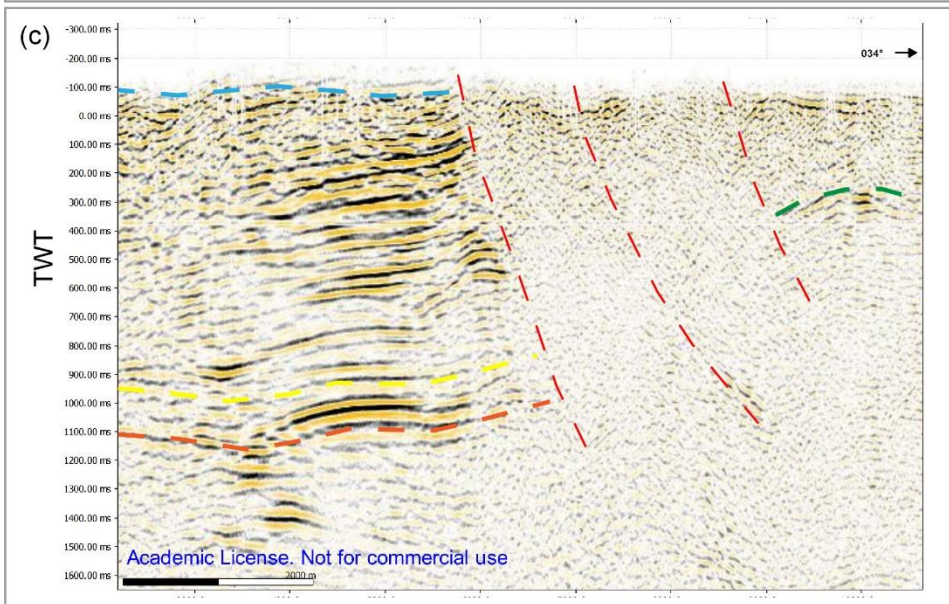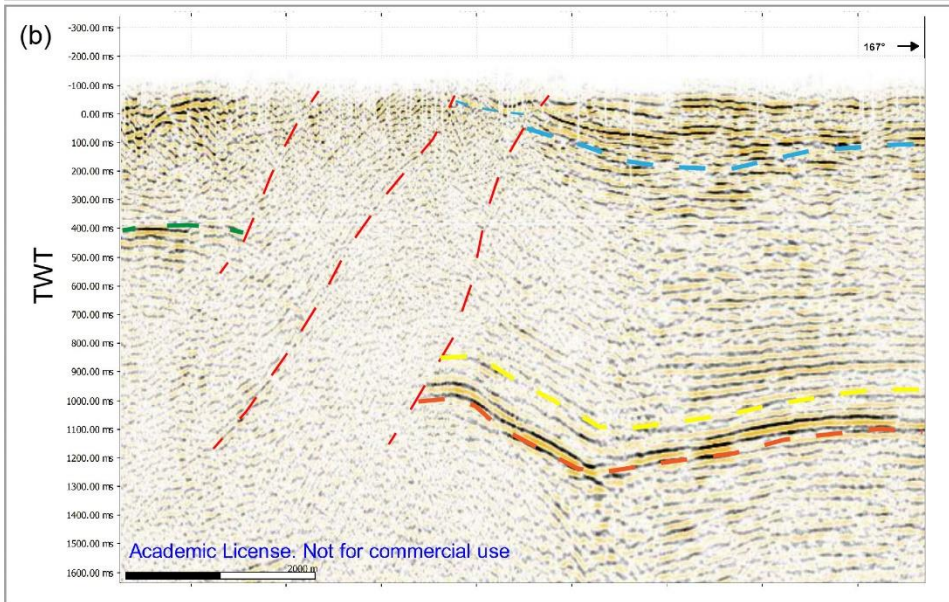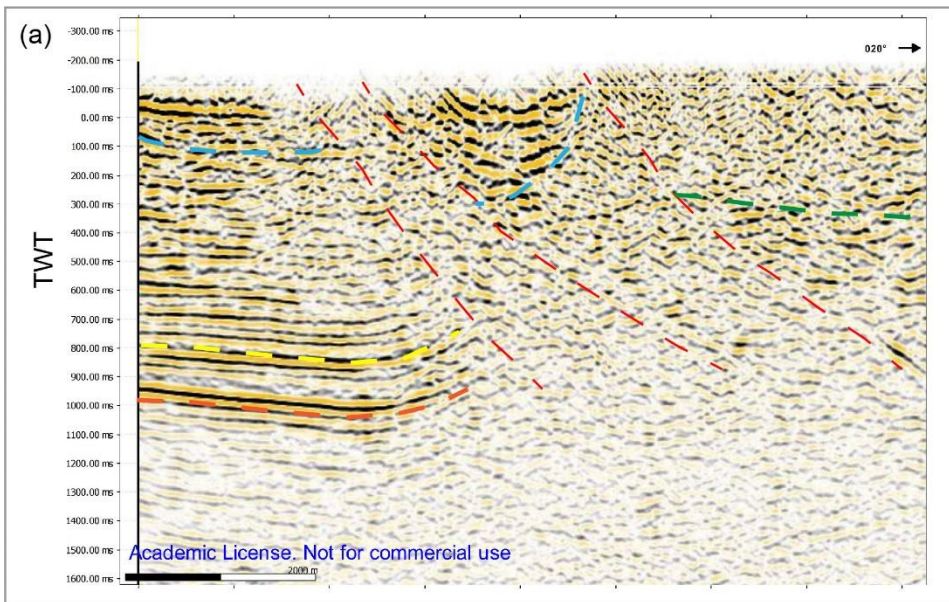In the most internal portion of the section H (Fig. 2.10 d) an additional low angle infra-Molasse reverse structure is present: the Osoppo thrust (OSP). This area is constrained by the close Col Vergnal relief and the homonymous geognostic well located about 250 m south. The relief is formed by Pliocene units (Osoppo conglomerates, Monegato, 2006; Monegato and Stefani, 2011; Monegato and Vezzoli, 2011; Zanferrari et al., 2013) on top of which the presence of LGM deposits (Spilimbergo Unit - SPB) is documented. Conversely, the Col Vergnal well stratigraphy is characterized by about 30 m Holocene deposits and 60 m LGM units, which lie on top of the upper Tortonian – lower Messinian sandstone-mudstone member of Montello conglomerate (MON2), at 83 masl (Zanferrari et al., 2013).

Following the elaboration of the geological cross sections, the 2D profiles were interpolated with the aim to reconstruct the 3D geometry of the main active fault systems of aastern Friuli (Fig. 2.12). It is worth noting that seismic lines allow to reconstruct the geometry of the tectonic structures only in their shallowest portion, deep up to 5 km depth.
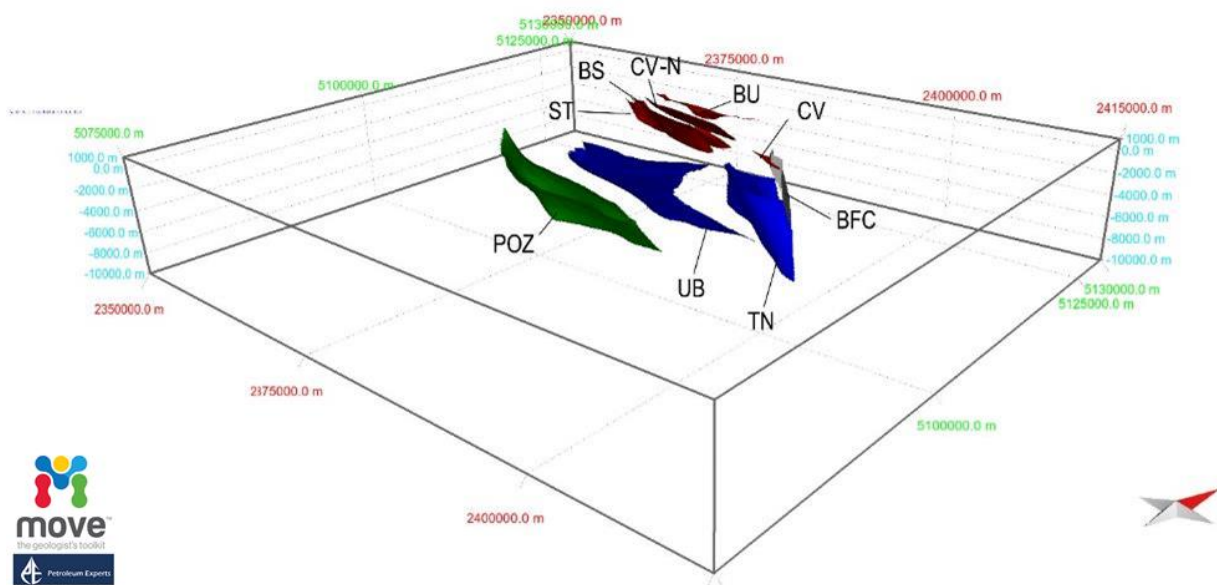

Fig.2.12 - Simplified 3D-model of the study area reconstructed through 3D Move Software thanks to ENI seismic lines interpretation. Green surface: Pozzuolo Thrust (POZ); blue surfaces: Udine Buttrio (UB) and Trnovo (TN) Thrusts, grey surfaces: Colle Villano – Borgo Faris – Cividale Fault System and red surfaces: Susans-Tricesimo (ST), Borgo Soima (BS) and Colle Villano (CV) Thrusts.

2.3 DISCUSSION

The elaborated 3D structural model well depicts the articulated tectonic setting of the four main fault-systems which characterize the study area.

The first active Thrust System is the Pozzuolo Thrust System (POTS). It represents an inherited medium to high angle SW-verging imbricate Dinaric structure, active since Paleogene and reactivated during the Neoalpine phase under a NNW-SSE compressive stress regime. The Pozzuolo 1 Thrust (POZ) represents the main structure of this thrust system (green surface in Fig. 2.12), which reveals a multiphase tectonic evolution. A kinematic variation from pure reverse to oblique can be hypothesized for POZ, during Dinaric (σ1 about NE-SW) and Neoalpine (σ1 about NNW-SSE) tectonic phases, respectively. In the present stress field, deformation is accommodated through a right-lateral transpressive motion on the NW-SE striking POTS. Differently, an almost pure dip-slip kinematics characterizes the Terenzano Thrust (TZ) under the present σ1, which probably represents a Paleogene (Dinaric) NE-SW striking lateral ramp, reactivated as a frontal one in the Neogene-Quaternary stress field. From industrial seismic lines and from geological and morphological evidence, both POZ and TZ Thrusts interest the Quaternary deposits. Particularly a Quaternary slip rate of 0.14 mm/yr and a minimum late Pleistocene rate of about 0.2 mm/yr have been estimated for the Pozzuolo Thrust. The slip rate values estimated for the different time intervals are summarized in Table 2.2.

The second active thrust system is the inner Trnovo Thrust System (TNTS, blue surfaces in Fig. 2.12). Within the Trnovo Thrust System, the Udine-Buttrio Thrust (UB) is the structure that shows the clearest evidence of Quaternary activity. A minimum Quaternary slip rate of 0.27mm/yr was calculated for the northern segment of UB (UB-N). If we restrict the time interval to the age of Canodusso subsynthem, the late Quaternary slip rate is of the order of 0.35 – 0.38 mm/yr (Tab. 2.2).

	Pozzuolo Thrust slip rate (mm/yr) (dip 65°)	Udine-Buttrio Thrust_NW slip rate (mm/yr) (dip 30°)	Udine-Buttrio Thrust_SE slip rate (mm/yr) (dip 30°)
Late LGM (Remanzacco subsynthem) (22.0 – 19.5 kyr cal BP, Fontana et al., 2014)	**0.20 - 0.23** Pozzuolo scarp (4 m)		
Late LGM (Canodusso subsynthem) (23–21 kyr cal BP, Monegato et al., 2007		**0.35 – 0.38** Pasian di Prato scarp (4 m)	
Quaternary (2,58 Myr)	**0.14**		**0.27**

Table 2.2 - Slip rate values estimated for Pozzuolo and Udine-Buttrio Thrusts, considering different late LGM and Quaternary time intervals (Patricelli and Poli, 2020).

The third active fault system is the Colle Villano – Borgo Faris Cividale (CV-BFC) transpressive Fault System (grey surfaces in Fig. 2.12), which develops at the hangingwall of TNTS. The pronounced morphotectonic evidence associated to CV-BFC testify its recent activity. As a matter of fact, it can be considered the westernmost dextral transpressive structure of the strike-slip domain of western Slovenia, presently affecting the elder reverse faults.

The fourth active thrust system is the Susans-Tricesimo Thrust System (STTS, red surfaces in Fig. 2.12). Regarding the fault's geometry, the reconstructed 3D structural model shows a medium-high angle deep geometry of ST, BS and CV-N. At the hanging-wall of CV-N, the Buia Thrust is present, which is characterized by a very low angle N-dipping plane and is responsible of Buia Eocene turbiditic outcrop (Zanferrari et al., 2013). Particularly, the elaborated sections well show the polyphasic evolution of the Susans-Tricesimo thrust. The displacement of the carbonate platform testifies the ST activity as thrust fault during the Dinaric phase and the displacement of the lower

and upper Molasse reveals that ST was involved even during the Neoalpine phase, probably with an oblique kinematics. Regarding the recent activity of ST, the deformation of the Plio-Quaternary succession clearly demonstrates that STTS presently accommodates deformation. Notably, ST, together with BS and CV-N, are interpreted as the surficial expression of a single masterfault (Galadini et al., 2005), responsible of the Eocene turbiditic outcrops at the NE Friuli plain border (Zanferrari et al., 2008a, 2013). According to Placer (2010), the Susans-Tricesimo and Trnovo Thrusts formed the same tectonic structure in the framework of the external Paleogene Dinaric front. However, starting from early Miocene, when σ1 turned to NNW-SSE, this Dinaric structure was segmented (Zanferrari et al., 2008a; Falcucci et al., 2018). Since then, STTS and TNTS underwent a different evolution. As a matter of fact, if comparing STTS and TNTS strike with respect to the Quaternary σ1, the Susans-Tricesimo Thrust System turns out to be more favorably oriented.

Regarding the faults activity rates, the late LGM to Present slip rates of Pozzuolo and Udine - Buttrio Thrusts (Tab. 2.2) are consistent with the slip rate calculated for the Arba Ragogna Thrust located in the eastern Carnian Prealps (about 0.2 mm/yr in Poli et al., 2009). Moving westward slip rates seem to be typically higher: the Polcenigo-Montereale Thrust-System (western Carnian Prealps) ranges from 0.2 and 0.5 mm/yr (Poli et al., 2015) and the Meduno Thrust reaches the 0.6 mm/yr (Monegato and Poli, 2015). This variation can be explained if considering the orientation of the tectonic structures with respect to the maximum compressional axis. In the western part of the eastern Southalpine Front (i.e. western Carnic Prealps), thrusts show a pure dip slip movement because they are WSW-ENE striking and sigma 1 is about NW-SE oriented (Bressan et al., 2018). In the eastern part, tectonic structures progressively reach a WNW-ESE/NW-SE striking but also sigma 1 rotates, reaching N-S direction in the central Friuli area (Slejko et al., 1999) and NNE-SSW direction in the Julian Prealps (Poli and Renner, 2004; Bressan et al., 2018). In the light of this, it is likely that on the NE-SW striking cross sections here studied, we record only the dip slip component of the

transpressive motion. In addition, the thrusts activity rates can be compared to GPS data. If assuming a constant deformation rate since Quaternary, the estimated slip rate values are well below the total 2 mm/yr velocities of Bechtold et al. (2009) and 1 mm/yr shortening of Serpelloni et al. (2016) and Cheloni et al. (2012). This gap confirms that the estimated rates represent only the dip-slip component of the faults, which act as transpressive structures, rather than purely reverse. Moreover, part of the accumulated deformation is absorbed by the NW-SE strike-slip structures that certainly interact with the transpressive/reverse structures (Poli and Zanferrari, 2018).

CHAPTER 3. SEISMICITY DISTRIBUTION

The distribution of seismic events registered by the Friuli Venezia Giulia Seismometric Network (http://www.crs.inogs.it/bollettino/RSFVG/RSFVG.en.html) shows that during the time interval 1978 – 2019 seismicity is mostly concentrated along the arcuate pre-alpine and alpine portion of eastern Southalpine Chain (Fig. 3.1). Towards the East, a cluster of events highlights the two recent sequences of 1998 and 2004, associated to the Raune fault (Kastelic et al., 2008). A clear reduction of seismicity characterizes the NW-SE elongated area located between the Southalpine domain and western Slovenia. Focusing on the southeastern portion of the Italian-Slovenian border, between Cividale del Friuli and Tolmin, most of the events are located at depth greater than 7 km, while only sparse shallower earthquakes are present.

Aiming at the study of the tectonic structures able to release strong earthquakes, the analysis of seismicity distribution was focused on the northern portion of the Friuli Plain (blue box in Fig. 3.1). As a matter of fact, at least two destructive earthquakes struck this area in the last 510 years (1511 and 1976). Through the analysis of 1978 – 2019-time interval seismicity, the seismogenic thickness of eastern Friuli was investigated and many aspects regarding the deep geometry and seismic behavior of the main tectonic structures emerged.
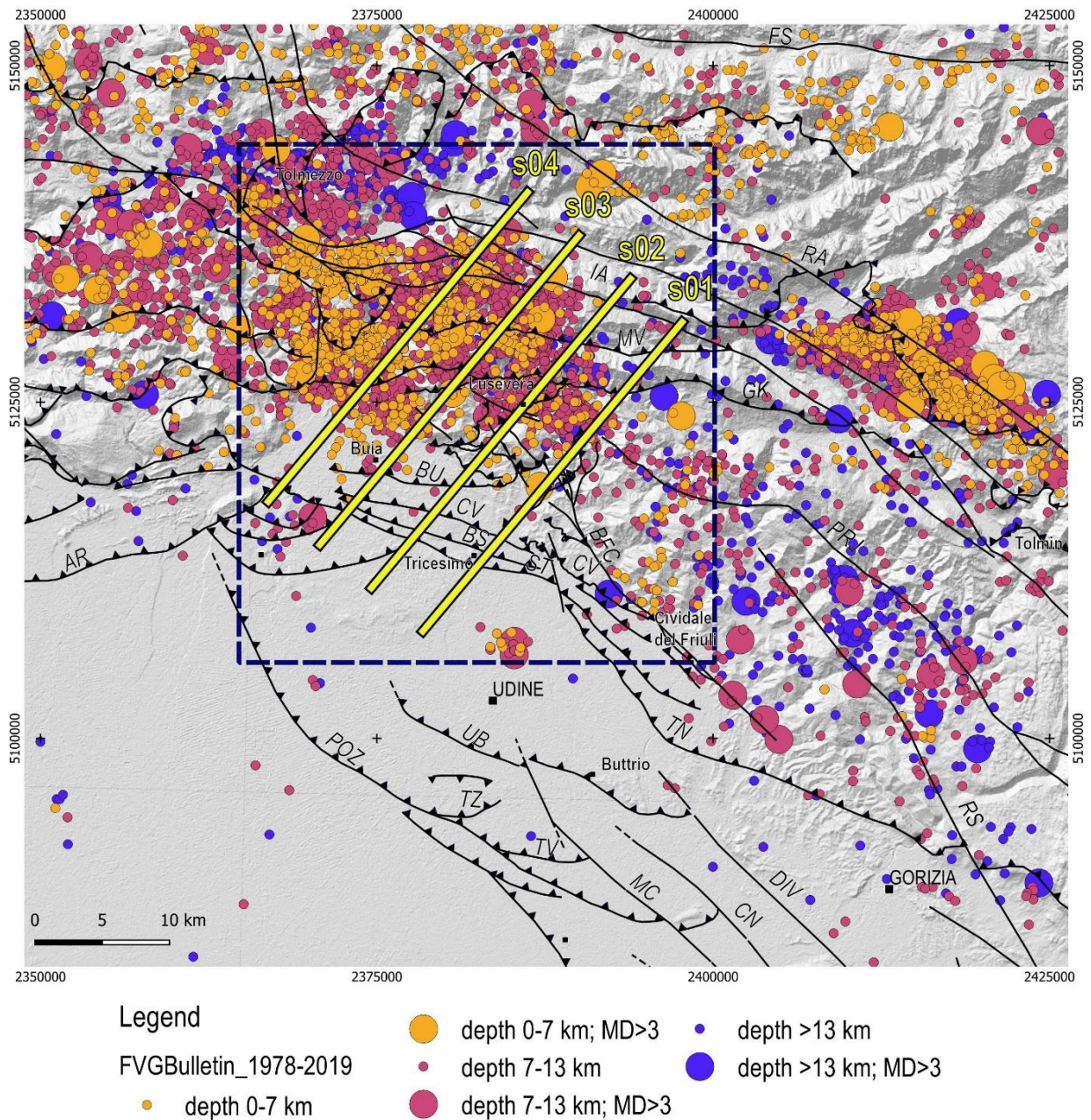
Fig. 3.1 – Seismicity distribution map of the eastern Friuli – western Slovenia. The events are extracted from http://www.crs.inogs.it/bollettino/RSFVG/RSFVG.en.html and classified per depth classes. Yellow lines: seriated section traces s01, s02, s03 an s04; blue dashed box: seismicity area of investigation.

3.1 METHODS

The seismogenic thickness of the studied area was reconstructed through the hypocentral distribution analysis of instrumental seismicity. At first, a seismological database was created by extracting all the events covering the time interval spanning from 1978 to 2019 of the study area,

registered by the CRS - OGS Seismometric Network and freely available on the Friuli Venezia Giulia Seismometric Network Bulletin (http://www.crs.inogs.it/bollettino/RSFVG/RSFVG.en.html). The database was filtered following three criteria (gap < 180°; vertical and horizontal error < 4 km and Md ≥ 1) and the 2726 collected events were classified based on depth and magnitude classes. Particularly, the 2D depth distribution was analyzed in terms of number of events per depth class. Moreover, the Md values were firstly converted in Ml through the Sitaram and Bora (2007) relation and then the corresponding energy value was calculated through the Richter (1958) formula, valid for Ml < 4.5 earthquakes. Differently, the Gutenberg and Richter (1956) relation for strong earthquakes was used for the only Ml 4.9 event. The total released energy per depth class distribution was then analyzed, differentiating by magnitude value.

The epicentral distribution of earthquakes was analyzed by plotting the events in map view. In detail, they were categorized in three depth classes (0-7 km; 7-13 km and > 13 km) and differentiated based on the magnitude value minor or major Md 3. Successively, the 3D earthquakes distribution was analyzed by plotting seismicity on the reconstructed fault surfaces. Four N40° trending seriated sections were elaborated with a length of 30 km, a spacing of 5 km and a projection distance of the events of 3 km. Following the recent focal mechanisms dataset revision performed by Saraò et al. (2021), 20 of the preferred solutions were extracted from the focal mechanism catalogue of earthquakes of southeastern Alps and surroundings area from 1928 to 2019 (https://essd.copernicus.org/preprints/essd-2020-369/; Saraò et al., 2021).

Regarding the 1976-77 seismicity, a distinct database was elaborated collecting the latest epicenter location of the mainshock elaborated by Slejko (2018) and the complete relocation of the sequence performed by Rebez et al. (2018). A recent update of the North-Eastern Italy Seismic Network catalogue was performed by Sandron et al., (2018), which revised and corrected magnitude estimation thanks to new linear empirical regressions between Ml and Md for eastern Southern

Alps. The magnitude values of 76-77 sequence events considered in this study were provided by A. Rebez by personal communication. As for the 1978-2019 events, the 1976-77 sequence depth and map distribution were analyzed. In this case, the time evolution of the sequence was analyzed too by grouping the events in three "*time classes*" (May-Aug. 1976; Sept.-Dec. 1976; Jan. – Dec. 1977).

3.2 RESULTS

3.2.1 1978-2019 SEISMICITY DISTRIBUTION

The collected and filtered 1978-2019-time interval seismicity contains 2726 earthquakes with Md values spanning from 1 to 4.9. The frequency-depth graph (Fig. 3.2 a), in terms of number of events per 1 km depth class, shows that the 90 % of earthquakes is located between 4 and 14 km depth. Moreover, an abrupt increase of seismicity is evident at 7 km depth. If considering the magnitude Md of the events, the total released energy per depth class graph (Fig. 3.2 b) shows that most of the energy is released between 6 and 16 km depth since only few Md > 3.5 are registered in the first 5 km. The depth distribution analysis of 1978-2019 seismicity testifies that the seismogenic thickness matches the first 14 km depth with a sharp increase of seismicity at depth exceeding 6 km, both in terms of number of events and in magnitude values.
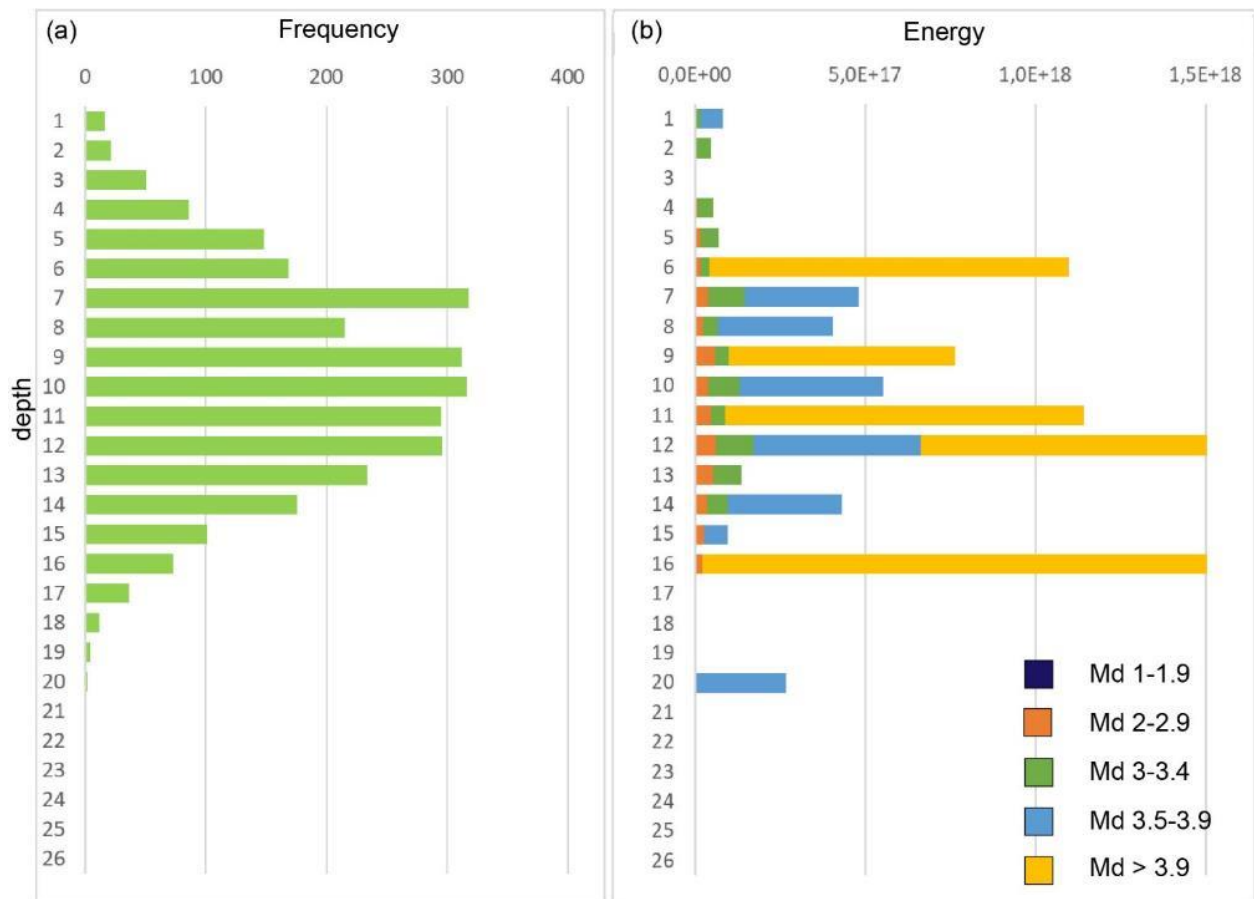
Fig. 3.2 - (a) Hypocentral frequency histograms of 1978-2019 seismicity in terms of number of events per depth class and (b) in terms of cumulated energy per depth classes differentiated per magnitude values. The collected events are located within the blue dashed box of Fig. 3.1.

In order to analyze the geometry of the seismogenic thickness, the collected events were classified in three macro-depth classes (0 – 7 km; 7 – 13 km and depth > 13 km) and the map distribution of each depth class was analyzed (Fig. 3.3).

Fig. 3.3 - Map distribution of 1978-2019 events. (a) earthquakes with depth > 13 km; (b) earthquakes with depth > 7 km; (c) earthquakes with depth > 0 km. Legend: orange circles = 0-7 km, purple circles = 7-13 km, blue circles = 7-13 km.
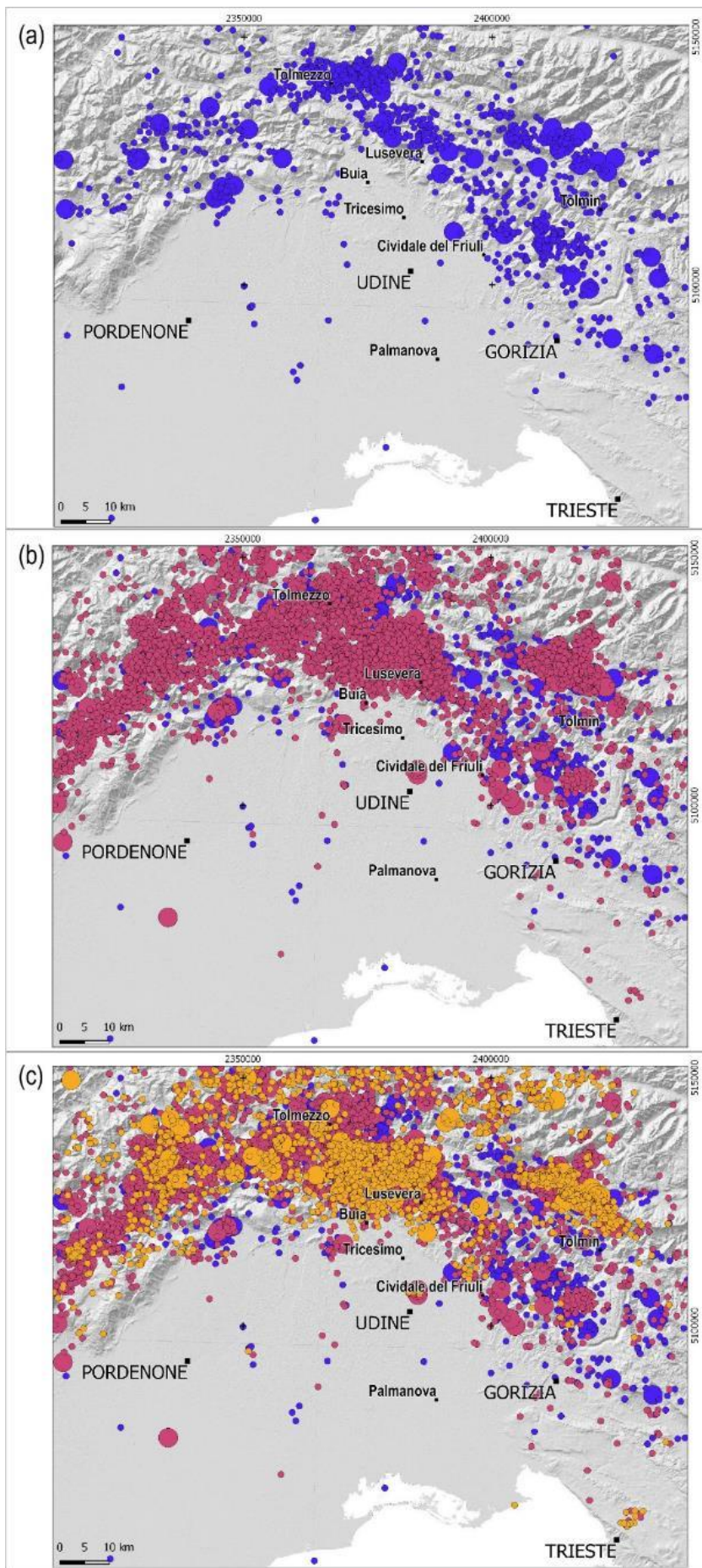
Starting from the deeper events, the map of Fig. 3.3a highlights the main structural elements, testifying that this area represents the junction zone between the western NE-SW trending front in the western Carnic Prealps and the NW-SE trending eastern front for the Julian Prealps and central Friuli area. Particularly, focusing on the study area, the events located at depth greater than 13 km (Fig. 3.3 a) depict a clear NW-SE alignment, from south of Tolmezzo to SE towards Cividale del Friuli. Moving up at shallower depth (Fig. 3.3 b), the earthquakes between 7 and 13 km depth affect a wider area, expanding south of the Tolmezzo – Cividale alignment. The southern border of 7 – 13 km seismicity is characterized by a WNW-ESE orientation in the central portion of the study area while SE of Tricesimo, seismicity is distributed along a NW-SE alignment matching the deeper (>13 km) seismicity distribution. Any major details can be added from the shallowest seismicity distribution analysis (0 - 7 km, Fig. 3.3 c), which is widely distributed. Regarding surficial seismicity, it is worth to remember that only the 17 % of earthquakes is located in the first 6 km depth with one event exceeding Md > 3.5. Anyhow, the three maps of Fig. 3.3 well highlight two active regions: the arcuate mostly compressive pre-alpine and alpine portion of Southalpine Chain and the strike-slip domain of western Slovenia, with a low-seismicity zone separating the two regions.

The seismicity distribution was analyzed with respect to the tectonic structures characterizing the study area through the elaboration of four NE-SW seriated sections (Fig. 3.1). The collected events were plotted together with the active faults of the area (Fig. 3.4), partly reconstructed in this study (Chapter 2) and partly extracted from the literature (Zanferrari et al., 2013). The strain pattern of the studied fault surfaces was investigated through the analysis of the available focal mechanisms (Saraò et al., 2021). Particularly, in order to better define the transpressive, rather than pure dip-slip character of the investigated faults, a special regard was dedicated to the events characterized by an oblique component (SS, SS-R and R-SS). All the analyzed events are identified with a number, listed in Table 1, and classified with different color based on their kinematics.
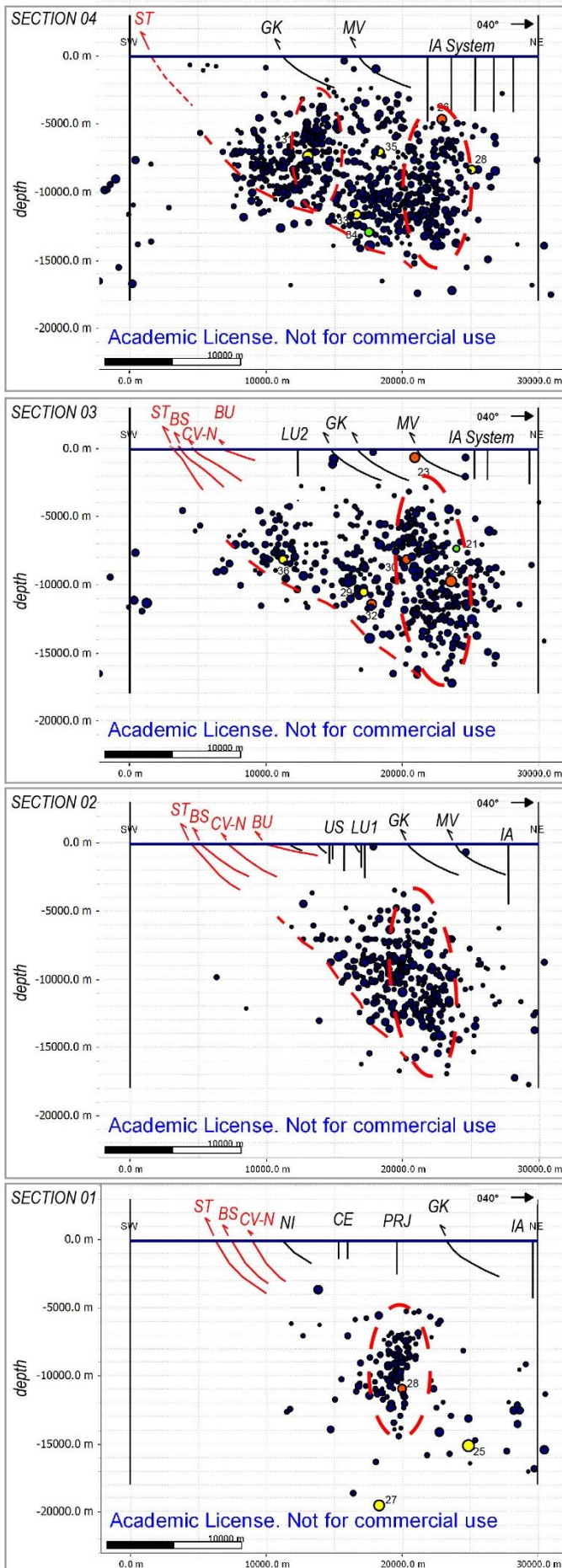
Fig. 3.4 - Seriated sections 01, 02, 03 and 04 (see Fig. 3.1 for section traces). The filtered 1978-2019 seismicity was plotted together with the active fault's surfaces reconstructed in this study (red thrusts) and tectonic structures known from the literature (black faults, Zanferrari et al., 2013). The symbols size is proportional to the magnitude value (Md), while the color refers to the kinematics as shown in the legend. Fault's acronyms: BS: Borgo Soima Th., BU: Buia Th., CE: Cergneu Ft., CV: Colle Villano Th., GK: Gemona-Kobarid Th., IA: Idrija-Ampezzo Fault System, LU1 – 2: Lusevera Unit Fts, MV: Musi-Verzegnis Th., NI: Nimis Th., PRJ: Predjama Ft.; ST: Susans-Tricesimo Th., US: Useunt Ft.

63

ID	DATE	TIME	M	DEPTH	REF	FT
1	06/05/1976	19:59	4.5	9.4	1	R
2	06/05/1976	20:00	6.4	7	1	R
3	07/05/1976	00:23	4.5	8.5	1	R
4	09/05/1976	00:53	5.3	11.6	1	R
5	11/05/1976	22:44	4.8	12.06	1	R
6	07/05/1976	11:15	3.3	11.69	1	R-SS
7	15/05/1976	16:50	2.8	10.25	1	SS
8	26/06/1976	11:13	4.3	5.95	1	R-SS
9	11/09/1976	16:31	5.1	8.9	1	R
10	11/09/1976	16:35	5.6	4.8	1	R
11	15/09/1976	03:15	5.8	7	1	R
12	15/09/1976	04:38	4.7	14	1	R
13	15/09/1976	09:21	6.1	12	1	R
14	15/09/1976	11:11	4.5	6.24	1	R
15	15/09/1976	20:34	3.5	5.42	1	R-SS
16	27/10/1976	04:25	3.1	5.13	1	R-SS
17	20/11/1976	00:01	2.7	5.83	1	R-SS
18	07/12/1976	03:37	3.4	7.39	1	R-SS
19	03/04/1977	03:18	4.5	12.23	1	R
20	24/08/1977	12:00	3.2	6.82	1	SS-R
21	02/04/1978	18:23	2.4	7.3	2	SS-R
22	03/04/1978	14:34	3.1	7	2	R
23	02/12/1978	04:05	3.5	0.6	2	R-SS
24	30/08/1981	23:30	3.9	9.7	2	R-SS
25	10/02/1983	22:30	4.2	15.1	2	R
26	20/12/1983	08:26	3.4	4.6	2	R-SS
27	05/10/1991	05:14	3.8	19.5	2	R
28	05/10/1991	14:56	3.1	10.9	2	R-SS
29	25/07/1995	11:53	3	8.1	2	R
30	22/12/1996	03:49	3.2	8.1	2	R-SS
31	09/12/1997	01:36	3.1	8.3	2	R
32	06/07/2002	08:30	3.5	11.4	2	R-SS
33	11/08/2006	01:35	3.1	11.6	2	R
34	23/03/2017	13:11	3.1	12.9	2	SS-R
35	09/05/2018	21:48	3.7	7.3	2	R
36	10/11/2018	07:59	3	10.5	2	R

Table 3.1. – Collection of analyzed focal mechanisms. The 1976-77 events location is from REF1 (Rebez et al., 2018), while the 1978-2019 earthquakes were extracted from REF2 (FVG Seismometric Network Bulletin). FT refers to the fault type classification by Alvarez Gomez (2019), as indicated in Saraò et al. (2021).

All the four sections of Fig. 3.4 show that seismicity affects the entire seismogenic thickness, with earthquakes located in the first 14 km depth. The events are confined to the north by the Idrija-Ampezzo (IA) structure: an anastomosed transpressive fault system of regional importance which has an almost N135° strike in western Slovenia and progressively assumes an almost WNW-ESE direction when entering the Italian territory (Zanferrari et al., 2013).

The southeasternmost section 01 (Fig. 3.4) shows that seismicity lies at depth between 5 and 15 km and a vertical grape shape cluster is evident at about 20 km NW from the section origin. This vertical alignment is located right in coincidence of the NW-ward continuation of the Predjama Fault (PRJ): a NW-SE trending steeply NE-dipping dextral strike-slip fault, which runs parallel to the Idrija fault towards the SW (Moulin et al., 2016; Poljak et al., 2000). The available focal mechanisms testify an oblique motion (R-SS) within the cluster (event 28), while reverse activity characterizes the deeper events (events 25 and 27). Moving northwestward seismicity of sections 02, 03 and 04 (Fig. 3.4) gets progressively sparser and the vertical structure detected in section 01 involves a progressively wider volume. Moreover, regarding the first 20 km length of the sections, the plotted earthquakes depict an about 40° NE dipping plane which well correlates with the Susans-Tricesimo Thrust System (STTS) reconstructed in this study. Fault plane solutions show an oblique (R-SS) kinematics based on the events 30 and 24, while a pure dip-slip motion (R) characterizes the frontal lower structure (events 36 and 29). However, it is worth noting that within the seismogenic volume some deep subvertical alignments can be recognized. Particularly, in S 02 and S 03 the subvertical cluster of events at around 20-22 km NW from the section origin is slightly still detectable and the event 21 confirms a transpressive kinematics (SS-R). Section 04 is dominated by a pure compressive seismicity (events 28, 31, 33 and 35). A subvertical cluster can be traced in coincidence of the Pioverno Fault, which represents the southern branch of the Idrija-Ampezzo Fault System (Zanferrari et al., 2013). Notably, the distribution of earthquakes does not highlight the activity of the Gemona-Kobarid structure.

3.2.2 1976-77 SEQUENCE SEISMICITY DISTRIBUTION

With the aim to make some attempts regarding the investigated tectonic structures as possible sources of the 1976-1977 earthquakes, the distribution of the events relocalized by Rebez et al. (2018) was analyzed (Fig. 3.5). Particularly, in order to investigate the spatial evolution of the sequence in time, the collected events were classified in 3 different "*time classes*": May-August 1976, September-December 1976 and January-December 1977. This aspect is also useful to explore the possibility that the sequence ruptured one single structure or whether many different sources activated.

The maps of Fig 3.5 clearly highlight the northwestward migration of the sequence, as already remarked by many Authors (Colautti et al., 1976; Finetti et al., 1976; Cagnetti and Console, 1977; Wittlinger et al., 1978; Slejko 2018). The depth frequency histogram for each of the three "*time classes*" show that most of seismicity occurred during the first year and particularly, that Sept-Dec 76 seismicity affected shallower depths with respect to the May-Aug 76 events. Moreover, the comparison between the two 1976-time classes shows that the mainshock of May-Aug 76 (Mw 6.4) is located at 7 km depth, which is the most active depth class. Conversely, during Sept-Dec 76 the most active thickness lies between 5 and 9 km depth, but the strongest event of September (Mw 6.1) occurred at greater depth (12.2 km).
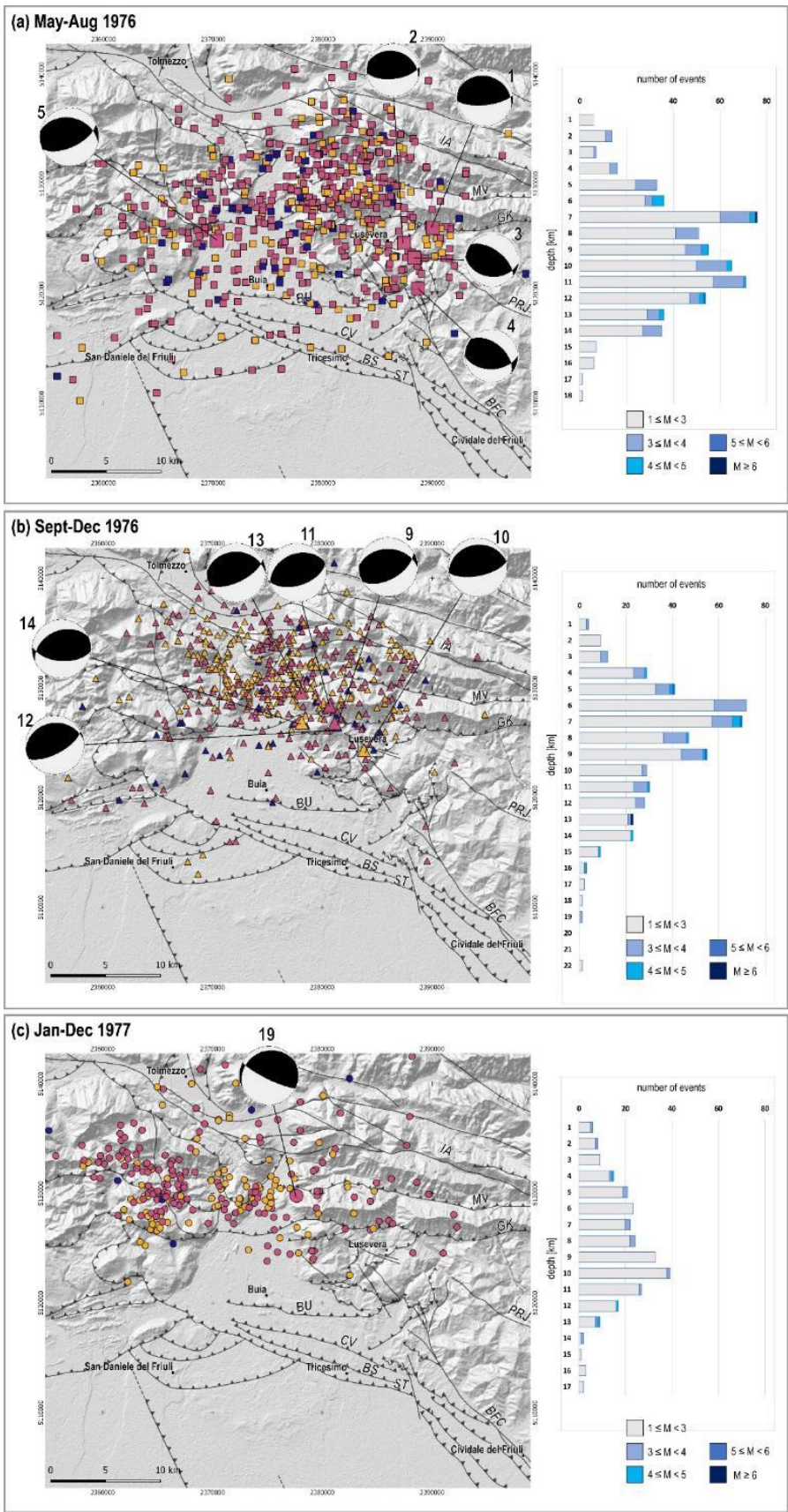
Fig. 3.5 - 1976-77 time classes map and depth distribution (locations from Rebez et al., 2018) with respect to the tectonic structures. (a) of May-August 1976 events; (b) September-December 1976 events; (c) 1977 events. The number of the events refers to Table 4.1, focal mechanisms are from Saraò et al. (2021).

In order to make some attempts regarding possible associations earthquake-structure, the distribution of 1976-77 sequence was analyzed with respect to the tectonic structures of the area. The 1976-1977 sequence events, classified per "*time classes*", were plotted on the seriated sections (Fig, 3.6, see traces in Fig. 3.1).
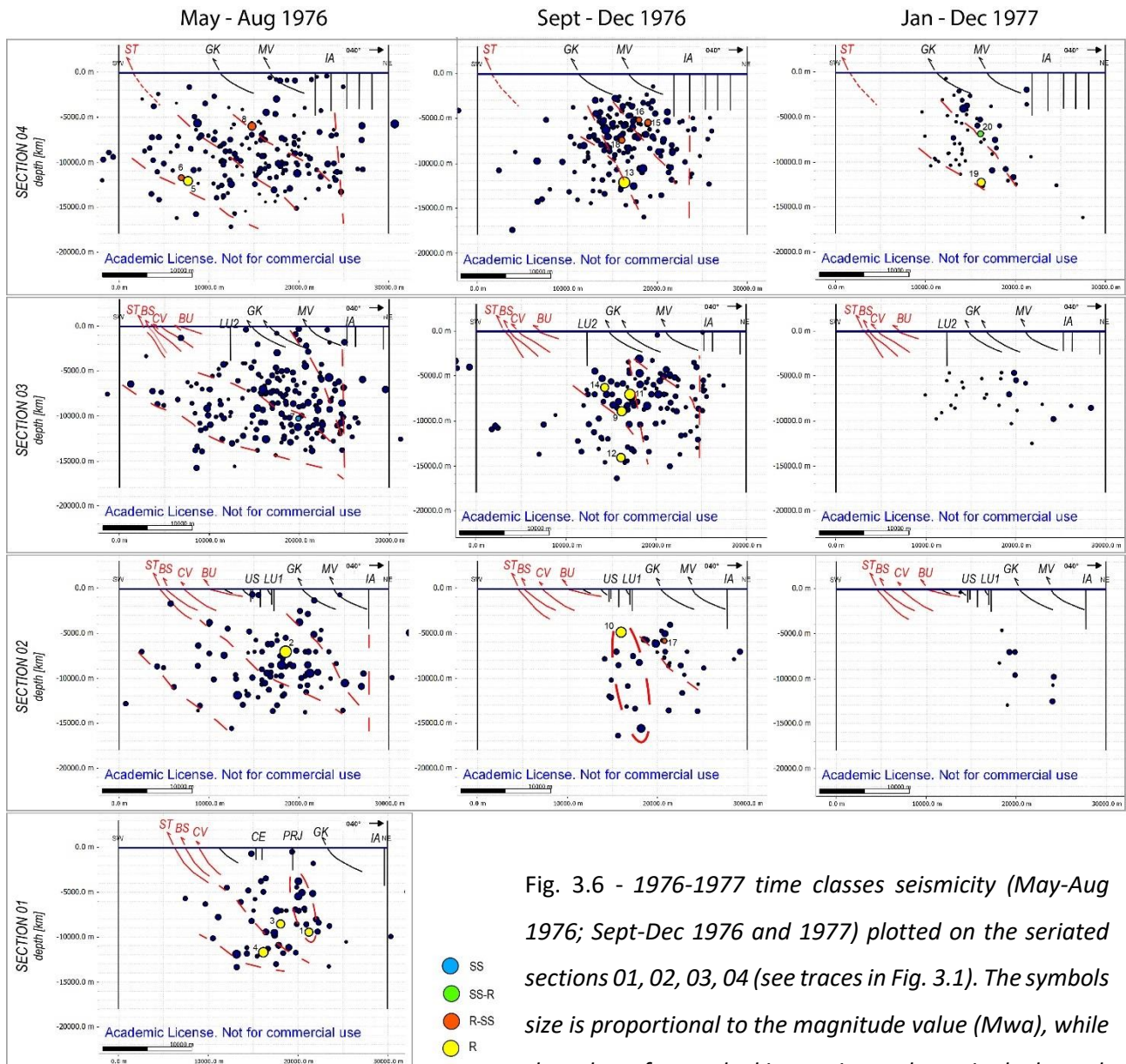

Fig. 3.6 - *1976-1977 time classes seismicity (May-Aug 1976; Sept-Dec 1976 and 1977) plotted on the seriated sections 01, 02, 03, 04 (see traces in Fig. 3.1). The symbols size is proportional to the magnitude value (Mwa), while the color refers to the kinematics as shown in the legend. Fault's acronyms: BS: Borgo Soima Th., BU: Buia Th., CE: Cergneu Ft., CV: Colle Villano Th., GK: Gemona-Kobarid Th., IA: Idrija-Ampezzo Fault System, LU1 − 2: Lusevera Unit Fts, MV: Musi-Verzegnis Th., NI: Nimis Th., PRJ: Predjama Ft.; ST: Susans-Tricesimo Th., US: Useunt Ft.*

The focal mechanisms of the strongest events, together with the oblique kinematics events were extracted from Saraò et al. (2021), as for the 1978-2019 time interval analysis.

Focusing on the strongest earthquakes, the preferred focal mechanism solutions (Saraò et al., 2021) reveal that both the NW-ward migration of the sequence with time, and a NW-ward variation of the activated faults geometry.

The 76-77 seismicity plotted on the seriated sections reveals a diffuse distribution, affecting the whole seismogenic thickness.

Focusing on May-Aug 1976 time interval, seismicity is confined between the frontal medium angle plane, well referable to the frontal Susans-Tricesimo Thrust System (STTS), while the innermost Idrija-Ampezzo fault system (IA) acts as a backstop. Regarding the strongest events (M >4.5) located in the SE portion of the area (Fig. 3.5 a), their focal mechanisms reveal the activation of both NW-SE and WNW-ESE oriented reverse structures with only minimum horizontal component (Saraò et al., 2021), matching the frontal Susans-Tricesimo Thrust System (sections 01 and 02, Fig. 3.6). Anyway, over the activation of the frontal reverse structures, the involvement of different additional structures can be assessed. Particularly, from sections 01 (Fig. 3.6) a vertical alignment is recognizable in the first 10 km depth, right in coincidence of the Predjama Fault (PRJ). In addition, moving to the NW-most sector, the hypocentral distribution of section 04 (Fig. 3.6) allows to assess the activation of three distinct planes characterized by medium-to low angle geometry. In detail, the NE-dipping intermediate plane well matches the deep geometry of the Susans-Tricesimo Thrust System, but the activation of an additional deeper structure is testified by the frontal plane seismicity, as suggested by Galadini et al., (2005).

Conversely, focusing on the second part of the sequence (September 1976-1977), most of seismicity is located NW-ward of the May-Aug 1976 area (Fig. 3.5 b and c). Particularly, the seismicity of

sections 03 and 04 (Fig. 3.6) is mostly located on planes consistent with high-angle geometries (about 60° dip). Moreover, the involvement of the Idrija-Ampezzo Fault-System (IA) and Gemona Kobarid Thrust (GK) can be assessed from seismicity distribution of section 03 and 04 (Fig. 3.6).

3.3 DISCUSSIONS

The hypocentral distribution analysis of the study area shows that the High Friuli Plain seismogenic volume extends deep up to 14 km and gets wider towards the NW.

In the study area, a few 40° dipping planes can be detected, well reliable to the frontal STTS. Moving towards the NW, the involvement of high-angle structure is more evident, both in the 1976-1977 and in the 1978-2019 seismic distribution. Particularly, regarding the post-77 seismicity, at about 12 km depth, the medium-to-high angle planes merge a subvertical structure which likely represents the NW-ward propagation of the dextral strike-slip fault-system of western Slovenia – eastern Friuli region. Even though located on the northwestern continuation of the Predjama Fault (PRJ), the detected subvertical structure could alternatively represents the right step of the Borgo Faris – Cividale Fault (BFC) or the NW segment of the Raša eastern strand. Since the scarce constraining don't allow a unique interpretation, the subvertical structure will be referred to as Vedronza Fault (VDR). It is likely that VDR propagates NW-ward up to section 03 between Gemona and Lusevera since a subvertical structure is still slightly recognizable moving towards the NW. In this area, seismicity clearly highlights the 40° dipping geometry of the frontal reverse structures. Based on the hypocentral distribution, the interaction at depth of STTS with the Vedronza Fault can be assessed at 13 km depth.

Focusing on the 1976-77 sequence, despite the wider seismicity distribution, the same structural setting is recognizable on the seriated sections. In this regard, it is worth to remark the crucial

improvement of the data acquisition thanks to the enlargement of the Seismometric Network coverage right subsequently to the May 1976 (Slejko et al., 2018). Therefore, over the structural complexity characterizing the area affected by the sequence, it is likely that the different reliability of the compared hypocentral distributions makes the interpretation more challenging. Despite this, many interesting aspects arise from the comparison between the May-August 1976 time interval and the second part of the sequence, regarding the evolution in time of 76-77 seismicity. Based on the hypocentral distribution analysis and faults plane geometry, most of the events of May-August 1976 are consistent with the activation of medium-to-low angle plane structure, well referable to the frontal Susans-Tricesimo Thrust System (STTS). It is worth to note that the focal mechanism solutions of 1976 strongest events show the activation of a very low angle plane (about 10°), in contrast with the 40° dipping planes identified in this study. The involvement of high-angle reverse structures during the 76 sequence was already suggested by Peruzza et al. (2002). Moreover, the activation of an additional distinct deeper plane can be assessed, likely matching the deep ramp of the frontal Palmanova Thrust System (PA), as proposed by Galadini et al. (2005), here referred to as Pozzuolo Thrust System. Conversely, the second part of the sequence (September 1976 – 1977) reveals the activation of high-angle plane structures (60° dip) located in the inner portion, at the hanging wall of the frontal reverse ST System. In regard of this, it is worth noting that differently from the first part of the sequence, the September 1976-77 seismicity seems to involve even the Idrija-Ampezzo Fault System (IA) and the Gemon a Kobarid Thrust (GK).

In addition, the activation of the Buia Thrust during the strongest earthquakes seems unlikely. As a matter of fact, the Buia Thrust is characterized by a very low angle geometry (10-20°) in the first 5 km depth. If excluding the chance of an abrupt verticalization of the Buia Thrust plane, the hypothesis of its activation as source of one of the mainshocks can be ruled out. Nevertheless, the possible involvement of BU as secondary structures seems more likely.

In the light of this, we can assess that spanning from the inner to the frontal sector the seismically released slip appears to be transferred from high angle structures to low-to-medium angle thrust faults. Particularly in the southeastern portion, the N130° trending high-angle structures result to be well oriented to the almost N-S sigma1, and probably release deformation through a transpressive motion. Moving NW-ward, the progressive rotation of faults strike (N100°) makes them almost orthogonally oriented with respect to the maximum compressional axis. In this case, despite the high obliquity value (i.e. angle between initial plate motion and the azimuth of the fault) and under the same fault strike, reverse faults are proven to be more efficient to accommodate the motion rather than subvertical structures, because of their lower dip angle (Vallage et al., 2014). Therefore, under the present almost N-S oriented sigma1, the motion of subvertical E-W striking planes is impeded while the frontal thrust planes, characterized by almost the same orientation and lower dip, are the favorably oriented structures for slipping. Seismicity distribution well confirms this pattern, highlighting that moving from the SE to the NW the subvertical inner structure detected in section 01 (VDR) is progressively less evident, and the sparser cloud of events can be mainly associated to the reverse structures. The analysis of the focal mechanisms clearly testifies the gradual transition from an oblique to a reverse kinematics spanning from the inner to the frontal sectors of the investigated area. However, the depicted setting well highlights the interaction at depth between the frontal WNW-ESE oriented reverse structures and the inner NW-SE trending strike-slip faults. Therefore, the possibility that reverse and strike-slip faults merge at depth forming a single major structure must be taken into account.

CHAPTER 4: MORPHOTECTONICS

4.1 METHODS

In order to further investigate the recent activity of the Quaternary fault systems of the eastern Friuli Plain, a morphotectonic survey was carried out. The analysis and interpretation of remote sensing data was aimed at the detection of surficial anomalies possibly related to the tectonic activity. The Digital Elevation Model of the whole regional territory are freely available on the Regional infrastructure of Environmental and Territorial Data (IRDAT) of the Regione Autonoma Friuli Venezia Giulia website (http://irdat.regione.fvg.it/CTRN/ricerca-cartografia/) in ARC/INFO ASCII GRID format in the original Projected Coordinate System Gauss Boaga Est. The 1 m DTM are derived from the 2006-2010 Lidar survey realized with a 4 m density points per square metre by the Protezione Civile FVG for institutional activities. Ortophotos, acquired simultaneously with the LIDAR survey, and hillshade models in *.tif format are also available on the regional website. The data, covering the study area, were processed in GIS ambient (QGIS 2.18 version). In detail, the microrelief of the area was realized through the extraction of the 1 m contour lines from the 1 m DTM grid files. In addition, from the digital elevation model the drainage network of the area was reconstructed in SAGA GIS. After the first fill sink step, the Flow Accumulation was performed with the aim to investigate the order of magnitude of the water volumes of the area. This input value is required in the successive River Channel processing step. Because of the detailed work scale, and since the minor water streams are more sensitive to deformation, an initiation threshold of 1000 was set.

Following the data processing, the mapping of the geomorphological features was performed in order to detect surficial anomalies, possibly related to the activity of the investigated tectonic structures. Particularly, the continuity of linear structures such as scarps, water streams, ridges was

analyzed, together with the identification of other topographic anomalies like suspended valleys, wreck surfaces, bulges and counter slopes. Successively, the field survey allowed to validate the detected surficial anomalies and to collect new structural and morphotectonic data. Many other considerations derive from the realization of detailed geologic profiles, where the collected field survey data were correlated with subsurface data extracted from geognostic well stratigraphies.

4.2 RESULTS

Following the morphostructural analysis, the newly collected surficial anomalies likely related to the tectonic activity were merged with the morphotectonic evidence available from the literature (see the attached Morphotectonic Map). A crop of the morphotectonic map focusing on the newly detected morphotectonic hints along the Julian prealpine border are presented in Fig. 4.1. On the map, grey symbology refers to bibliographic data while red color was used for the newly detected morphostructural elements. As shown in the legend, the collected surficial linear data mainly deals with anomalous traits of the drainage networks, morphological scarps, and saddle alignments, while areal data include counterslopes, upwarped surfaces, isolated pre-LGM relieves and pre-LGM units outcrops, suspended glacis. The buried scarps detected thanks to the reconstructed Quaternary surface were also mapped (see Chapter 2). The numbered black hammer symbology refers to field stops, commented on the following sections from the NW to the SE and divided into four investigation sites: Montegnacco, Qualso-Savorgnano del Torre, Campeglio and Cividale del Friuli. In Montegnacco and Qualso-Savorgnano sites the CV-N reverse structure was investigated, while in Campeglio and Cividale del Friuli sites the CV-BFC transpressive structure was analyzed.
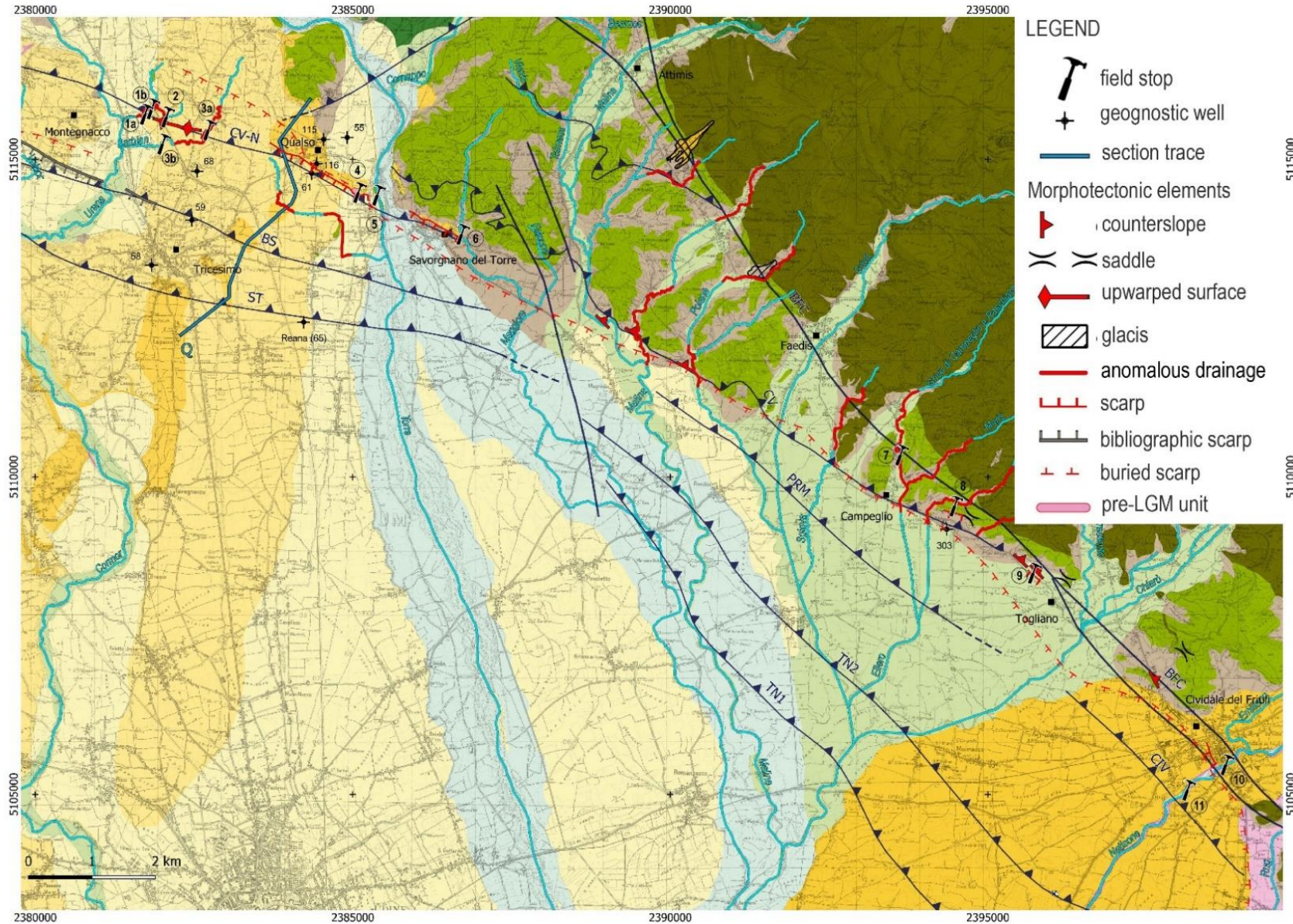
Fig. 4.1 – Crop of the morphotectonic map, representing the morphostructural elements collected during the morphotectonic survey along the Julian prealpine border. Red colour: data collected in this study; grey symbols: bibliographic data. The geological base cartography from the "049-Gemona del Friuli" and "066-Udine" sheets of the Geological Map of Italy (Zanferrari et al., 2008a and 2013), the "067-Cividale del Friuli" and "088-Gorizia) sheets of the Geo-CGT Project (GEO-CGT; 2008) and the Map of the geological units of the Friuli Venezia Giulia Plain (Fontana et al., 2019).

4.2.1. MONTEGNACCO SITE

The DTM analysis of the Montegnacco area (Fig. 4.2) allowed to detect, between Montegnacco locality and Tricesimo village, a gentle WNW-ESE elongated upwarping of the topographic surface. Moreover, in this area the Borgo Soima and Barbian streams flow in a NNE-SSW direction, but addressing the topographic bulge, they abruptly change in direction and assume an about E-W orientation until merging the Urana-Soima river (Fig. 4.2).

Along the Borgo Soima riverbed, folded and fractured (155/60) SVO turbiditic unit outcrops (field stop n°1a, Figs. 4.1 and 4.2). On top of this unit S-dipping tilted pre-LGM conglomerates are present and both units are truncated by an erosional surface which represents the basal surface of unconsolidated (LGM?) gravels (Fig. 4.3 a). Moreover, 60 m upstream (field stop n°1b, Figs. 4.1 and 4.2), where the stream bends about 90° towards the West, the N-dipping Eocene Savorgnano Marls and Sandstones (SVO) unit (S0: 330/30) is interested by a shear zone (Fig. 4.3 b) with a fault plane (040/50) displacing a second subvertical N110° striking plane.

In addition, even the ENE-WSW flowing incision, presently representing a dextral tributary of the Borgo Soima channel, abruptly turns towards the West when addressing the bulging area (field stop n°2, Figs. 4.1 and 4.2). The ENE-WSW flowing trait of the water stream is characterized by a stagnating meandering riverbed and in the proximity of the 90° angle deflection, the buried lodgment till crops out in the riverbed (Fig. 4.4), in correspondence of the bulging surface.
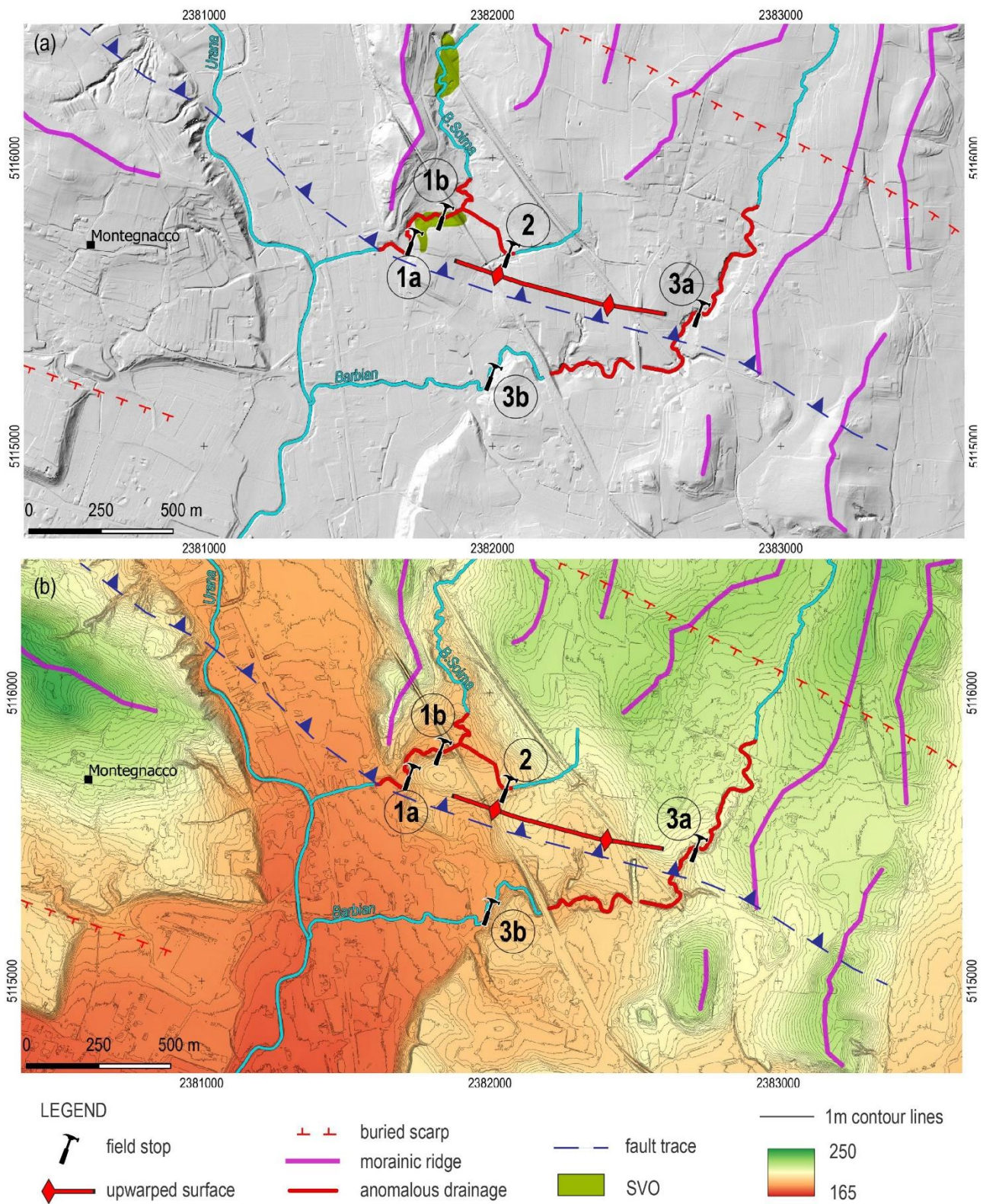
Fig. 4.2 - Morphotectonic elements mapped in the Montegnacco site (a) on the 1 m – hillshade and (b) on the 1 m dtm with 1 m contour lines showing the detailed topography of the area.

Fig. 4.3 – Outcrops of field stop n°1a (a) and n°1b (b) (see location Figs. 4.1 and 4.2). The stereographic plots show attitude observed in the Eocene turbiditic unit.

Fig. 4.4 – Outcropping lodgment till in coincidence of the 90° bend of the water stream located between the Borgo Soima and Barbian streams (see Figs. 4.1 and 4.2 for the location).

In the Barbian riverbed (field stop n°3a, Figs. 4.1 and 4.2), no pre-Quaternary bedrock outcrops, but the water stream erodes a thick glacial unit (lodgment till) of the Canodusso Subsynthem (Zanferrari et al., 2008a). Particularly, in the Barbian riverbed a subvertical plane (050/60) separates the lodgment till from a well stratified sandy unit, possibly representing a glacial contact deposit (Fig. 4.5 a). However, the discontinuity is marked by the presence of sub vertically aligned clasts (Fig. 4.5 b). Right above this outcrop, the field on the right bank of the river, North of the railway, is characterized by an upwarped surficial shape, where the Fraelacco trench was dug (Chapter 5).
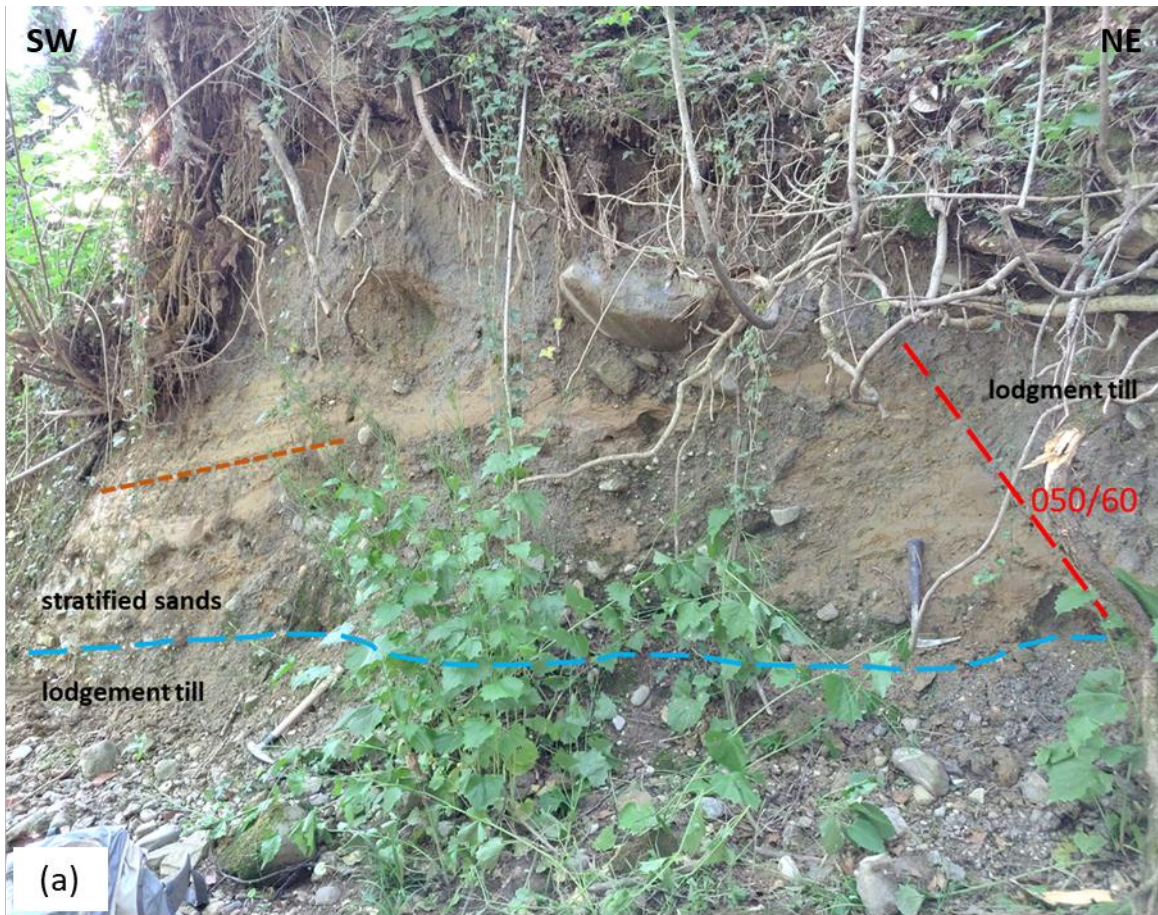
(a)

(b)

Fig. 4.5 – Outcrop of field stop n°3a (a) (see Figs. 4.1 and 4.2 for the location) and a detail of the high-angle plane (b). Note the presence of iso-oriented clasts parallel to the high-angle contact.

About 750 m downstream, always in the Barbian riverbed, the outcropping light blue grey lodgment till is characterized by the presence of subvertical features (Fig. 4.6 a). The filling material is composed of brow-yellowish deposits, with a slightly coarser particle size with respect to the silty-clayey lodgment till (Fig. 4.6 b). Upwards, the glacial unit is overlaid by the LGM alluvial gravelly unit.
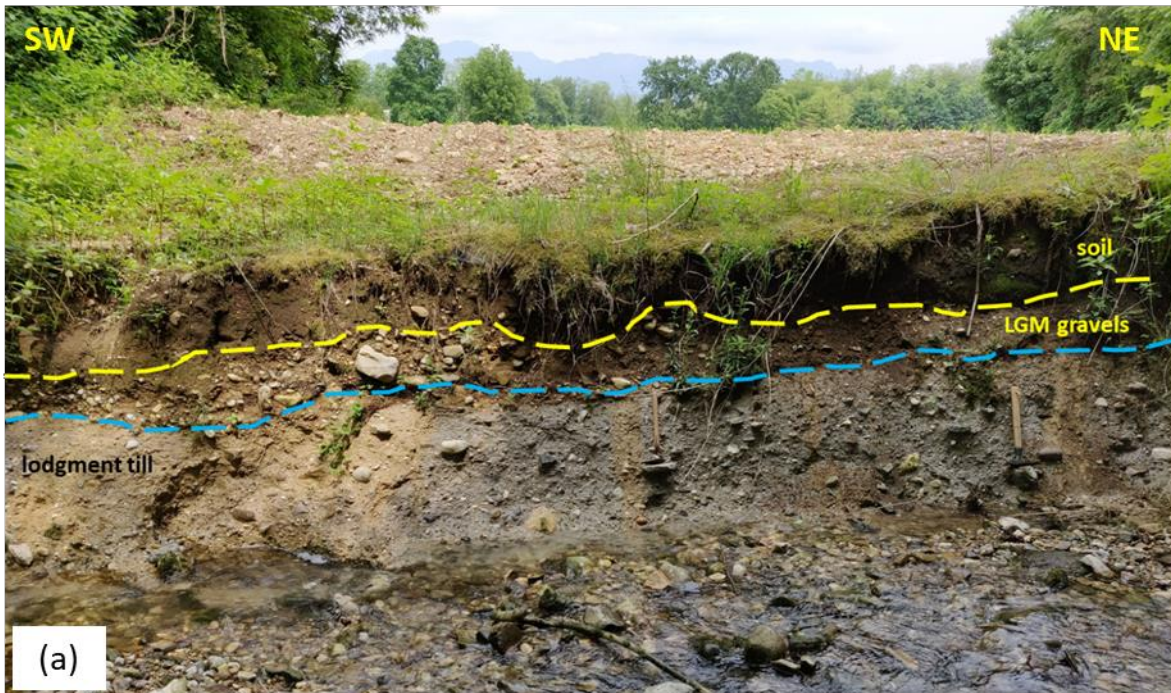

(a)

(b)

Fig. 4.6 - (a) Outcrop of the lodgment till in the Barbian riverbed (field stop n° 3b, Figs. 4.1 and 4.2) affected by subvertical features. (b) Detail of the brown-yellowish veins within the glacial unit.

4.2.2. QUALSO – SAVORGNANO DEL TORRE SITE

Moving Southeast, a sharp NW-SE oriented scarp borders towards the SW both the Qualso relief
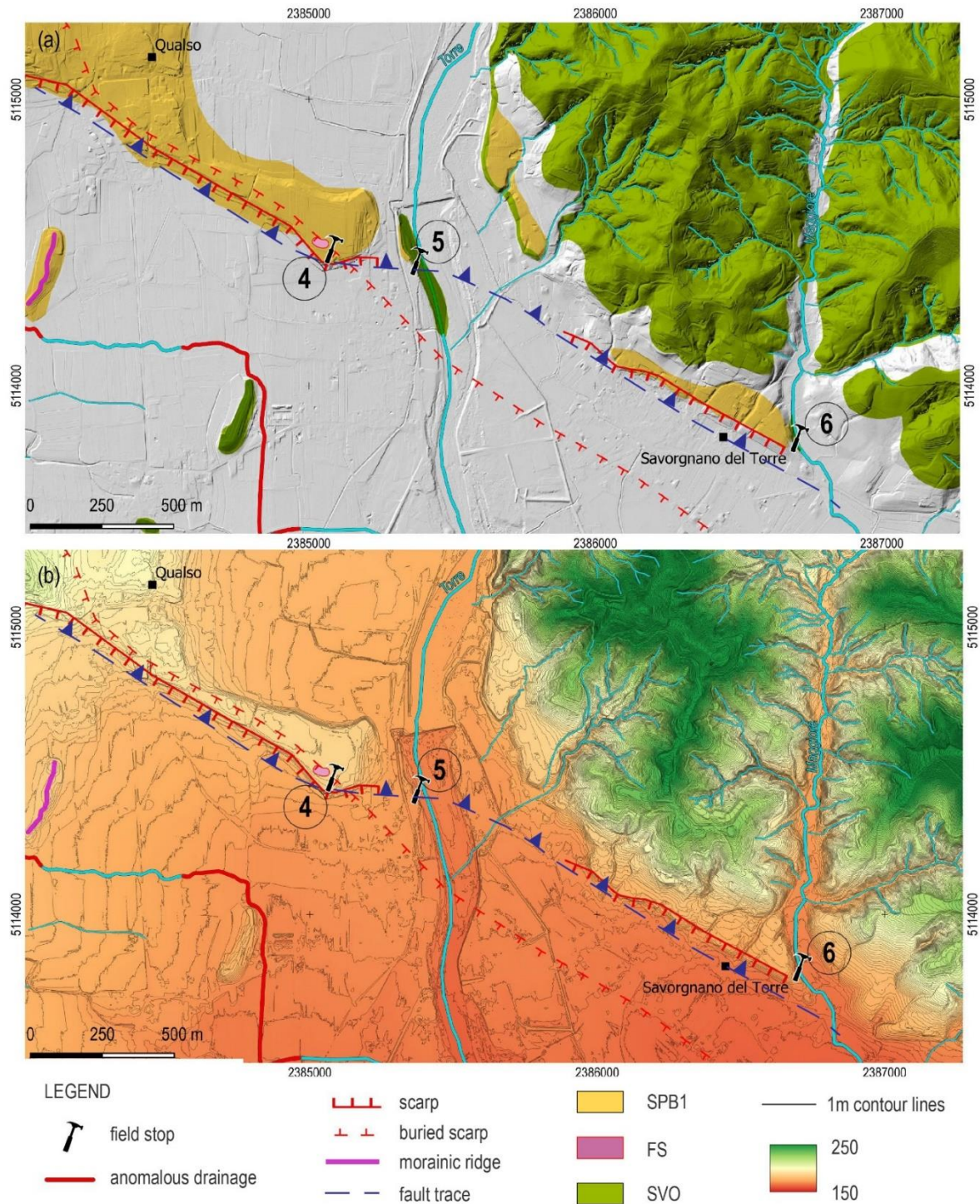and the Savorgnano del Torre terrace (Fig. 4.7).

*Fig. 4.7 - Morphotectonic elements mapped in the Qualso - Savorgnano del Torre site (a) on the 1 m –
hillshade and (b) on the 1 m dtm with 1 m contour lines showing the detailed topography of the area.*

Both Qualso and Savorgnano del Torre terraces are mainly formed by fluvioglacial Santa Margherita (SPB1) deposits that are doubtfully attributed to the first last glacial maximum Tagliamento glacier advance (Zanferrari et al., 2008a); note that the same Authors assess that these deposits may belong to a pre-LGM unit.

In this regard, on top of the southeasternmost border of Qualso scarp, the outcrop of a carbonate conglomeratic unit was detected (field stop n°4, Figs. 4.1 and 4.7). The well cemented deposit, which is strongly karstified and probably has a pre-LGM age (Fig. 4.8), is located 10 m higher than the LGM plain surface.

Fig. 4.8 – Outcrop of pre-LGM conglomerates at field stop n°4 (see location on map of Figs. 4.1 and 4.7).

Between the two scarp strands, in the Torre riverbed (field stop n°5, Figs. 4.1 and 4.7), the outcropping SVO unit is interested by an about 5 m wide shear zone (Fig. 4.9). Particularly, shear

planes range from 290/40 to 350/50 and an intense cleavage affects the marly levels (Fig. 4.10 a and b). Moreover, a change of attitude characterizes the Eocene SVO unit (from 178/40 to 320/25) downstream and upstream of the shear zone, respectively. Within the damage zone the turbiditic layers (SVO) are verticalized.

Fig. 4.9 – (a) Damage zone affecting the Eocene turbiditic unit (SVO) in the Torre riverbed (field stop n° 5, Figs. 4.1 and 4.7). In the stereographic plot the intense cleavage affecting marly SVO layers (b).

Fig. 4.10 – Details of the S-C planes on marly layers.

On top of the pre-Quaternary bedrock a well cemented gravelly unit is present (SPB1). In analogy with the basal SVO unit, also the LGM gravelly unit shows a different attitude at the hanging wall and at the foot wall of the fault zone, spanning from 080/50 to 160/35 (Fig. 4.11).

Fig. 4.11 – Detail of the well cemented gravelly unit (SPB1) on top of the Eocene turbiditic unit (SVO).

In the Rio Maggiore riverbed (field stop n°6, Figs. 4.1 and 4.7), the Savorgnano Marls and Sandstones (SVO) crop out with a vertical attitude (150/75) (Fig. 4.12 a).
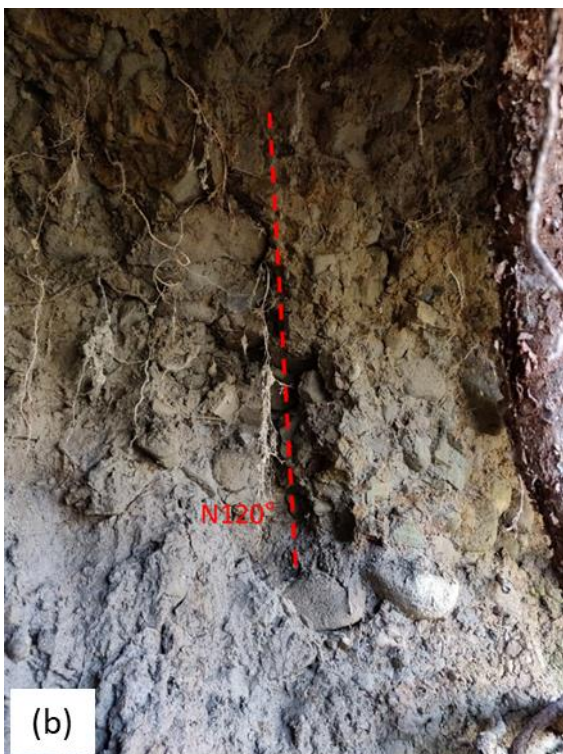

Fig. 4.12 – Outcrop of field stop n°6 (a) (see Figs. 4.1 and 4.7 for the location) and a detail of the subvertical fracture affecting the continental Holocene unit (b).

The pre-Quaternary bedrock is interested by subvertical open N110°-N120° striking fractures which also affect the upper Holocene continental unit (UIN) (Fig. 4.12 b).

Zanferrari et al. (2008a) considered the Qualso - Savorgnano del Torre WNW-ESE morphological feature as an erosional fluvial scarp. However, in order to investigate a possible tectonic component, an about NE-SW oriented detailed topographic profile (section trace in Fig. 4.1) was elaborated (Fig. 4.13). Section Q crosses the culminations of the Santa Margherita external morainic system, including Qualso hill. By integrating the collected surficial data with subsurface data deriving from geognostic well stratigraphies, the following aspects arise.
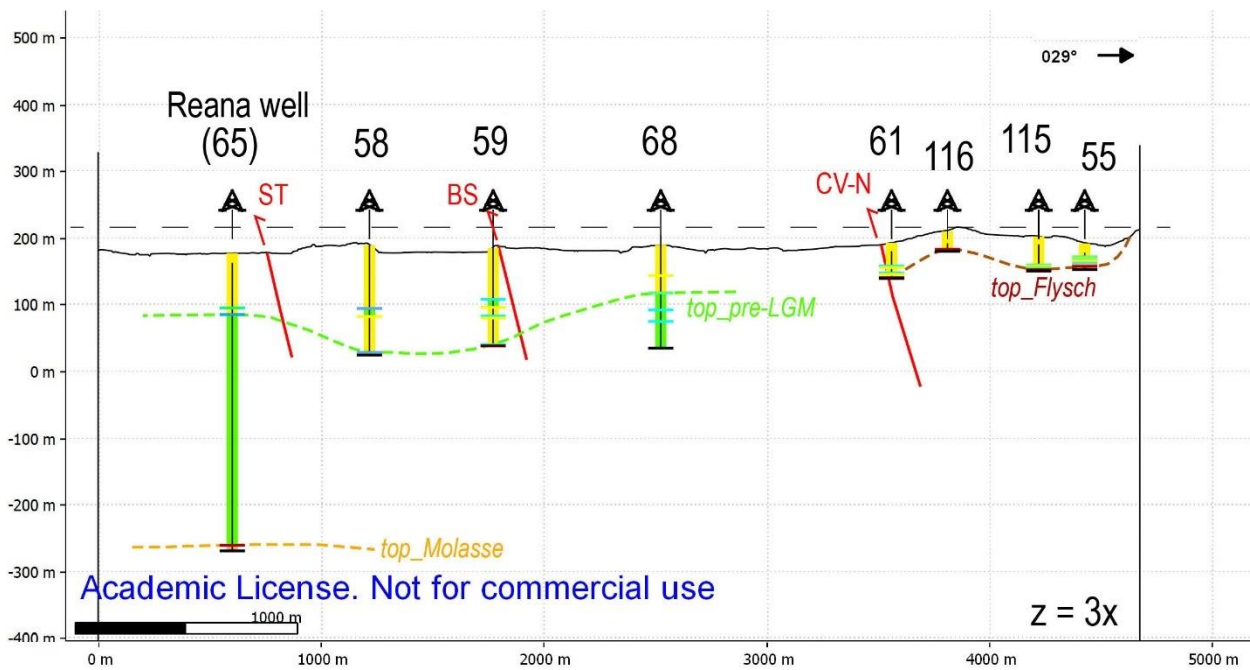

Fig. 4.13 - Detailed topographic profile Q (see section trace in the Fig. 4.1). The projected geognostic wells show the deepening of the pre-Quaternary bedrock and the thickening of the pre-LGM and LGM units, at the footwall of CV-N Thrust.

The available geognostic well stratigraphies projected onto the profile show that the Qualso relief is mainly composed of Savorgnano Marls and Sandstones unit (SVO), overlaid by thin gravel units. Differently, the geognostic wells located at the base of the scarp never cut the pre-Quaternary

bedrock, thus revealing a deepening of the bedrock of the order of at least 100 m. Pre-Quaternary bedrock, in terms of middle-late Miocene Molasse, was drilled by the Reana well at about -260 masl (well n°65 in Fig. 4.1). Focusing on the Quaternary deposition, the geognostic wells testify the presence below the Plain surface of 65 to 150 m thick gravel prevalent unit, which overlies cemented gravels and conglomerates. The first cemented layers in the geognostic well stratigraphies are interpreted as the base of the LGM units (Zanferrari et al., 2008a). Therefore, a possible correlation can be hypothesized between the underlying cemented layers and the conglomeratic unit outcropping on top of the Qualso relief (stop n°4, Fig. 4.8), in the southernmost portion of the hill. Another point of reflection arises from the topographic profile, which reveals that the external morainic S. Margherita ridges altitudes range between 187 and 194 masl, while the northwesternmost portion of Qualso hill, where SPB1 is documented, has an altitude of 218 masl. Therefore, the glacial SPB1 unit on top of Qualso relief is located 20 m higher with respect to the other SPB1 relieves. From profile Q it is evident that both pre-LGM and LGM units are characterized by higher thickness at the footwall of CV-N Thrust with respect to the hanging wall. Particularly, at the footwall of CV-N the boundary between pre-LGM and LGM is located at least 30 m lower respect to the hanging wall (Fig. 4.13).

4.2.3. CAMPEGLIO SITE

Moving towards the SE (Campeglio and Cividale del Friuli sites), the CV-BFC transpressive structure was investigated. Campeglio site is located about 15 km SE of Tricesimo and represents the area where the Colle Villano Thrust locks on BFC. Here, on the gentle hills bordering the plain area, the Eocene Savorgnano Marls and Sandstones (SVO) outcrop (Figs. 4.1 and 4.14).
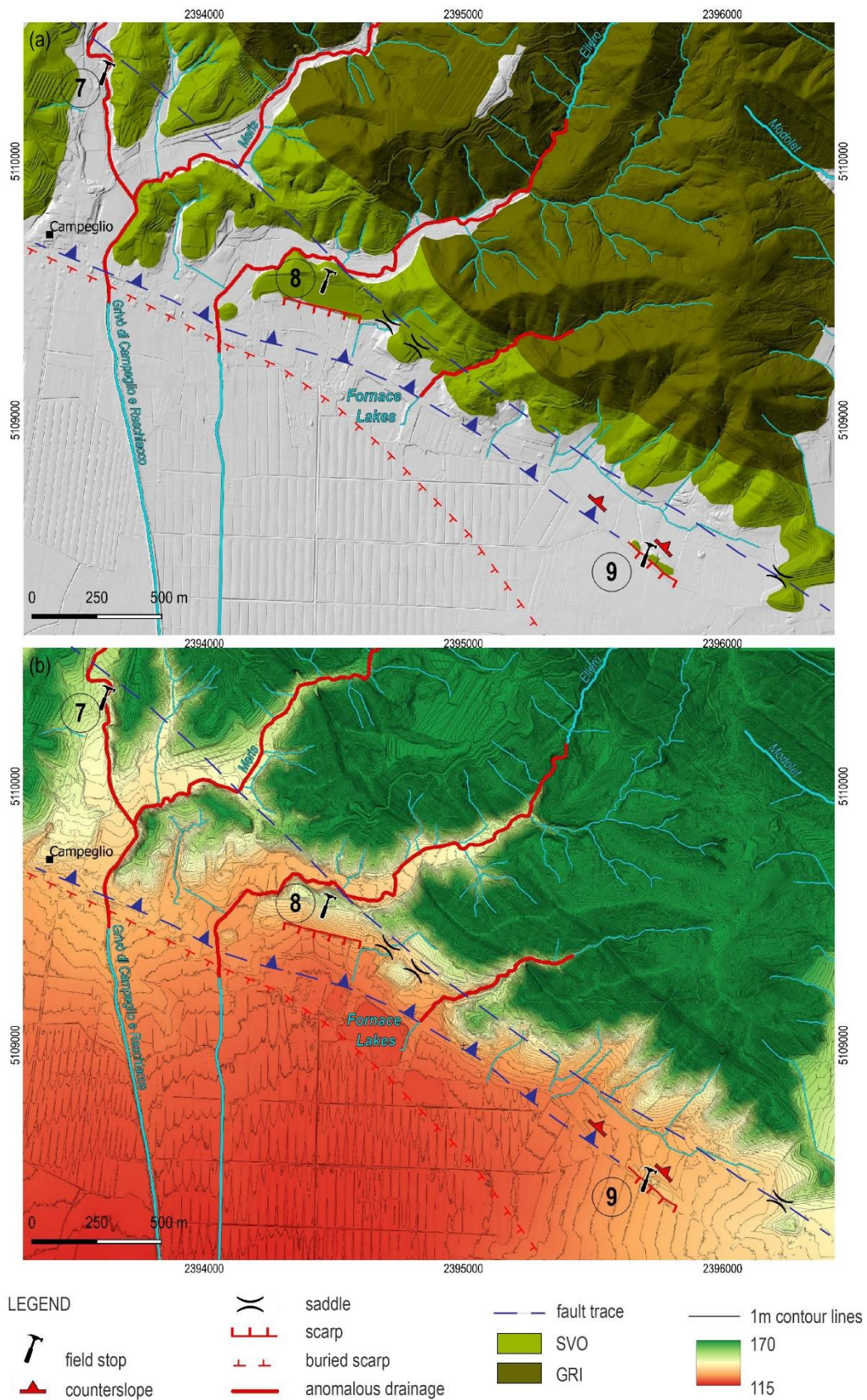
Fig. 4.14 - Morphotectonic elements mapped in the Campeglio site (a) on the 1 m – hillshade and (b) on the 1 m dtm with 1 m contour lines showing the detailed topography of the area.

Particularly, in the Grivò di Raschiacco riverbed (field stop n°7, Figs. 4.1 and 4.14), the presence of a fault plane (230/80) on a calcarenitic bed of SVO was detected (Fig. 4.15 a). A bedding variation characterizes the NE (about 050/55) and the SW (about 320/25) sides of the discontinuity. On the shear plane mineral fibers and horizontal striae are present, testifying a dextral kinematics (Fig. 4.15 b). It is worth noting that both Meris and Ellero waterstreams, located on the SE extension of this structural trend, show anomalous drainage (Fig. 4.14)

Fig. 4.15 – Outcrop of field stop n°7 (a) (see Figs. 4.1 and 4.14 for the location). The stereographic plot indicates both flysch and strike-slip attitude; (b) detail of the horizontal dextral striae on calcite plane.

On the SW slope, upstream of the Fornace Lakes (field stop n°8, Figs. 4.1 and 4.14), the outcrop of Eocene SVO strongly affected by deformation was detected (Fig. 4.16). The shear planes of the main system are characterized by an about 330/50 attitude and a double set of striae on mineral fibers, revealing both a pure dip-slip and an oblique kinematics. Many associated secondary planes are present, and the thin marly layers are affected by intense cleavage. Additional displaced fault planes, characterized by sinistral movement, were measured (190/80, 230/75, 160/89, Fig. 4.16). The structural analysis of the shear zone allowed to assess that the about 330/50 reverse/oblique system represents the Colle Villano structure, while the subvertical left-lateral planes can be referred to the Dinaric stress field.
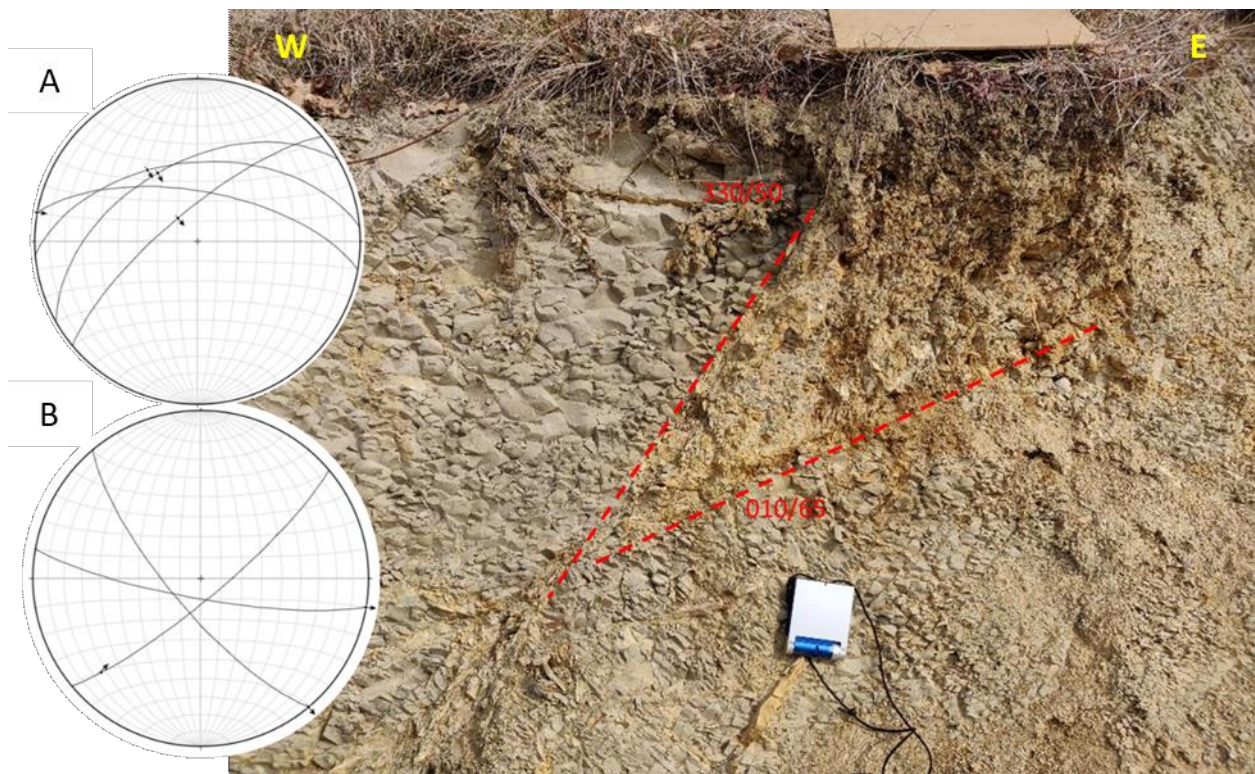

Fig. 4.16 - Outcrop of the shear zone detected near Campeglio affecting the Eocenic SVO unit. Field stop n°8 (see Figs. 4.1 and 4.14 for the location). Plot A shows the reverse S-verging plane of CV; plot B shows the left lateral fractures probably linked to the W-verging Paleogene (Dinaric) tectonic phase.

About 100 m downstream of the deformed Savorgnano Marls and Sandstone outcrop, a WNW-ESE trending 1 m high scarp borders a field covered by thick colluvium (> 1 m) (Fig. 4.17 a). A geognostic well located about 370 m SW (n° 303, Fig. 4.1), which intersects the pre-Quaternary bedrock 25.5 m below topography, confirms the colluvium thickening. In the field, rills and gully erosion features highlight the presence of sub vertical veins filled by gray to light blue silt within the colluvium (Fig. 4.17 b).

Fig. 4.17 – (a) WNW-ESE trending 1 m high scarp bordering the thick colluvium field; (b) detail of the blue-grey vein intruding the thick colluvium. Field stop n°8 (see Figs. 4.1 and 4.14 for the location).

Further SE, near Togliano locality (field stop n°9, Figs. 4.1 and 4.14), a wide back tilted surface is bordered towards the SW by a NW-SE oriented scarp (Fig. 4.18 a). Particularly, the scarp cuts the SW side of a 3 m high isolated relief. The outcrop of Eocene turbiditic unit (SVO) on top of the relief testifies that the gentle hill is affected by tectonic deformation (Fig. 4.18 b).

Fig. 4.18 – Field stop n° 9 (see Figs. 4.1 and 4.14 for location). (a) NW-SE trending scarp in Togliano locality; (b) deformed SVO unit outcropping on top of the isolated relief.

4.2.4 CIVIDALE DEL FRIULI SITE

Moving towards the SE, the investigation focused on the Borgo Faris-Cividale Fault (BFC) structural setting. In particular the Cividale del Friuli old town is located on top of a gentle relief, which is bordered towards the SE by a NW-SE trending scarp (Fig. 4.19). At the base of the scarp the Natisone river flows in a wider riverbed with a sinuous pattern. Conversely, upstream of the scarp the river forms an incised channel eroding its own cemented deposits, and a widespread deformational zone (about 100 m) affects the pre-LGM conglomerates (FS).

The pre-LGM conglomeratic unit outcropping at Cividale old town (FS) is interested by sharp subvertical fractures (field stop n°10, Figs. 4.1 and 4.19), with a medium NNW-SSE orientation (Fig. 4.20).
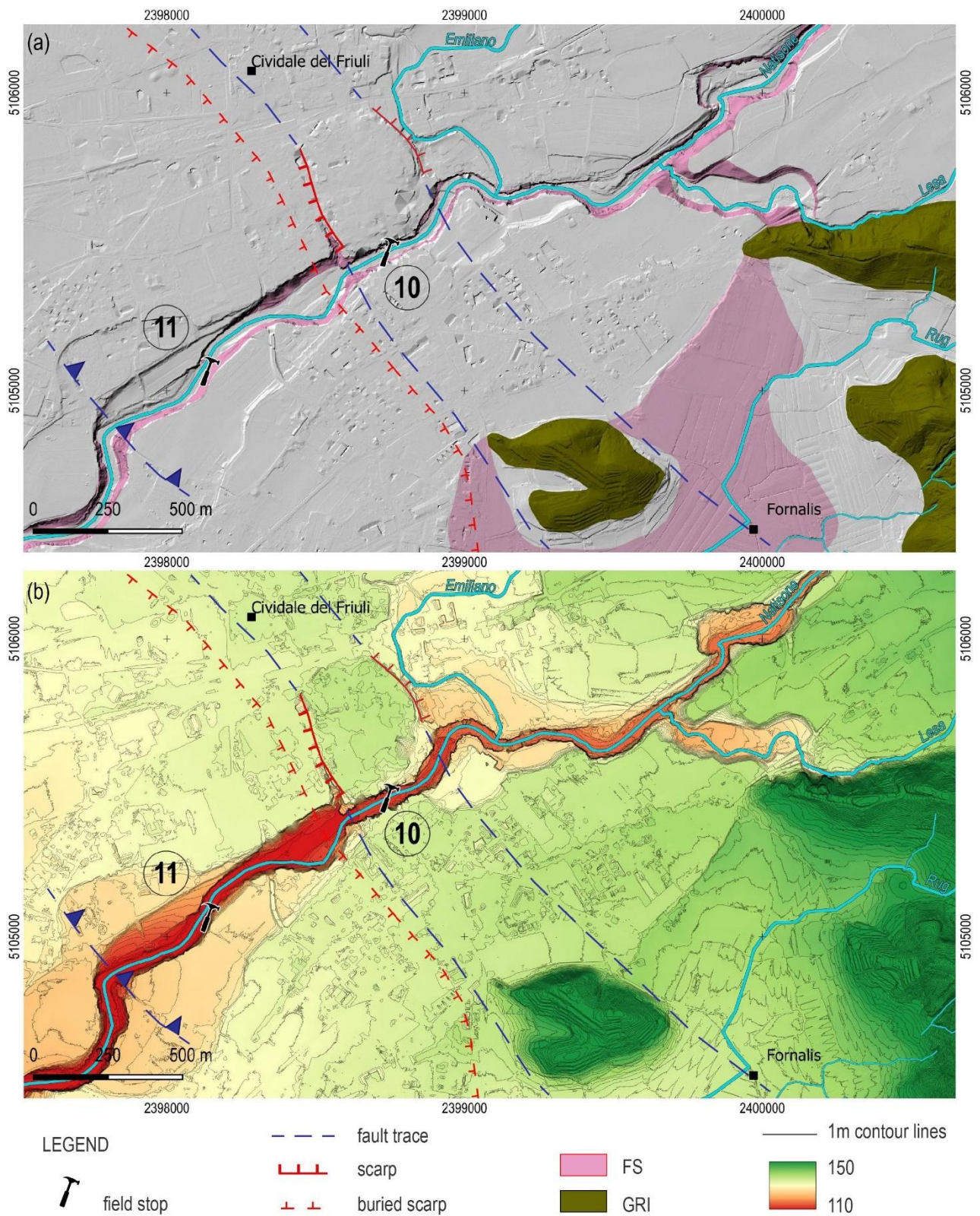
Fig. 4.19 - Morphotectonic elements mapped in the Cividale del Friuli site (a) on the 1 m – hillshade and (b) on the 1 m dtm with 1 m contour lines showing the detailed topography of the area.

Fig. 4.20 – (a) pre-LGM conglomerates outcropping at field stop 10 (Figs. 4.1 and 4.19); (b) detail of subvertical fractures on pre-LGM conglomeratic (FS); (c) Detail of the altered and karstified pre-LGM conglomeratic unit (FS) outcropping in the Natisone riverbed.

About 500 m downstream of the Cividale old town (field stop n°11, Figs. 4.1 and 4.19), the outcrop on the left Natisone bank well shows the late Quaternary continental succession composed of two different units (Fig. 4.21). The basal unit is made by a pre-LGM stratified conglomeratic body with a folded red brown palaeosoil on top (7.5 YR 4/6). The upper unit deals with LGM unconsolidated sandy gravels, composed of a basal channel-filling body with cross bedding features and an upper sub-horizontal well stratified body. Focusing on the structural elements, the basal conglomeratic layers, with an attitude spanning from 150/40 to 185/37, are clearly deformed as lithon shape. Moreover, the wavy geometry of the palaeosoil (S0 spanning from 135/25, 170/35, 150/30 to 142/07) on top of the conglomerates testifies its involvement in the deformation. The structural analysis revealed the presence of an about NS trending fracture system affecting the pre-LGM conglomeratic unit. Right in correspondence of the fracture, the thinning of the palaeosoil is evident (Fig. 4.22 b). The C-14 dating of a palaeosoil sample performed at Beta Analytic confirmed its pre-LGM age (>43500 years BP). Differently, the LGM upper unit sub-horizontal layering, in onlap on the basal unit, appears to seal the deformation.

Fig. 4.21 – Outcrop of field stop n° 10 at Cividale del Friuli (see location in Figs.4.1 and 4.19). (a) Pre-LGM (FS) basal conglomerates and overlying subhorizontal LGM gravelly unit (CIV); (b) palaeosoil on top of the pre-LGM conglomerates.
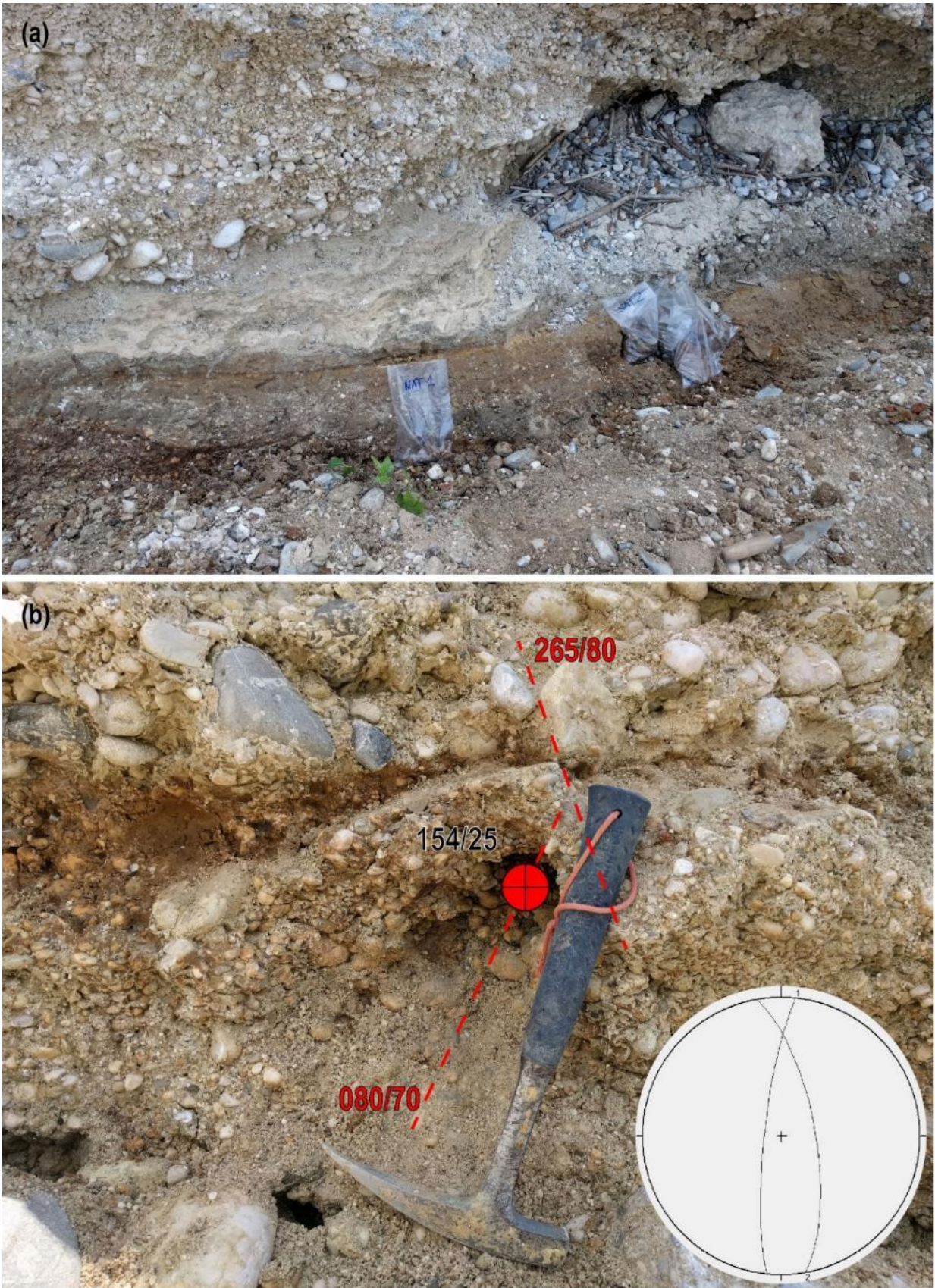
Fig. 4.22 – (a) Detail of the palaeosoil on top of the pre-LGM conglomeratic unit (FS). (b) Detail of the fractures affecting the pre-LGM conglomeratic units. Note that right on the fracture the palaeosoil thickness reduces.

4.3 DISCUSSION

The morphotectonic survey carried out in the Julian prealpine area allowed to confirm that the investigated tectonic structures (Colle Villano-N and Colle Villano-Borgo Faris – Cividale Faults) strongly controlled the sedimentary continental deposition during the Upper Pleistocene – Holocene time span. Moreover, the buried scarp mapped from the Quaternary base surface geometry (Chapter 2), together with the abrupt thickening of the Quaternary succession at the base of the scarp, well highlights the surficial geometry of the fault systems testifying their Quaternary activity.

In detail, the morphotectonic data collected in the investigated area depict an about N110°-130° striking deformation band, located along the prealpine border, from Tricesimo to Cividale del Friuli.

Focusing on the northern portion (Colle Villano North Thrust, CV-N), the NW-SE aligned scarps between Qualso and Savorgnano del Torre, where LGM Santa Margherita Subunit and pre-LGM Friuli Superunit outcrop in the hangingwall of CV-N, highlight the Upper Pleistocene tectonic activity of the thrust. Considering that the orientation of the scarps well coincides with the outflow directions of Tagliamento fluvioglacial bodies during LGM, a fluvial erosion component could not be excluded. However, it is worth noting that the boundary between LGM and pre-LGM deposits (gravels vs conglomerates) is located at about 142 masl in the hanging wall of the CV-N and at about 113 masl at its foot wall. Moreover, crossing the fault surface, the pre-LGM deposits strongly thicken S-ward.

Moreover, along the Torre and Maggiore rivers, in correspondence of the morphogenic scarp, an about N90°-110° striking subvertical fault affects not only the pre-Quaternary bedrock (Eocene Savorgnano Marls and Sandstone) but also the Upper Pleistocene succession (Santa Margherita deposits).

Following these observations, we can assess that the CV-N acted during the last 30 ky uplifting the Upper Pleistocene fluvioglacial deposits with a maximum displacement of about 1 mm/yr.

Moving SE, the morphostructural data collected near Campeglio di Faedis and Cividale del Friuli testify the activity of the complex Colle Villano – Borgo Faris – Cividale transpressive Fault-System (CV-BFC).

Near Campeglio locality, where the CV closes on the BFC, a NW-SE striking shear zone referable to the tectonic effects of the Borgo Faris – Cividale fault matches with aligned drainage anomalies of two minor creeks. Deformational effects referable to the reverse CV Thrust can be interpreted as the infill of a subsided area at the footwall of the reverse frontal splay of Colle Villano. Moreover, recent tectonic activity was indicated by the back-tilted surface in the northern wall of a clear morphogenic scarp developing along the fault trace.

Additional tectonic evidence referable to the Upper Pleistocene Borgo Faris – Cividale strike-slip fault were mapped along the Natisone valley, at Cividale del Friuli site (field stops n°10 and 11, Fig. 4.1). Here, the sub-horizontal pre-LGM conglomerate unit crops out at about 135 masl in the Cividale old town. A set of NNW-SSE striking planes strongly fractured the conglomerates that are covered by a small thickness of LGM gravels. The LGM-pre-LGM boundary crops out a few hundreds of meters downstream, at Macello locality. Here, the pre-LGM conglomerates lie below 25 m thick gravel unit, at about 100 masl and dip 40° towards the South. Therefore, we can speculate that the transpressive motion of BFC should be responsible of a 35 m vertical offset on the LGM-pre-LGM boundary, thus revealing a throw rate of about 1 mm/yr for the last 30 kyr.

CHAPTER 5: PALAEOSEISMOLOGY

All the structural, seismological and morphotectonic data collected in the previous sections highlight that topography of the Julian Prealps was/is strongly controlled by the tectonic activity of the faults bordering the relieves. In addition, according to macroseismic and instrumental seismological data, this area experienced two M>6.0 since 1000 (1511 and 1976 earthquakes, CPTI15 v3.0). With the aim to investigate the Upper Pleistocene-Holocene tectonic activity and the possible surface rupturing potential of the investigated faults (Colle Villano-N and Colle Villano-Borgo Faris-Cividale transpressive active Faults), two palaeoseismological trenches were dug across each segment (see the Morphotectonic map for the locations).

5.1 METHODS

In order to better define the excavation site, some geophysical investigations were conducted. Particularly, in site 1 (Fraelacco trench, location on the Morphotectonic map) two overlapping Electric Resistivity Tomographies were realized by IND.A.G.O. snc: ERT1 with a total length of 115 m and offset electrodes of 5 m and a more detailed ERT2 with a total length of 47 m and offset electrodes of 1 m. This geophysical technique allows to investigate the resistivity potential trend in the subsoil and the detection of abrupt lateral variation of resistivity potential can be associated to the presence of a tectonic discontinuity. Differently, thanks to a cooperation with the Direzione Centrale Risorse Agroalimentari, Forestali e Ittiche of the Regione Autonoma Friuli Venezia Giulia, site 2 (Campeglio trench, location on the Morphotectonic map) was investigated through seismic tomography and HVSR analysis techniques. Both geophysical surveys are based on seismic waves propagation in the subsoil. The seismic tomography technique allows to detect the presence of discontinuity in the subsoil, based on the first arrival of the generated P waves. Differently from

seismic tomography, the HVSR technique helps to detect the presence of discontinuity in the subsurface by applying the spectral ratio of the vertical and horizontal component of the ambient noise Rayleigh waves.

In the light of the anomalies detected from geophysical investigations, the excavation area in the two sites was defined and two palaeoseismological trenches were realized, with the aim to investigate the deformation potential of the Colle Villano thrust and its possible activation during the strong earthquakes which affected the area. Following the excavation work, the study wall was brushed and armed with a 1m grid. The log, representing the geometry of the identified stratigraphic units were designed on graph paper and a detailed photographic report of the wall was realized. Later, many samples useful for laboratory analysis were collected. Particularly, the radiocarbon dating analysis performed by Beta Analytics allowed to estimate the age of the excavated units, while the grain size analysis, performed at the Geotechnical Lab of the University of Udine, was useful for investigating the liquefaction potential of the collected material.

5.2 FRAELACCO TRENCH

The morphotectonic elements collected in the NW portion of the Julian prealpine border area depict a clear WNW-ESE alignment consistent with the Colle Villano northern portion (CV-N). Particularly, an upwarped surface located between the Barbian and the Borgo Soima water streams analyzed in the previous chapter revealed suitable for the palaeoseismological analysis (Morphotectonic map).

Fig. 5.1 – (a) Ortophoto of the Fraelacco site. The yellow line is the trace of ERT survey, the blue box is the excavated trench, and the red square represents the deformation zone in the Barbian riverbed (field stop n°3a, Chapter 4); (b) Field investigated through the palaeoseismological analysis.

5.2.1 RESULTS

The higher resolution profile (ERT2, Fig. 5.2) realized by dr. Farinatti (IND.A.G.O. snc) in the Fraelacco site shows that the northern portion is characterized by high resistivity bodies, while medium resistivity values characterize the southern part of the investigated area. At around 32-36 m from the profile origin a sharp NE-dipping discontinuity separates the two domains.
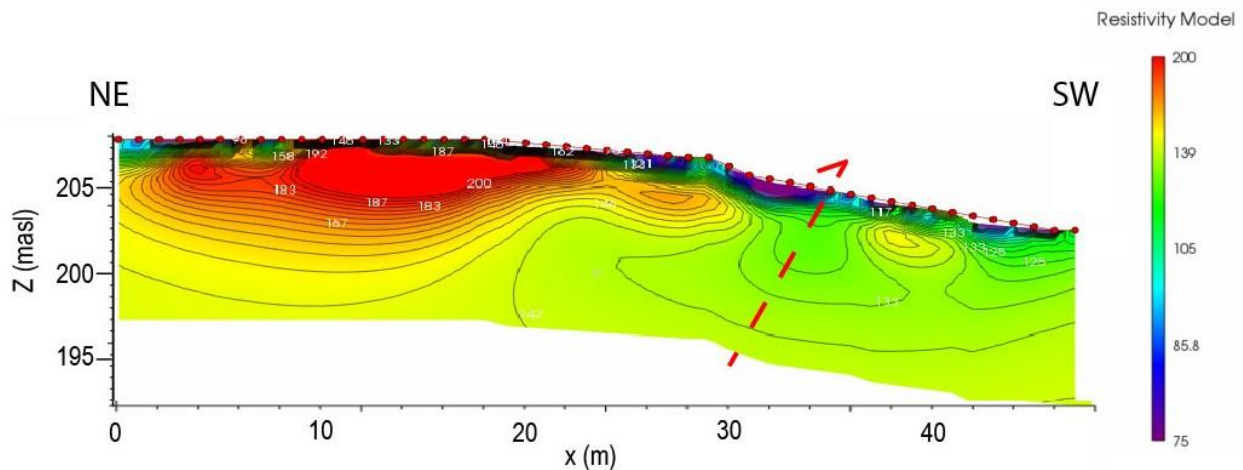

Fig. 5.2 – ERT2 profile (see trace in Fig. 5.1).

Based on the geophysical results, a 30 m long and 2.5 m deep trench was dug across the detected discontinuity (blue box in Fig. 5.2a). The excavated sedimentary sequence showed sub-glacial and glacial units of the LGM Tagliamento glacier underlying a post-glacial debris-flow. Particularly, from the bottom to the top of the trench 5 different units were identified (Fig. 5.3):

-   Unit A: sub-glacial roughly organized deposit composed of alternating sandy and gravelly layers. It develops in the basal portion for the whole length of the trench. The sandy layers (2.5 Y 6/4), locally characterized by sub-parallel and cross laminations, reveal a S-dipping geometry (20-25°). Within the gravelly layers, characterized by sandy matrix, the presence of alteration pouches (7.5 YR 6/4) was detected, likely caused by locally suspended water-table.
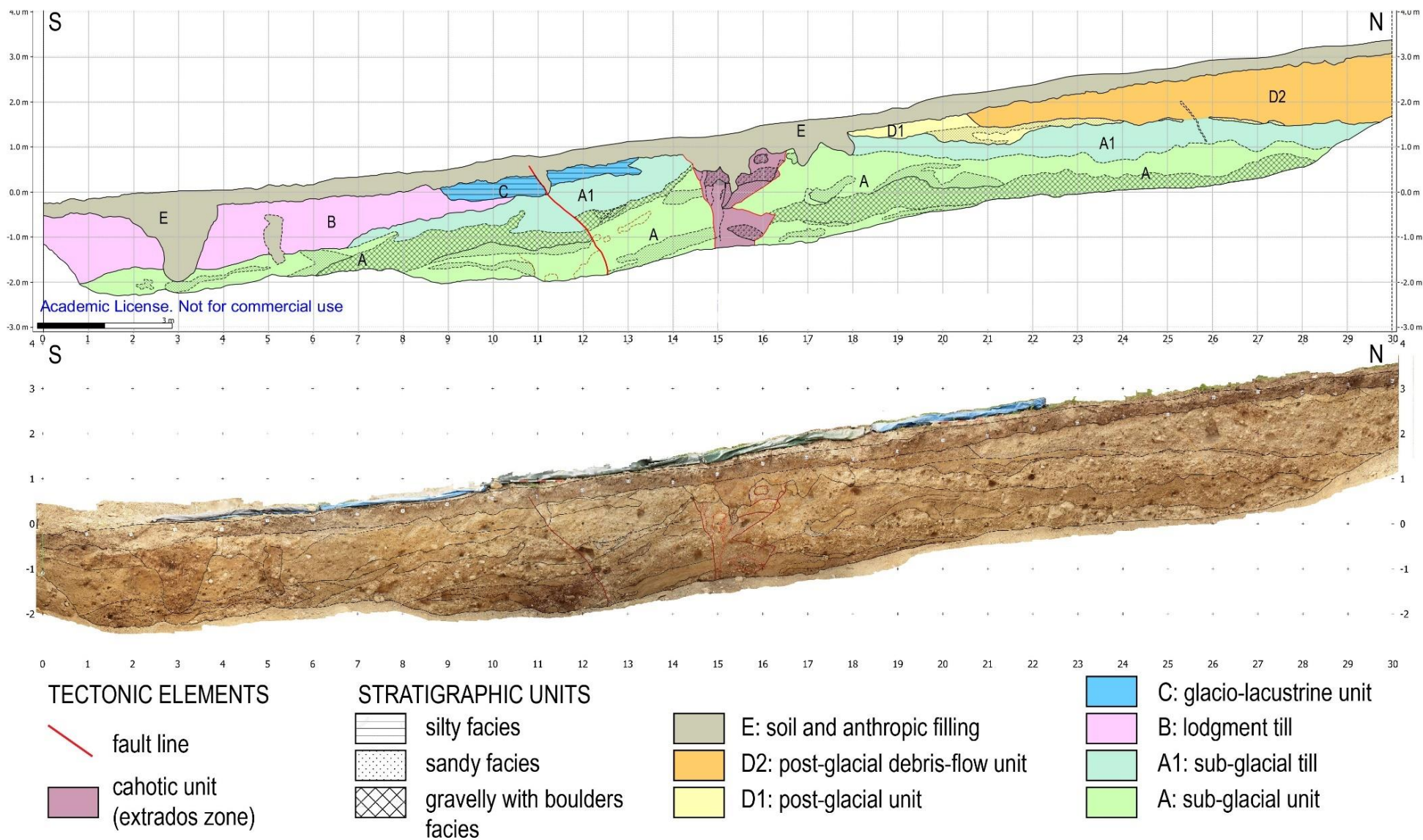
Fig. 5.3 – (a) interpretation and (b) elaborated orthomosaic of the excavated wall in the Fraelacco site.

- Unit A1: sub-glacial over-consolidated diamicton deposit with grey silty lenses (2.5 Y 6/2).

- Unit B: lodgment till deposit which develops between sections 0 and 11. Over-consolidated diamicton deposit with multi-faceted glacial clasts up to 20 cm dimensions in silty matrix (2.5 Y 6/6). The composition of the clasts allowed to attribute the deposit to the Tagliamento glacier. The upper 40 cm thick represents the weathered portion (10.5 YR 4/6), characterized by many altered clasts. The basal limit shows an irregular shape, while upwards the unit is truncated.

- Unit C: glacio-lacustrine deposit composed of a basal 10-12 cm thick well laminated silty portion within which the presence of a dropstone was detected. Upwards, the lamination is less evident, and the deposit is truncated by the overlying arable unit E.

- Unit D1: roughly organized alluvial post-glacial unit which develops from sections 18 to 28. It is composed of clasts supported gravelly layers in sandy matrix with an about 10 cm thick layer of silty fine sand (2.5 Y 5/4).

- Unit D2: post glacial debris-flow unit which develops from sections 20 to 30. It is composed of clasts supported gravels with boulders, sand and silt. The upper part of the unit corresponds to the weathered portion (10 YR 5/6), characterized by the presence of intensely altered carbonatic clasts, locally completely dissolved.

- Unit E: gravelly sandy unit corresponding to the arable layer (10 YR 4/4). Locally the presence of roots is recognizable. Between sections 2 and 4 an anthropic infill at the base of the arable layer is present, characterized by calcarenitic clasts in a silty matrix (7.5 YR 4/6).

The trench shows that the whole stratigraphic succession is warped up and truncated by the erosional soil surface. It is worth noting that the upwarped convexity of the stratigraphic succession coincides with the topographic bulge and, between sections 10 and 17, many deformation items

were detected. Particularly, between sections 10 and 13, a vertical offset of 30 cm can be identified on the base of unit B and upwards, the presence of a verticalized clast highlights the clear 18 cm displacement of the base of the glacio-lacustrine unit C (Fig. 5.4).
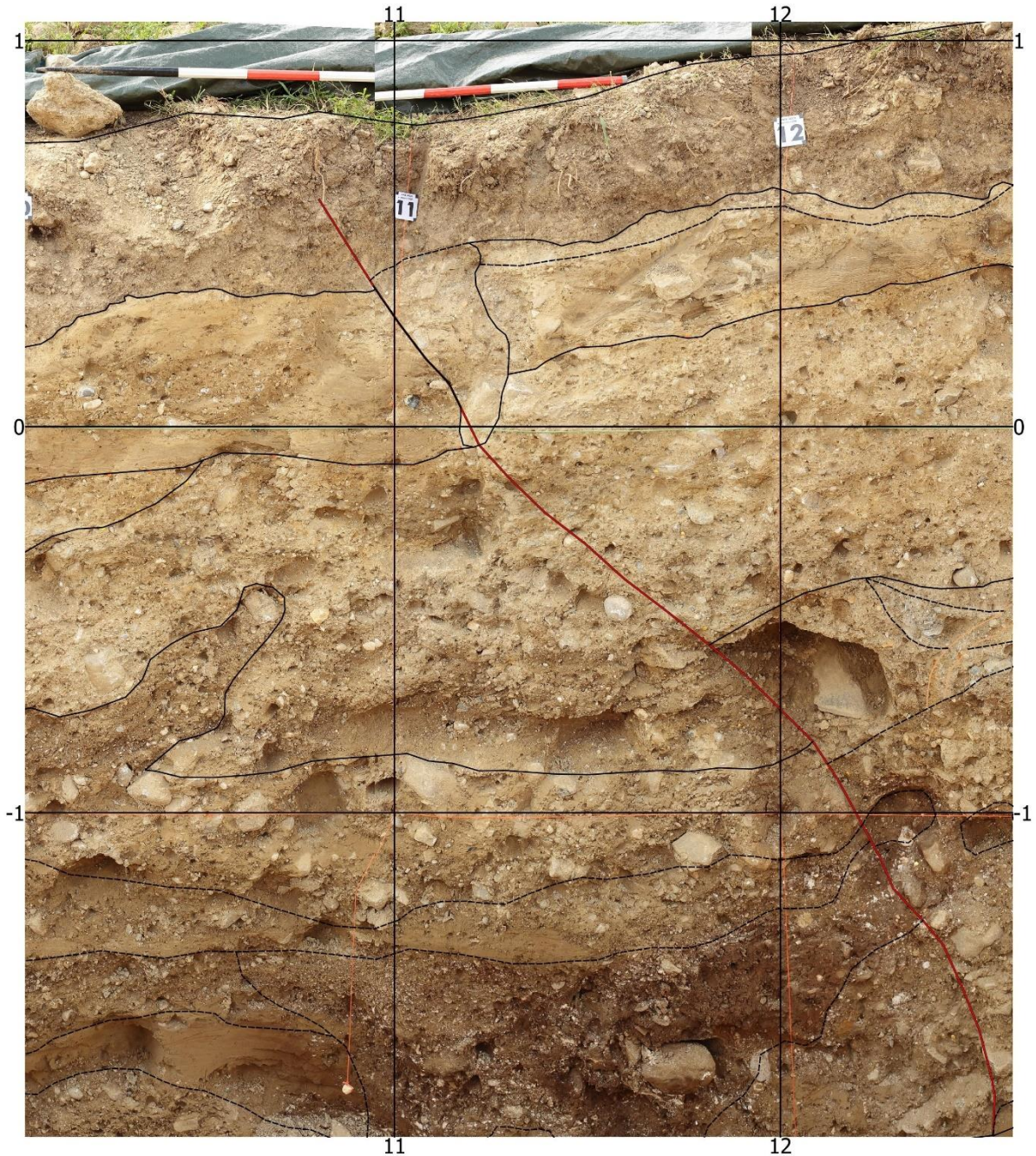

Fig. 5.4 – Detail of the dislocated base of the glacio-lacustrine C unit, marked by the orange thumbtacks. Note the presence of the anthropic infill in coincidence of the offset point highlighted by a verticalized clast.

Focusing on the most surficial thickness, in coincidence of the detected offsets, the presence of a cone shape filling body can be identified. The clasts composition of the filling material only deals with carbonatic clasts, thus suggesting an anthropic intervention. Both the LGM units of the Tagliamento basin and the post-glacial debris-flow units are characterized by a varied composition where carbonatic and calcarenitic clasts prevail. However, on top of the infill the base of the brownish arable layer can easily be detected and, focusing on its geometry, the SW-ward thickening of the soil is marked by the presence of a 6 cm step (Fig. 5.4).

Only a few meters North, in coincidence with the anticlinal hinge between sections 14 and 17, the lateral continuity of the stratigraphic units is abruptly interrupted by the presence of a vertical funnel-shape 1-1.5 m wide discontinuity (Fig. 5.5). Within the chaotic unit filling the funnel shape discontinuity, it is possible to distinguish many coarse-sandy and fine-sandy lenses characterized by high-angle lamination, locally parallel to the northern border of the discontinuity. Differently, the southern border of the discontinuity is marked by the presence of a 20 cm wide vertical body filled by gravels (Fig. 5.5), while the upper portion of the infill deals with calcarenitic clasts in a brownish silty matrix.
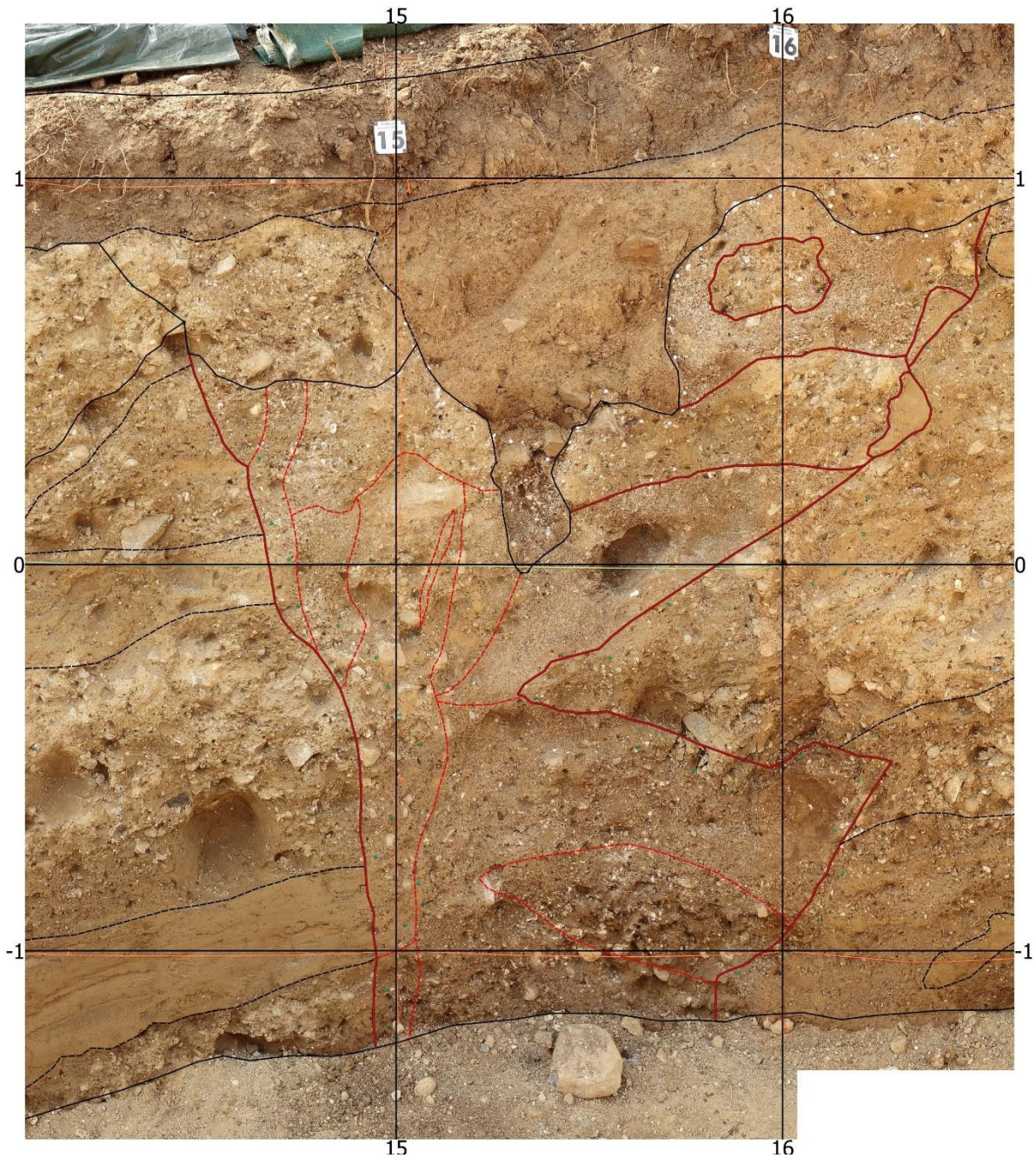
Fig. 5.5 – Detail of the chaotic unit filling the funnel shape body between sections 15 and 16.

5.2.2 INTERPRETATION

The basal and eldest stratigraphic units deposited during the Canodusso maximum advance (21 – 23 kyr cal BP; Monegato et al., 2007). In this area the Tagliamento glacial body flowed from the NW to the SE (coming out of the excavated wall) and deposited the glacial and glacio-lacustrine B and C

units. Meanwhile, the melting water at the base of the glacial body were responsible of the deposition of the sub-glacial A and A1 units. Following the Canodusso maximum advance, the retreat of the glacial bodies occurred and during the successive Remanzacco advance, the Tagliamento sub-lobes didn't reach the study area (Zanferrari et al., 2008a). Therefore, D1 and D2 units must have deposited during the last 21 kyr.

The excavated stratigraphic sequence is characterized by an antiformal geometry, which reflects the upwarped shape of the field surface. Moreover, the numerous deformation elements testify that the investigated area is affected by active tectonics. Particularly, the presence of an about N-dipping high-angle reverse plane is evident, which is responsible of the vertical offset of B and C units. In detail, based on the 30 cm vertical offset of the B unit and the 18 cm throw on the base of unit C, the occurrence of at least two deformational events can be identified. The first event E1 must have occurred during the Canodusso maximum advance (23 and 21 cal kyr BP), but certainly before the deposition of the glacio-lacustrine C unit, causing a vertical offset of 12 cm. A subsequent deformational event E2 on the same thrust fault caused an 18 cm vertical displacement of the unit C. This event, which certainly post-dates the Canodusso maximum advance, probably occurred in historical times. As a matter of fact, the anthropic infill located right in coincidence of the tectonic discontinuity can be interpreted as an attempt to fill and level the deformations of the topographic surface. In addition, the detection of a 6 cm high step on the well continuous base of the arable soil right above the dislocation of B and C unit suggests the possibility that the tectonic discontinuity was reactivated in a third most recent event E3. If this interpretation is valid, the E3 event must be very recent, since it post-dates the anthropic infill.

At the back of the identified shear plane, the chaotic unit filling the funnel-shape discontinuity can be interpreted as the extrados zone associated to the reverse fault. In detail, the geometry of the sandy lenses within the chaotic units, together with the presence of vertical veins filled by gravels,

allow to hypothesize that this portion of the damage zone was not only filled by the sediments coming from above. Indeed, it is likely that the chaotic zone was also used as a preferential zone of material upwelling from below. As a matter of fact, during the 1976 seismic sequence many liquefaction phenomena were documented in a wide area spanning from Majano to Gemona. Although in most cases it dealt with sand mixed with water, many gravelly and sandy ejecta were documented in the Avasinis and Bordano area (Martinis, 1977). The recent study conducted by Rollins et al. (2020) confirmed that gravelly sand liquefied in Avasinis in occurrence of the Friuli 1976 earthquake.

In the light of these results, it must be assessed that the excavated trench cut through the active Colle Villano-N Reverse Fault. This structure registered at least two deformational events (E1 and E2), with E2 likely occurred in historical times. If considering the historical seismicity of the area, two Mw > 6.0 historical earthquakes are documented in the CPTI15 v3.0 (Rovida et al., 2021): the 1511 and the 1976 earthquakes. Both events affected this area and are characterized by a potential consistent with the deformation features detected through palaeoseismological analysis.

5.3 CAMPEGLIO TRENCH

Based on the collected morphotectonic data (Chapter 4), the Campeglio site revealed suitable for palaeoseismological investigation. Particularly, the geophysical survey investigated the about E-W oriented scarp in the field located downstream of the outcropping fractured bedrock and characterized by thickened colluvium affected by vertical features (Fig. 5.6).
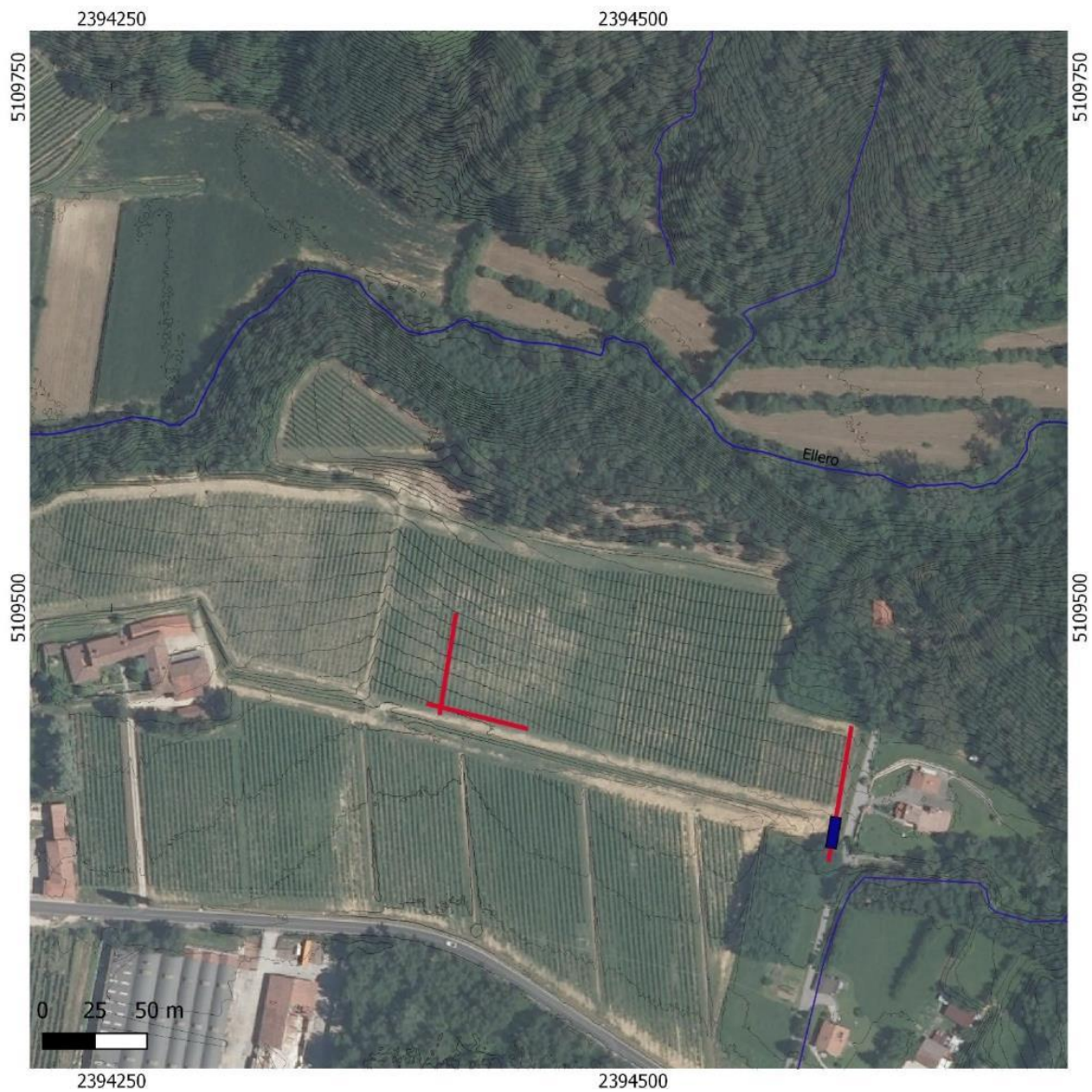
Fig. 5.6 – Ortophoto of the Campeglio site. Purple lines represent the geophysical survey traces, the blue box is the excavated trench.

5.3.1 RESULTS

In the western portion of the investigated field at Campeglio site two perpendicular seismic tomographies (tomo_A and tomo_B profiles, Fig. 5.7) were realized, characterized by a length of 48 m and a geophone offset of 3 m (Fig. 5.7). Note that the color bar is slightly different for the two profiles.
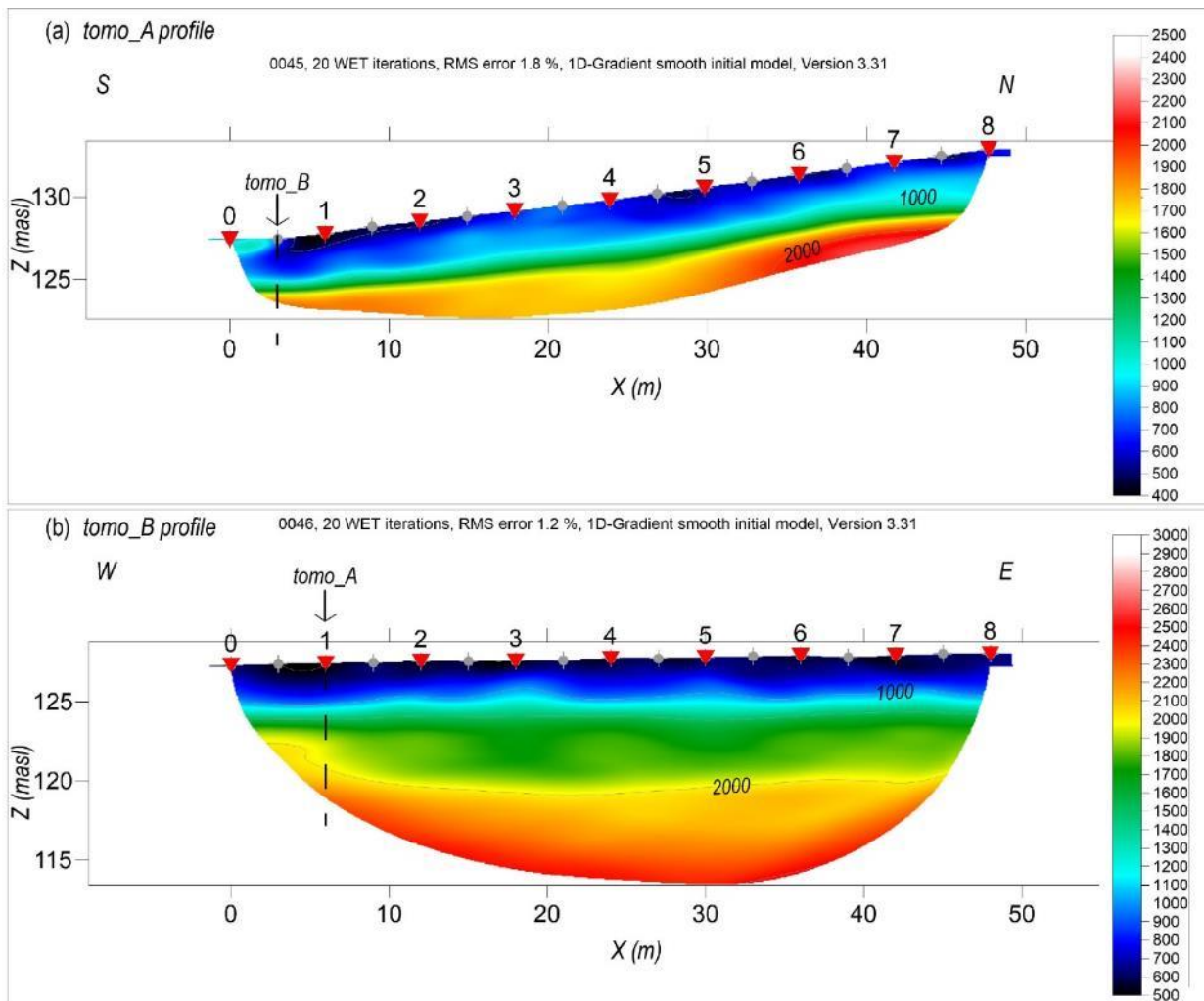
Fig. 5.7 – (a) N-S oriented A and (b) E-W oriented B tomographic seismic profiles realized in the western portion of the Campeglio site (see trace location in Fig. 5.6).

The N-S oriented tomo_A profile reveal a gently S-dipping stratigraphy, almost parallel to the topography. The E-W tomo_B profile reaches a higher depth (about 12 m below the surface) and shows a thickening of the green body immediately east of the crossing point with the N-S tomography. It is worth noting that in the northern portion of tomo_A profile the Vp = 2000 m/s lies at about 3 m below the surface. Conversely, in the E-W tomo_B profile the Vp = 2000 m/s isoline runs at a depth of about 7.5 m below the surface for most of the section and tends to get shallower in the western portion, accompanying the thickening of the green body.

In the eastern portion of the investigated field the N-S oriented tomographic seismic section (tomo_C, Fig. 5.8), characterized by a total length of 64 m and a geophone offset of 4 m, illustrates a plane parallel, slightly S-dipping stratigraphy and clearly shows the presence of a discontinuity at around 25 m from the section origin.
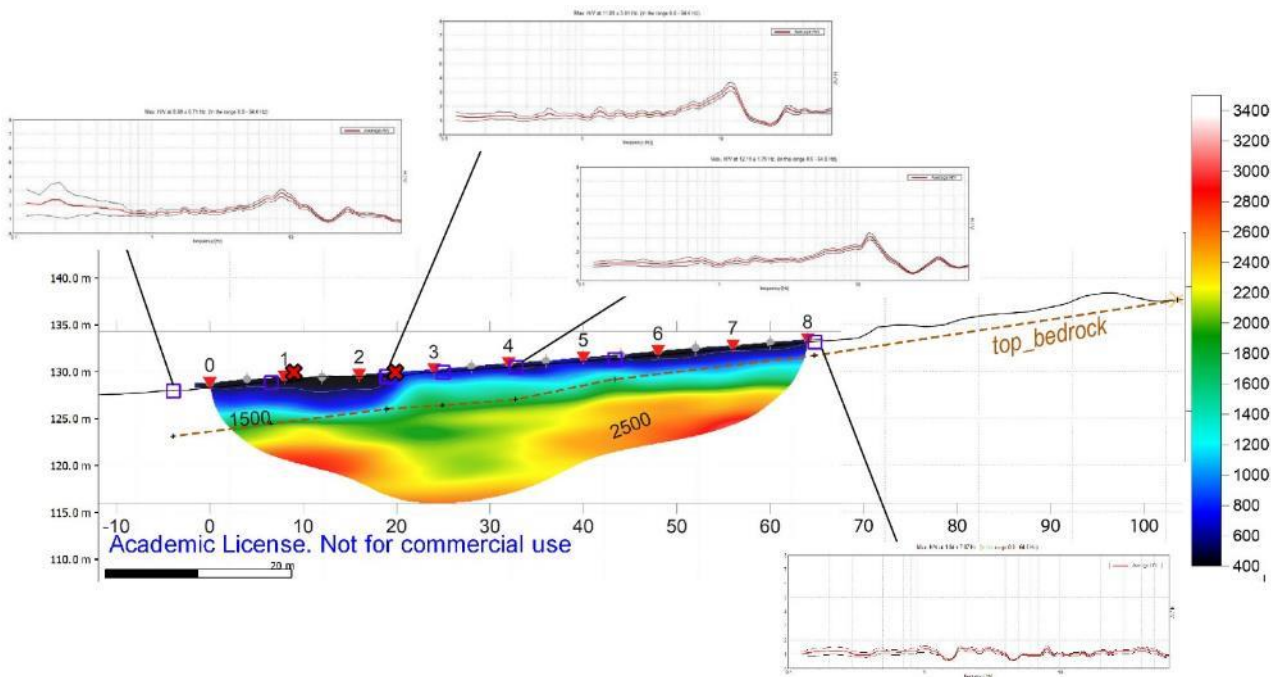

Fig. 5.8 – N-S oriented C tomographic seismic profile (see trace location in Fig. 5.6) and HVSR measurements (blue squares) realized in the eastern portion of the Campeglio site.

Moreover, along the tomo_C profile 4 HVSR measures were realized in order to investigate the depth of the bedrock, which outcrops about 40 m upstream of the seismic line (Fig. 6.8). The northernmost located measure, in coincidence with geophone 8, doesn't show any peak, thus testifying the proximity of the bedrock to the surface. Conversely, the H/V peaks of the other 5 measures reveal that sedimentary cover is present above the bedrock. The geometry of the top of the bedrock was reconstructed by considering a Vs value of 170 m/s for the surficial layer, measured through Refraction Microtremor (ReMi) method. Particularly, the green -yellow subtle layer has been interpreted as the altered uppermost portion of the bedrock. In this regard, the green-yellow

funnel shape located at 25-30 m from the section origin, and in coincidence with the thickening of the blue surficial body, could represent the bedrock damage zone.

Based on the geophysical evidence, a 9 m long and 2.5 m deep palaeoseismological trench was realized (blue box in Fig. 5.6). The excavated stratigraphic sequence deals with colluvial units (Fig. 5.9).
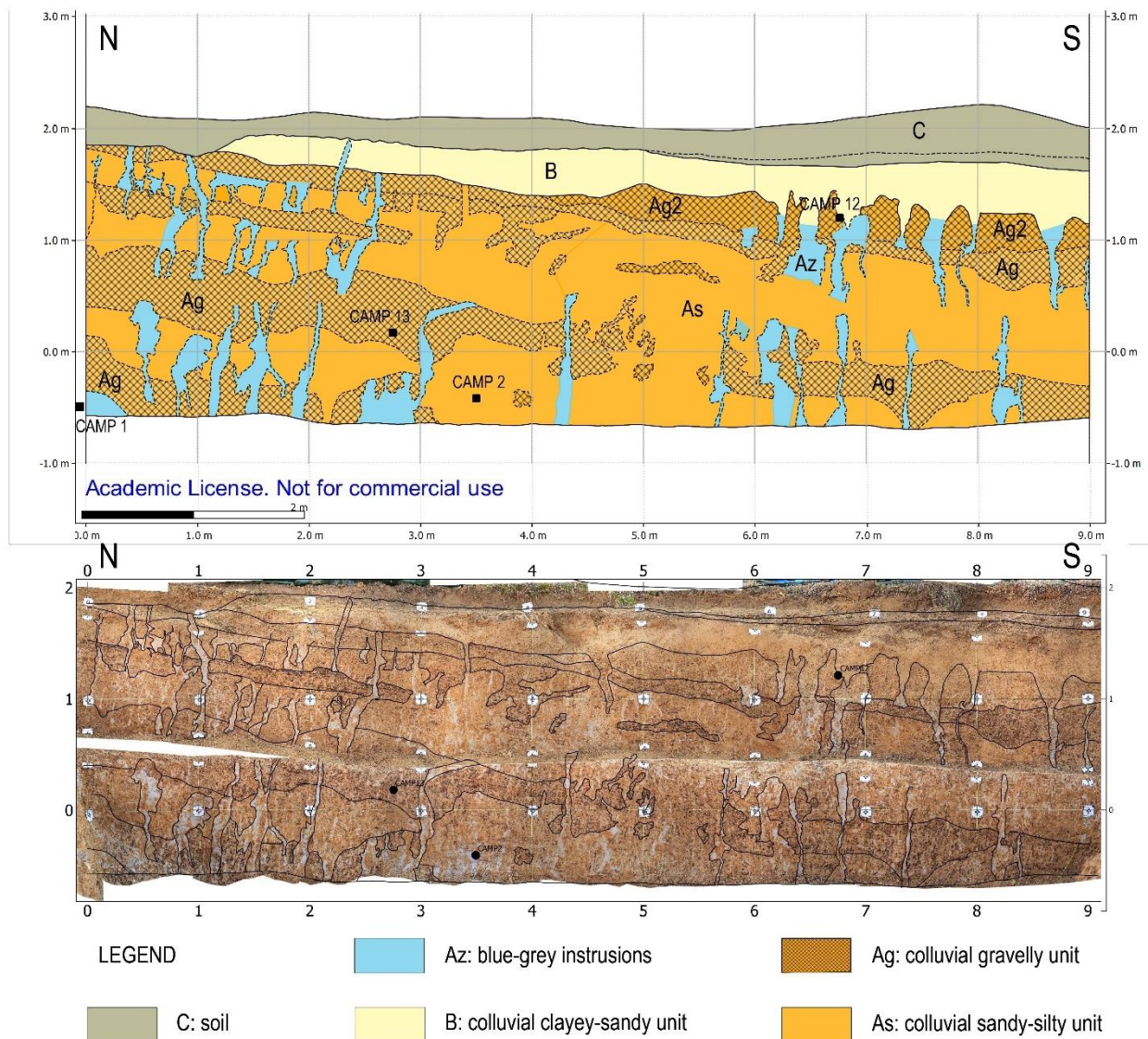

Fig. 5.9 – (a) interpreted and (b) elaborated orthomosaic of the excavated wall at Campeglio site.

In detail, three units were identified: the basal A unit occupies most of the wall and is composed of brown/yellow sandy silt (As) with pebbly levels (Ag). The clastic component of the coarse gently S-

dipping levels is mainly represented by chert. However, an abundance of nodules of iron and manganese oxides is present. Upwards, unit A is truncated by the soil (unit C) in the first 1.5 m from the origin, while south of the 1.5 m vertical section, unit A is overlaid by the clayey-sandy unit B. The uppermost unit C is represented by the arable soil.

The abundant presence of Fe-Mn nodules provides information regarding the long-term soil pedogenetic processes, revealing alternating oxidizing and reducing conditions within the soil. Particularly, during wet periods Fe (III) and Mn (III/IV) are reduced and dispersed throughout the soil matrix, while during drying periods when the soil environment becomes more oxidized and oxygen levels gradually increase, they reprecipitate filling matrix pores. As a matter of fact, soil Fe-Mn concretions and nodules have been found to be widespread in soils with some internal drainage restrictions (Vidhana Arachchi et al., 2004; Zhang and Karathanasis, 1997).

Concerning the presence of deformational elements, the most relevant feature of the wall stratigraphy is the pervasive presence of vertical blue-grey veins filled by sandy-silt (Az). The brushing of the wall step allowed to reconstruct the 3D dense network geometry of the intrusions, which pass through the whole basal unit A, locally interrupting the pebbly levels continuity (Fig. 5.10 a), and die out upwards within unit B.

Fig. 5.10 – Details of the vertical blue-grey dikes characterizing the excavated wall. (a) Abrupt interruption of the lateral continuity of the coarse levels; (b) detail showing the yellow-reddish sandy borders and the blue-grey infill; (c) detail showing the shallow-up color gradation of the dikes, not accompanied by size gradation.

In detail, the veins show a width up to 10 cm and are characterized by yellow-reddish sandy borders and blue-gray silty-sandy infill (Fig. 5.10 b). It is worth noting that from section 0 to section 9 both the density and the dimensions of the veins reduce. The shallow-up transition from the blue-grey infill of the intrusions to the yellow-brown material which composes the B unit is gradual, but any vertical grain gradation is evident (Fig. 5.10 c). Between sections 2 and 3, the blue-grey vertical veins seem to intrude even unit B. Differently, the arable soil is not affected by intrusions.

In order to investigate the liquefaction potential, the grain size of two infill material samples was investigated at the Geotechnical Lab of the University of Udine. The elaborated particle size curves (Fig. 5.11) show that the collected intruding material well fits the poorly sorted potentially liquefiable grain size (Tshucida and Hayashi. 1971). Conversely, if compared to the well sorted grain size graph (Fig. 5.11 b), only the 50 % of the elaborated curves fit the potentially liquefiable area. However, recent studies focused on textural parameters show that silty sands and silts characterized by relatively high content of fines can also liquefy (Fontana D. et al., 2019). Therefore, also coarse silts and silty sands are fully susceptible to liquefaction. In this regard, it is worth noting that the presence of the Fornace Lakes located less than 100 m South testifies the surficial depth of the water table.

The dating of two samples CAMP13 and CAMP12 were performed by Beta Analytics and provided an age of 19020 ± 30 BP for Ag unit and of 7170 ± 60 BP for the Ag2 (upper gravel) unit (Fig. 5.9).
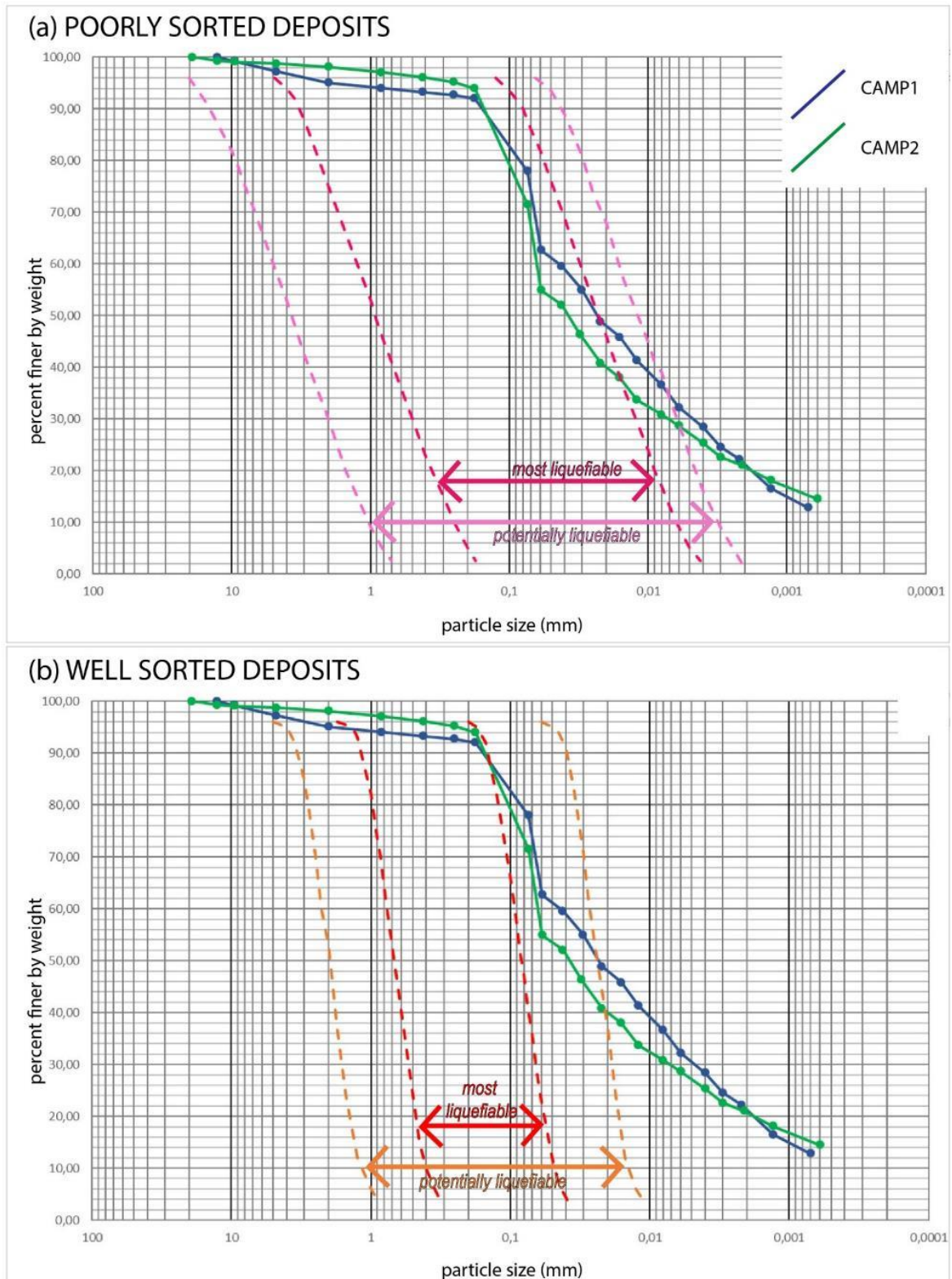
Fig. 5.11 – Size curve of the collected CAMP1 and CAMP2 samples, compared to the potentially liquefiable and most liquefiable (a) poorly sorted and (b) well sorted deposits (Tshucida and Hayashi, 1971).

5.3.2 INTERPRETATION

The realized palaeoseismological trench interested slope colluvial depositional units, as the S-dipping geometry of the pebbly levels testifies. The excavated wall, located 40 m downstream of the outcropping Eocene units, reached a depth of 2.5 m below the surface and no pre-Quaternary bedrock was excavated. Therefore, the downstream thickening of the colluvial body filling the abrupt deepening Eocene turbiditic unit is confirmed. Moreover, the abundant presence of Fe-Mn nodules in the soil testifies that this area is characterized by an impeded drainage, thus favoring alternating wet (reducing) and dry (oxidating) periods.

The pervasive presence of a dense network of dikes and diapirs, clearly interrupting the lateral continuity of the stratigraphy, testifies that this area experienced seismic shaking. Another interesting aspect arises from the upward continuity of the dikes and the silty-sandy unit B, which could represent the upwelled material and thus be interpreted as a sand blow (Tuttle et al., 2019).

The dating of samples CAMP 13 and CAMP 12 testifies that basal silty-sandy unit A deposited between 19020 ± 60 BP and 7170 ± 30 BP. Since sand dikes cut through the entire A unit, the most recent liquefaction event must have occurred later than 7170 ± 30 BP. However, the lack of carbon material useful for the dating of the upper units doesn't help to constrain the time of the latest shaking event.

In the light of these results, no shear surface was detected in the excavated trench. However, the proximity of a tectonic structure, possibly responsible of the shaking which caused liquefaction, is clear. Some attempts regarding the possible strong earthquake responsible for the liquefaction phenomenon in this area was made by considering the historical seismicity (CPTI15) together with the empirical magnitude over distance relationships for liquefaction (Kuribayashi and Tatsuoka, 1975; Ambraseys, 1988; Papadopulos and Lefkopulos, 1993; Galli, 2000) (Fig. 5.12).
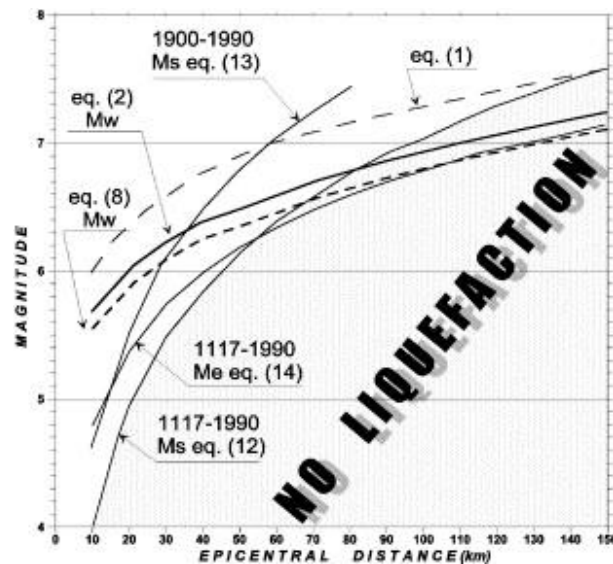
Fig. 5.12 – Comparison among different equations provided by different Authors (from Galli et al., 2000).

(1): Kuribayashi and Tatsuoka (1975); (2): Ambreaseys (1988); (8): Papadopulos and Lefkopulos (1993); (12)

and (14): Galli et al. (2000).

In this context both the 1511 earthquake (Mw 6.3), located at about 15 km NNW (CPTI15), and the seismicity of the 1976 sequence (Mw up to 6.45), located at a distance minor than 30 km, could have induced liquefaction in the Campeglio area.

CHAPTER 6: DISCUSSION

Following the individual previous sections, all results were integrated with the aim to depict a comprehensive seismotectonic model for eastern Friuli region, focused on the characterization of the active faults presently accommodating deformation and able to release strong earthquakes. The interpretation of ENI seismic lines allowed to reconstruct the deep geometry (up to 5 -7 km depth) of the active fault-systems which characterize the study area: Pozzuolo (POTS), Trnovo (TNTS), Susans-Tricesimo (STTS) and Colle Villano-Borgo Faris – Cividale (CV-BFC) Fault-Systems. Particularly, the elaborated 3D-structural model (Chapter 2) well reflects the polyphasic compressional tectonic evolution which affected the study area since late Cretaceous – Paleogene, testifying that each distinct successive tectonic phase superimposed on pre-existing structures. The LGM Friuli Plain subsurface is characterized by the presence of NW-SE trending inherited Dinaric fronts of Pozzuolo (POTS), Trnovo (TNTS) and Susans- Tricesimo (STTS) Thrust-Systems (Fig. 6.1).
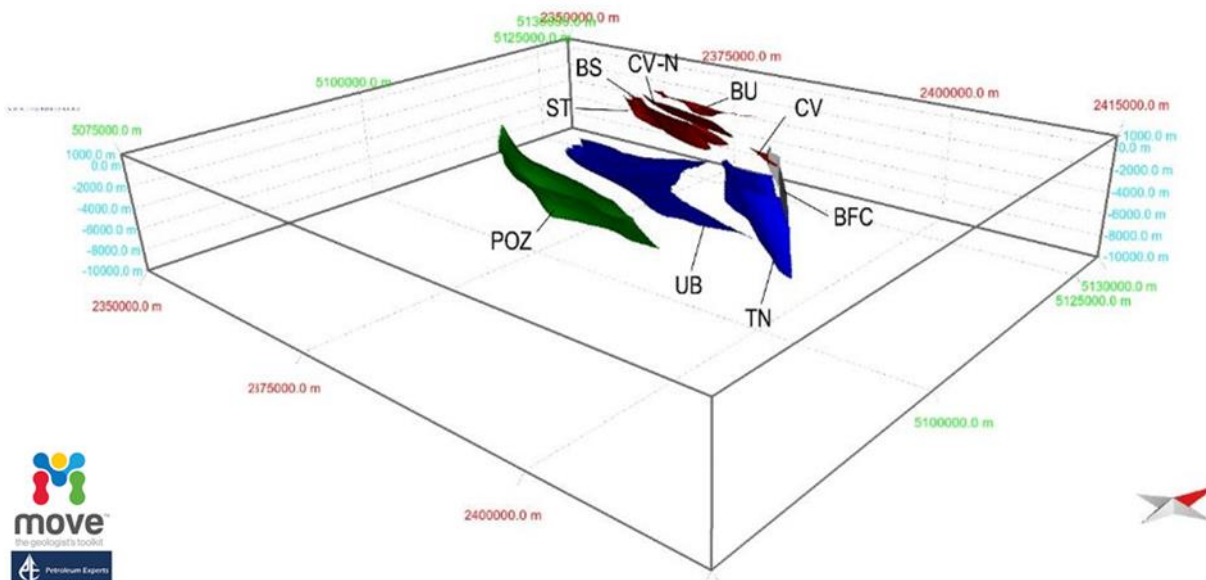

Fig. 6.1 – 3D structural model reconstructed through the interpretation of ENI seismic lines. Green surface: Pozzuolo thrust (POZ); blue surfaces: Udine Buttrio (UB) and Trnovo (TN) Thrusts, grey surfaces: Colle Villano – Borgo Faris – Cividale Fault System and red surfaces: Susans-Tricesimo (ST), Borgo Soima (BS) and Colle Villano (CV) Thrusts.

During the Dinaric phase, STTS and TNTS formed a single structure, the Trnovo Nappe (Placer et al., 2010) and, together with the frontal POTS, accommodated deformation as SW-verging reverse faults under a N30° oriented sigma1 (Doglioni and Bosellini, 1987). These same structures were reactivated during the successive Neoalpine phase, under an almost N-S oriented compression (Zanferrari et al., 2013). Particularly, following the Serravallian-Tortonian event (N340° sigma 1), a kinematic change affected both POTS and TNTS: the inherited lateral ramps were activated as Neoalpine fronts with a reverse kinematics (Terenzano Thrust), while the NW-SE oriented strands (POZ) accommodated deformation with a transpressive kinematics. Since the Mio-Pliocene transition, the combined action of the NW-ward motion of Adria microplate and its counterclockwise rotation caused the activation of dextral motion along the strike-slip fault-systems of western Slovenia and eastern Friuli region (Vrabec and Fodor, 2006). The development of these structures affected the pre-existing reverse planes, by displacing and/or reactivating them. Besides, the inherited Dinaric fronts were still favorably oriented to accommodate deformation with an oblique (NW-SE trending faults) to reverse (E-W oriented strands) kinematics. The ongoing deformation caused the segmentation of the pre-existing reverse planes through the NW-ward propagation of the NW-SE trending strike-slip fault-systems. The CV-BFC transpressive Fault-System represents the NW-ward segment of the Raša strike-slip Fault, which is the westernmost transpressive structure of the dextral strike-slip systems characterizing western Slovenia (Idrija, Raune, Predjama) (Vrabec and Fodor, 2006; Kastelic et al., 2008; Moulin et al., 2014 and 2016; Atanackov et al., 2020).

Although evidence of tectonic activity referable to the frontal thrust-systems (POTS and TNTS) testify the late LGM activity of these structures, many surficial anomalies (both morphological and structural) highlight that the Susans-Tricesimo Thrust-System (STTS)and the Colle Villano-Borgo Faris – Cividale (CV-BFC) Fault-System strongly affect Holocene deposition (Chapter 4). The

estimated late Pleistocene throw rates of the analyzed tectonic structures (Chapters 2 and 4) well match the activity rates of the dextral strike-slip fault-systems reported on the Database of active faults in Slovenia (Atanackov et al., 2021), which range from 0.06-2 mm/yr for the Idrija Fault, 0.05-1.45 mm/yr for the Predjama Fault and 0.23-1.3 mm/yr for the Raša East and West segments. Particularly, the data collected in this study (Table 6.1) highlight that the STTS and CV-BFC are characterized by higher activity rates with respect to POTS and TNTS, suggesting that deformation is mainly released by the inner reverse-oblique to transpressive fault-systems (STTS and CV-BFC) bordering the Julian Prealps rather than the frontal systems (POTS and TNTS).

	Pozzuolo Thrust	Udine-Buttrio Thrust_NW	Udine-Buttrio Thrust_SE	Colle Villano-N Thrust	Borgo Faris-Cividale Fault-System
Late LGM (Remanzacco subsynthem) (22.0 – 19.5 kyr cal BP, Fontana et al., 2014)	0.18 - 0.2 Pozzuolo scarp (4 m)				
Late LGM (Canodusso subsynthem) (23–21 kyr cal BP, Monegato et al., 2007		0.17 – 0.19 Pasian di Prato scarp (4 m)			
LGM (30 kyr)				1 LGM base surface displacement	1.1 LGM base surface displacement
Quaternary (2,58 Myr)	0.14		0.13		

Table 6.1 – Throw rate values (mm/yr) of the main fault systems investigated in this study.

The seismicity distribution well confirms this issue, showing that most of the earthquakes are located beyond the prealpine border (Chapter 3). In western Friuli, slip is presently accommodated

by the ENE-WSW trending Neoalpine fronts bordering the western Carnic Prealps, while moving towards the East seismicity is mainly referable to the structures bordering Julian alpine and prealpine mountain area (STTS and CV-BFC), rather than by the frontal systems of the Friuli Plain (POTS and TNTS). Corresponding to the transition area from the western pure reverse domain of western Friuli and eastern strike-slip domain of western Slovenia, the kinematic model of eastern Friuli here reconstructed (Fig. 6.2 a) testifies that in the study area deformation is presently accommodated by transpressive fault-systems. Across these structures, slip is partitioned between a reverse-oblique component on the high-angle reverse frontal splay and a horizontal dextral component on the subvertical strike-slip faults. In addition, considering the rotating strike of the tectonic structures under the present almost N-S oriented sigma1, the kinematic model here proposed suggests that the eastward transition from pure reverse to pure strike-slip domains occurs through the gradual eastward increase of the horizontal component and the mutual eastward decrease of the reverse component. Particularly, the hypocentral seismicity distribution depicts a NW-ward widening seismogenic volume, matching at depth the STTS, and revealed the presence of a subvertical inner plane (VDR) (Chapter 3). Considering the structural setting of the area, many interpretations for this subvertical structure are possible. It could represent the NW-ward propagation of the Predjama dextral strike-slip Fault (PRJ) or alternatively, if taking into account the E-W oriented band of PRJ towards the NW, the detected subvertical fault can be interpreted as the right step of the Borgo Faris – Cividale strike-slip Fault. The third option contemplates the possibility that VDR represents the NW propagation of the inner Raša Fault (RS).
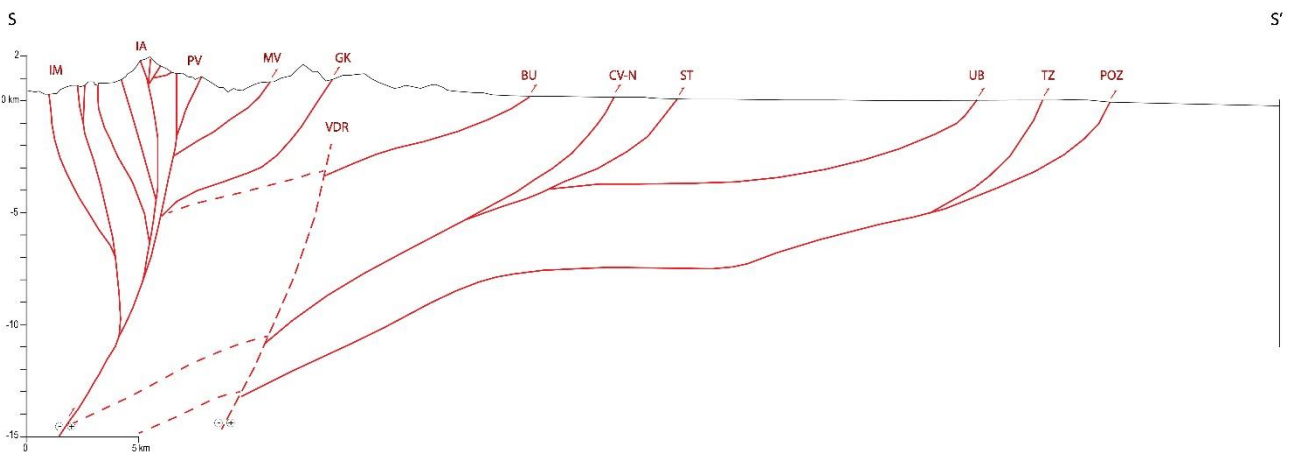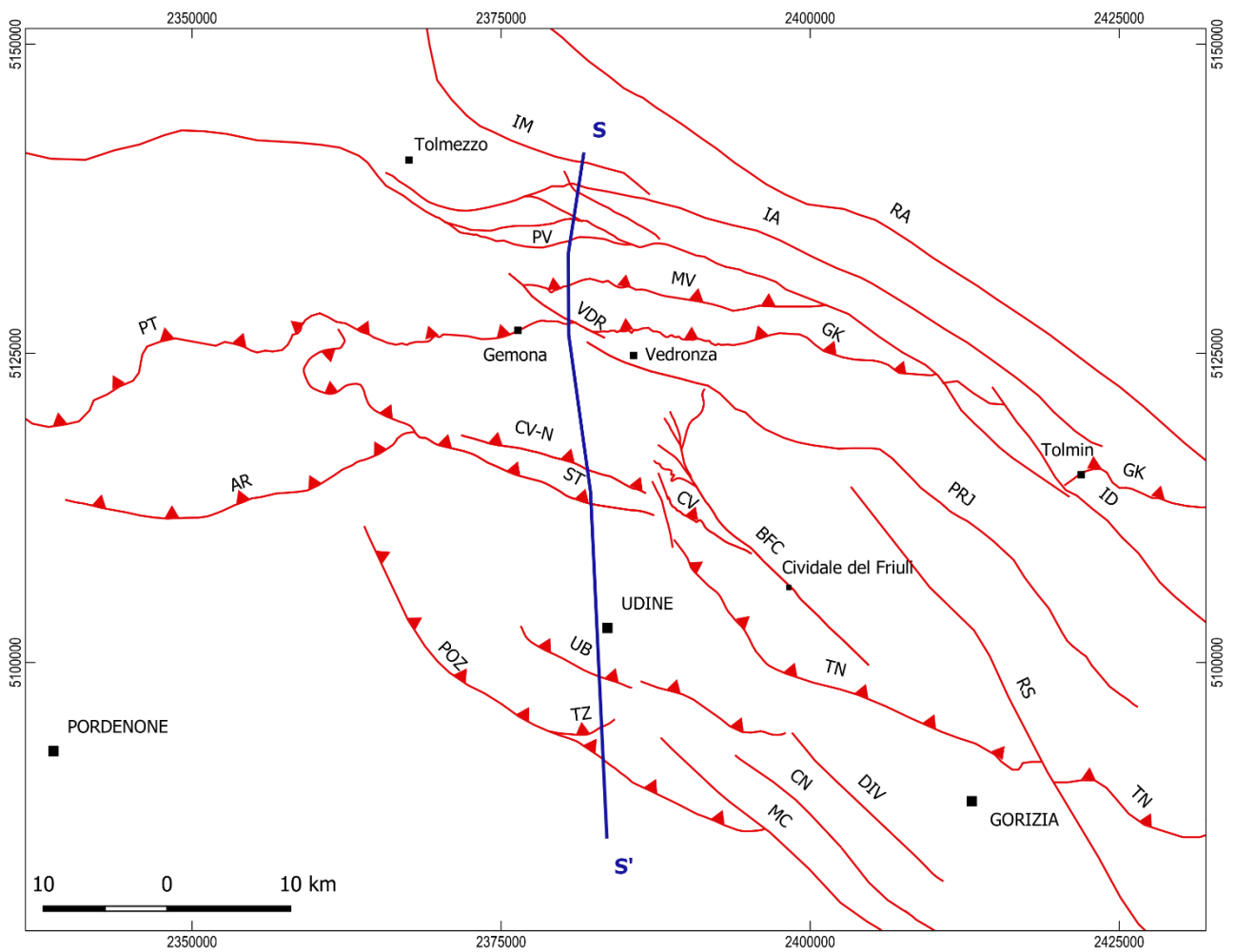
Fig. 6.2 – (a) Kinematic model of eastern Friuli region. (b) N-S oriented SS' structural cross section (modified after Poli and Zanferrari, 2018), explanation in the text. Faults acronyms: AR: Arba-Ragogna Th; BFC: Borgo Faris-Cividale Ft, CN: Colle Nero Ft, CV-N: Colle Villano-North Th, CV: Colle Villano Thrust; DIV: Divača Ft, GK: Gemona-Kobarid Th, IA: Idrija-Ampezzo Ft, ID: Idrija Ft; IM: Idrija-Moggio Ft, MC: Monte Cosici Ft, MV: Musi-Verzegnis Th; POZ: Pozzuolo Th; PRJ: Predjama Ft; PT: Periadriatic Th; PV: Pioverno Fault; RA: Raune Ft; RS: Raša Ft; ST: Susans-Tricesimo Th, TN: Trnovo Th, UB: Udine-Buttrio Th, VDR: Vedronza Ft.

In any case, the presence of a subvertical NW-SE oriented structure testifies the recent-to-current NW-ward deep propagating of the dextral strike-slip fault-system of western Slovenia – eastern Friuli region, which affects the pre-existing NNE-dipping reverse/oblique structures like STTS. As a matter of fact, based on the hypocentral location of the events, the interaction at depth of the imbricate STTS with the detected subvertical plane VDR can be hypothesized, in good agreement with the transpressive seismotectonic model proposed by Poli and Zanferrari (2018) for the study area (Fig. 6.2 b).

Following the reconstruction of the structural setting of eastern Friuli, the additional goal of this work was the characterization of the seismogenic potential of the study area. The Susans-Tricesimo Thrust System is considered the surficial expression of the seismogenic source responsible of the M 6.4 mainshock of May 1976 (Galadini et al., 2005). Currently, the updated DISS 3.2.1 version (http://diss.rm.ingv.it/dissmap/dissmap.phtml) displays the Susans-Tricesimo source segmented into two individual sources, Gemona South and Tarcento (Burrato et al., 2008). They both belong to the Composite Seismogenic Source of Gemona-Tarcento, extending South up to Cividale del Friuli.

The seismotectonic analysis conducted in this study allows to hypothesize two different and partly new scenarios in terms of seismogenic sources, with implications regarding the source of the May 1976 sequence. Both scenarios are based on the interaction between the frontal NE-dipping planes of STTS with the subvertical fault highlighted by the hypocentral distribution analysis (VDR). The interaction depth is always located at the base of the seismogenic thickness (13.5 km depth), however an abrupt increase of seismicity at depth greater than 7 km is testified by the distribution frequency histogram (Fig. 3.2, Chapter 3). This depth value can be interpreted as the depth where the subvertical fault connects to the reverse inner front of STTS (Colle Villano-N Thrust).

- In the first hypothesis (Fig. 6.3 a) two distinct seismogenic sources characterize the study area: CV-BFC and ST-DVR. Along the southeastern Julian Prealpine border, the Colle Villano

– Borgo Faris-Cividale transpressive Fault-System is interpreted as the surficial expression of a single transpressive seismogenic source, probably responsible of the 1511 earthquake (Falcucci et al., 2018). The CV-BFC source extends for a total length of 25 km, thus capable of a Mmax 6.7 (Wells and Coppersmith, 1994) and then consistent with the 1511 released potential. Regarding the NW portion of the study area, this hypothesis considers ST and DVR as a positive flower structure, representing the surficial expression of a single transpressive source (ST-DVR, Fig. 6.3 a). In this context, the transpressive source model proposed by Falcucci et al. (2018) for the CV-BFC can tentatively be adopted for the ST-DVR source. However, the definition of seismogenic sources in transpressive (or transtensive) domains is still a matter of debate and many aspects concerning the source-to-fault relationship are worth to be explored. Particularly, in order to properly define the transpressive seismogenic source (in terms of geometric and kinematic parameters), the location of the depth interaction between the strike-slip fault and the frontal splay within or rather at the top of the seismogenic thickness could represent a fundamental issue in terms of seismogenesis. A further aspect which is worth to explore concerns the surficial volume affected by an earthquake originated on the deep source, and the possible activation of both the strike-slip and the reverse splay. This aspect certainly has important implications in terms of seismic hazard assessment.
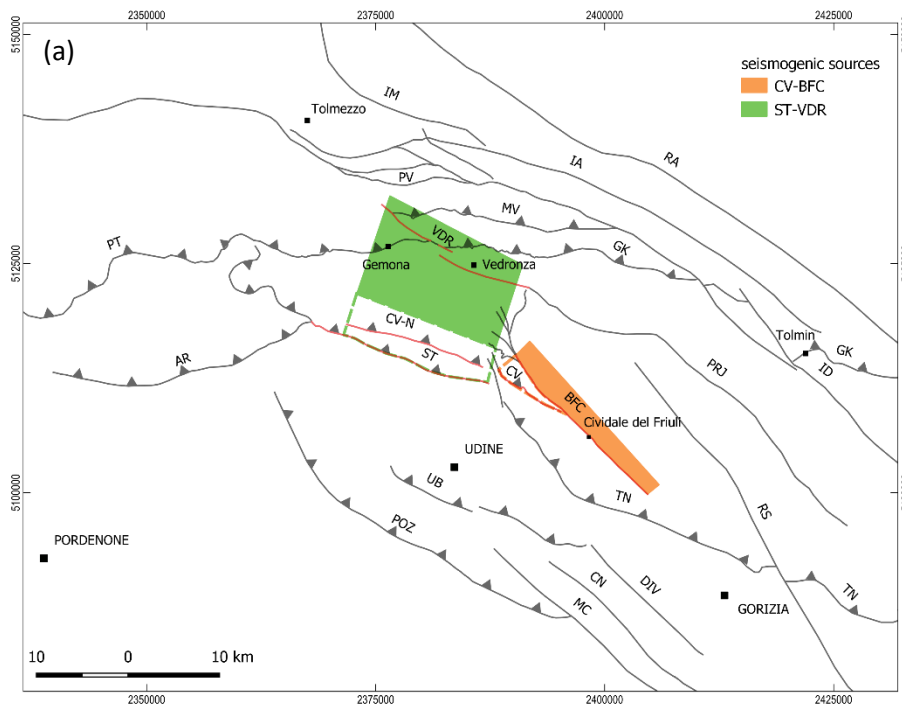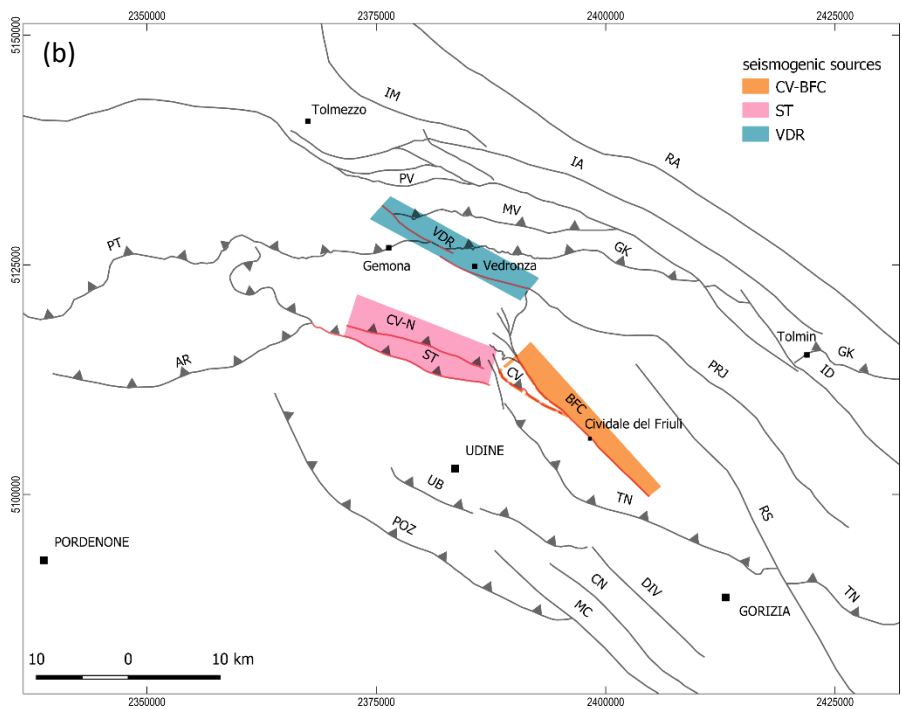
Fig. 6.3 – schematic representation of the seismogenic sources elaborated for the study area considering two different scenarios (a) and (b).

- The second hypothesis is consistent with the presence of three seismogenic sources: CV-BFC, as previously described, ST and VDR (Fig. 6.3 b). ST source is characterized by a length (SRL) of 15 km and extends deep up to 13.5 km depth, in analogy with the ST source proposed by Galadini et al. (2005). Based on the measured geometric source parameters, a

Mmax of 6.4 can be estimated for ST through the Wells and Coppersmith (1994) empirical relationship. This seismogenic potential value is comparable to both the M 6.3, 1511 events and the M 6.4 mainshock of May 1976. The palaeoseismological study conducted in this study across the Colle Villano-N Thrust allowed to confirm the recent activation of the structure, highlighting at least two deformative episodes (Section 5.2, Chapter 5). The most recent event possibly occurred in historical times, being compatible both with the 1511 and 1976 events. However, the hypocentral distribution analysis of the 1976 sequence strongly testifies the activation of a NNE-dipping reverse plane with only a minor oblique component (section 3.3, Chapter 3), referable to the STTS. In this scenario, ST and VDR are considered two distinct structures and the definition of VDR as an independent source is evaluated, even though it is scarcely constrained and has no association with a strong earthquake. In this view, the DVR source represents the most recent NW-ward deep propagating segment of the dextral strike-slip fault-system of western Slovenia and eastern Friuli region. The development of this structure certainly interferes with the elder source of ST, which is still favourably oriented to accommodate deformation. As a matter of fact, the interaction between the two structures is located where the tectonic systems change their strike (Fig. 6.2). In addition, it is worth to note that the M 4.5 foreshock of 06/05/1976 is located on the DVR structure (Fig. 3.6, Section 3.2.2, Chapter 3). Therefore, the activation of the DVR source during the earliest 1976 sequence can be hypothesised, and the possibility that its activation could have triggered the ST source, responsible of the mainshock of May 1976, must be taken into account. Differently, the seismicity distribution of the second part of the sequence (September-December 1976) are mainly referable to high-angle inner planes (Section 3.2, Chapter 3), suggesting the activation of a deeper source and the involvement of the Idrija-Ampezzo Fault System.

Based on the results of this study, which strongly highlight the inheritance of preexisting structures and their interaction with the newly developing systems, the second hypothesis can be considered more representative of the proposed seismotectonic model.

CONCLUSIONS

This thesis project aimed at the seismotectonic characterization of the eastern Friuli region, with particular focus on the area between the High Friuli Plain and the Julian prealpine border. The used multidisciplinary methodology followed a multilayer approach, spanning from the investigation of the 3D deep structural setting of the upper crustal volume (up to 15 km depth) to the detection of the surficial evidence related to the recent activity of the tectonic structures. In detail, the study was articulated in four sections, each one aiming to a specific goal.

- The first part of this study aimed to reconstruct the 3D-model of the NE Friuli Plain. The structural setting of the NE Friuli Plain was updated through the interpretation of dense grid of industrial seismic lines gently supplied by ENI. Four active Thrust-Systems were characterized: the Pozzuolo (POTZ), Trnovo (TNTS), Susans Tricesimo (STTS), and Colle Villano-Borgo Faris-Cividale (CV-BFC). Tectonic structures clearly show a polyphasic evolution in response to distinct successive tectonic phases affecting the NE Italy up to Present.

- The second part of this study focused on the analysis of the instrumental seismicity (1976-1977 and 1978-2019) collected by the OGS-TS. Hypocentral distribution clearly shows that seismicity affects the Southalpine crust for about 12-15 km in depth. Seismicity develops in the external fronts by means of the activation of a set of WNW-ESE striking middle angle reverse faults mainly corresponding to the Susans Tricesimo Thrust System. Moving towards the inner portion of Julian Prealps, a set of high angle to subvertical faults accommodates deformation.

- The third part of this study aimed at investigating the recent activity of the analyzed tectonic structures through the detection of the surficial evidence related to tectonic activity. The

morphotectonic survey allowed both to validate the recent activity of the Pozzuolo Thrust System and the Udine-Buttrio Thrust, and to collect new data related to the CV-N Thrust and BFC Fault-System. The estimated LGM throw rates within the whole study area range from 0,17 - 0,2 mm/yr calculated for the frontal Pozzuolo (POZ1) Thrust and Udine-Buttrio Thrust (UB) to the about 1 mm/yr estimated for the CV-N Thrust and BFC Fault-System.

- The fourth part of this study investigated the potential surface rupturing along the CV-N and CV-BFC structures. Two palaeoseismological trenches were dug across the surficial trace of these faults. Particularly, the excavated wall of the Fraelacco trench cut through a reverse plane responsible for a vertical displacement of 30 cm, cumulated during 2 or 3 events occurred in the last 23-21 ky. Differently, the Campeglio trench revealed the presence of secondary coseismic effects (palaeoliquefaction features) testifying that the area experienced seismic shaking.

Based on these results, the seismotectonic model here proposed shows that the upper crustal volume of eastern Friuli presently accommodates deformation through transpressive motion. In detail, the Pliocene-Quaternary strike-slip fault-systems presently control deformation, both displacing and re-activating the frontal splays. In this regard the segmentation of the Colle Villano structure into two different strands can be assessed: a southern segment presently representing the transpressive splay of the Borgo Faris Cividale Fault System and a northern Colle Villano-N segment, referable to the Susans Tricesimo Thrust System. Moreover, the strong interaction at depth between the frontal Susans- Tricesimo Thrust System and a subvertical deep structure (VDR) is highlighted. In this context, the association for both sources with one strong earthquake can be considered: the 1511 event for the CV-BFC structure (as already proposed by Falcucci et al., 2018) and the May 1976 earthquake for the ST source. It is worth noting that the September 1976

seismicity involved high-angle structures deeply connected to the Idrija-Ampezzo Fault-System that at present plays as backstop for the whole crustal volume of the study area.

Slip partitioning across oblique systems is documented in many areas from across the world (Wesnousky and Jones, 1994; Walker et al., 2003; King et al., 2005; Gulik et al., 2013; Fitzgerald et al., 2014; Vallage et al., 2014; Bemis et al., 2015; Koehler and Carver, 2018). In this context, the right step between BFC and VDR structures surely represents a key point within the seismotectonic framework of eastern Friuli. Further investigation dealing with the parametrization of VDR and the understanding of its mutual relationship with the frontal reverse structures would better clarify how the slip is partitioned along the continuously rotating transpressive system. Finally, this study highlights the surficial effects of the active faults of eastern Friuli, testifying that they are not necessarily buried. Therefore, additional morphotectonic and palaeoseismological investigation certainly represent the future developments of this study, with the aim to further explore the surface rupturing potential of the active faults of eastern Friuli.

REFERENCES

Álvarez-Gómez, J. A.; 2019: *FMC—Earthquake focal mechanisms data management, cluster and classification.* SoftwareX, **9**, 299-307.

Ambraseys N.N; 1991. *Engineering seismology*. Int. J. Earthquake Eng. Struct. Dyn., **17**, 1-105.

Amato A., Barnaba P.F., Finetti I., Groppi G., Martins B. and Muzzin A.; 1976: *Geodynamic outline and seismicity of Friuli Venetia Julia region.* Boll. Geof. Teor. Appl., **18**, 217-256.

Aoudia A., Saraò A., Bukchin B. and Suhadolc P.; 2000: *The 1976 Friuli (NE Italy) thrust faulting earthquake: a reappraisal 23 years later.* Geophys. Res. Lett., **27**, 573-576.

Arachchi, L. P., Tokashiki, Y., & Baba, S.; 2004. *Mineralogical characteristics and micromorphological observations of brittle/soft Fe/Mn concretions from Okinawan soils*. Clays and clay minerals, **52(4)**, 462-472.

Atanackov J., Jamšek Rupnik J., Jež P., Celarc B., Novak M., Milanič B., Markelj A., Bavec M. and Kastelic V.; 2021. *Database of active faults in Slovenia: compiling a new active fault database at the junction between the Alps, the Dinarides and the Pannonian Basin tectonic domains*. Front. Earth. Sci., doi: 10.3389/feart.2021.604388.

Bajc J., Aoudia A., Saraò A. and Suhadolc P.; 2001: *The 1998 Bovec-Krn mountain (Slovenia) earthquake sequence.* Geophys. Res. Lett., **28 (9)**, 1839-1842.

Bavec M., Atanackov J., Celarc B., Hajdas I., Jamšek R., Jež J., Kastelic V., Milanič B., Novak M., Skaberne G. and Žibret G.; 2013: *Evidence of Idrija fault seismogenic activity during the Late Holocene including the 1511 Mm 6.8 earthquake.* In Grützner C., Rudersdorf A., Pérez-López and Reicherter K. (eds): Proceedings of the 4th International INQUA Meeting on Paleoseismology, Active Tectonics and Archeoseismology (PATA), 9-14 October 2013, Aechen, 23-26, ISBN: 987-3-00-042796-1.

Bechtold M., Battaglia M., Tanner D.C. and Zuliani D.; 2009: *Constraints on the active tectonics of the Friuli/NW Slovenia area from CGPS measurements and three-dimensional kinematic modeling*. J. Geophys. Res., **114**, B03408, DOI 10.1029/2008JB005638.

Bemis S.P., Weldon R.J. and Carver G.A.; 2015: *Slip partitioning along a continuously curved fault: Quaternary geologic controls on Denali fault system slip partitioning, growth of the Alaska Range, and the tectonics of south-central Alaska.* Litosphere, **7**, 235-246, doi: 10.1130/L352.1.

Bernardis G., Poli M.E., Snidarcig A. and Zanferrari A.; 2000: *Seismotectonic and macroseismic characteristics of the earthquake of Bovec (NW Slovenia: April 12, 1998).* Boll. Geof. Teorica Appl., **41 (2)**, 133-148.

Bosellini A., Masetti D. and Sarti M.; 1981: *A Jurassic "Tongue of Ocean" infilled with oolitic sands: the Belluno trough, Venetian Alps, Italy.* Marine Geol., **44**, 59-95.

Bressan G., Barnaba C., Bragato P., Ponton M. and Restivo A.; 2018: *Revised seismotectonic model of NE Italy and W Slovenia based on focal mechanism inversion*. J. Seismol., DOI: https://doi.org/10.1007/s10950-018-9785-2.

Burrato P.; Poli M.E., Vannoli P., Zanferrari A., Basili R. and Galadini F.; 2008: *Sources of Mw 5+ earthquakes in northeastern Italy and western Slovenia: an updated view based on geological and seismological evidence.* Tectonophysics, **453 (1-4)**, 157-176, DOI https://doi.org/10.1016/j.tecto.2007.07.009.

Buser S.; 1989: *Development of the Dinaric and the Julian carbonate platforms and of the intermediate Slovenian basin (NW Yugoslavia).* Mem. Soc. Geol. It., **40**, 313-320.

Cagnetti V. and Console R.; 1977: *Space-time distribution of the Friuli (1976) earthquake.* Ann. Geofis., **30**, 107-183.

Camassi R., Caracciolo C.H., Castelli V., and Slejko D.; 2011: *The 1511 Eastern Alps earthquakes: a critical update and comparison of existing macroseismic datasets.* J. Seismol., **15**, 191-213, DOI: 10.1007/s10950-010-9220-9.

Caputo R.; 1996: *The polyphase tectonics of eastern Dolomites, Italy.* Memorie di Science Geologiche, **48**, 93-106.

Caputo R. and Hally B., 2008: *The use of distinct disciplines to investigate past earthquakes.* Tectonophysics, **453**, 7-19, doi:10.1016/j.tecto.2007.05.007.

Caputo R., Poli M.E. and Zanferrari A.; 2010: *Neogene-Quaternary stratigraphy of the eastern Southern Alps, NE Italy*. J. Struct. Geol., **32**, 1009-1027, DOI 10.1016/j.jsg.2010.06.004.

Carulli G.B.; 2006: *Carta geologica del Friuli Venezia Giulia alla scala 1:150.000.* Regione Autonoma Friuli Venezia Giulia – Direzione centrale ambiente ed energia – Servizio Geologico. S.E.L.C.A. Firenze.

Cassola Guida P. and Calosi M.; 2012: *Una sepoltura monumentale dell'antica età del bronzo: il tumulo di Sant'Osvaldo (Udine). Scavi 2000-2002 –* In: Studi e ricerche di protostoria mediterranea, (Quasar Eds), pp. 208. Isbn: 978-887140-461-5.

Castellarin A., Cantelli L., Fesce A.M., Mercier J.L., Picotti V., Pini G.A., Prosser G. and Selli L.; 1992: *Alpine compressional tectonics in the Southern Alps. Relationships with the N-Apennines.* Annales Tectonicae, **6**, 62-94.

Castellarin A. and Cantelli L.; 2000: *Neo-Alpine evolution of the Southern Eastern Alps*. J. Geodyn., **30**, 251-274.

Castellarin A., Nicolich R., Fantoni R., Cantelli L., Sella M. and Selli L.; 2006: *Structure of the lithosphere beneath the Eastern Alps (southern sector of the TRANSALP transect).* Tectonophysics, **414**, 259-282, DOI 10.1016/j.tecto.2005.10.013.

Cati A., Sartorio D. and Venturini S.; 1987: *Carbonate platforms in the subsurface of the northern Adriatic area.* Mem. Soc. Geol. Ital., **40**, 295-308.

Cheloni D., D'Agostino N., D'Anastasio E. and Selvaggi G.; 2012: *Reassessment of the source of the 1976 Friuli, NE Italy, earthquake sequence from the joint inversion of high-precision levelling and triangulation data.* Geophys. J. Int., **190**, 1279-1294, DOI 10.1111/j.1365-246X.2012.05561.x.

Colautti D., Finetti I., Nieto D., Pupis., Russi M., Slejko D. and Suhadolc P.; 1976: *Epicenter distribution and analysis of 1976 earthquakes and aftershocks of Friuli.* Boll. Geof. Teor. Appl., **18**, 457-548.

Comel A.; 1947: *Una nuova concezione sull'origine dei terrazzi prewürmiani friulani.* In Alto, s. 2, **44 (2)**, 1-9.

Comel A.; 1955: *Monografia sui terreni della pianura friulana II. Genesi della pianuracentrale connessa all'antico sistema fluvioglaciale del Tagliamento.* N. Ann. Ist. Chim. Agr. Sperim. Gorizia, **6**, 216 pp.

Cousin M.; 1981: *Les rapports Alpes-Dinarides. Les confines de l'Italie et de la Yugoslavie.* Soc. Géol. Nord., **5 (I-II)**, 521 pp.

D'Agostino N., Cheloni D., Mantenuto S., Selvaggi G., Michelini A. and Zuliani D.; 2005: *Strain accumulation in the southern Alps (NE Italy) and deformation at the northeastern boundary of Adria observed by CGPS measurements.* Geophys. Res. Lett., **32**, L19306, DOI 10.1029/2005GL024266.

D'Argenio B. and Alvarez W.; 1980: *Stratigraphic evidence for crustal thickness changes on the southern Tethyan margin during the Alpine cycle.* GSA Bulletin, **91 (12)**, 681-689, https://doi.org/10.1130/0016-7606(1980)91<681:SEFCTC>2.0.CO;2.

DISS Working Group (2018). *Database of Individual Seismogenic Sources (DISS), Version 3.2.1: A compilation of potential sources for earthquakes larger than M 5.5 in Italy and surrounding areas.* http://diss.rm.ingv.it/diss/, Istituto Nazionale di Geofisica e Vulcanologia, DOI: 10.6092/INGV.IT-DISS3.2.1.

Devoti R., Esposito A. Pietrantonio G., Pisani A.R and Riguzzi F.; 2011: *Evidence of large scale deformation patterns from GPS data in the Italian subduction boundary.* Earth Planet. Sci. Lett., **311**, 230-241, DOI 10.1016/j.epsl.2011.09.034.

Doglioni C. and Bosellini A.; 1987: *Eoalpine and mesoalpine tectonics in the Southern Alps.*Geol. Rundsch., **76**, 735-754.

Falcucci E., Poli M.E., Galadini F., Scardia G., Paiero G. and Zanferrari A.; 2018: *First evidence of active transpressive surface faulting at the front of the Eastern Southern Alps, northeastern Italy. Insight on the 1511 earthquake seismotectonics*. Solid Earth, **9**, 911-922, DOI https://doi.org/10.5194/se-9-911-2018.

Fantoni R., Catellani D., Merlini S., Rogledi S. and Venturini S.; 2002: *La registrazione degli eventi deformativi cenozoici nell'avampaese Veneto-Friulano*. Mem. Soc. Geol. It., **57**, 301-313.

Feruglio E.; 1925c: *La zona delle risorgive del basso Friuli tra il Tagliamento e il Torre. Parte I: descrizione geologica e litologica.* Annali Staz. Chim. Agr. Sperim. Udine, **3 (1)**, 1-343.

Finetti I., Giorgetti F., Haessler H., Hoang Trong P., Slejko D. and Wittlinger G.; 1976: *Time space epicenter and hypocenter distribution and focal mechanism of 1976 Friuli earthquakes*. Boll. Geof. Teor. Appl., **18**, 637-655.

Fitzgerald P.G., Roeske S.M., Benowitz J.A., Riccio S.J., Perry S.E. and Armstrong P.A.; 2014: *Alternating asymmetric topography of the Alaska range along the strike-slip Denali fault: strain partitioning and lithospheric control across a terrane suture zone.* Tectonics, **33**, 1519-1533, doi: 10.1002/2013TC003432.

Fitzko F., Suhadolc P., Aoudia A. and Panza G.F.; 2005: *Constraints on the location and mechanism of the 1511 Western-Slovenia earthquake from active tectonics and modeling of macroseismic data.* Tectonophys., **404**, 77-90, doi: 10.1016/j.tecto.2005.05.003.

Fontana A.; 1999: *Aspetti geomorfologici dell'area di Sammardenchia.* In: Ferrari A., Pessina A., (Eds.), Samardenchia – Cueis, Contributi per la conoscenza di una comunità del Primo Neolitico. Monografie Museo Friulano Storia Naturale, **41**, 11-22.

Fontana A., Mozzi P. and Bondesan A.; 2004: *L'evoluzione geomorfologica della pianura veneto-friulana.* In: Bondesan A., Meneghel M. (a cura di), Note illustrative della Carta geomorfologica della provincia di Venezia, Esedra, 113-138.

Fontana A., Mozzi P. and Bondesan A.; 2010: *Late pleistocene evolution of the Venetian-Friulian Plain.* Rend. Fis. Acc. Lincei, **21**, S181-S196. DOI: 10.1007/s12210-010-0093-1.

Fontana A., Monegato G., Devoto S., Zavagno E., Burla I. and Cucchi F.; 2014a: *Geomorphological evolution of an Alpine fluvioglacial system at the LGM decay: the Cormor type megafan (NE Italy).* Geomorphology, **204**, 136-153.

Fontana A., Mozzi P. and Marchetti M.; 2014b: *Alluvial fans and megafans along the southern side of the Alps.* Sediment. Geol., **301**, 150-171, DOI http://dx.org/10.1016/j.sedgeo.2013.09.003.

Fontana A., Monegato G., Rossato S., Poli M.E., Furlani S and Stefani C., 2019. *Carta delle Unità Geologiche della Pianura del Friuli Venezia Giulia alla scala 1:150.000.* Regione Autonoma Friuli Venezia Giulia, Direzione centrale ambiente ed energia, Servizio Geologico, Trieste, Italy.

Galadini F., Poli M.E: and Zaferrari A.; 2005: *Seismogenic sources potentially responsible for earthquakes with M≥6 in the eastern Southern Alps (Thiene-Udine sector, NE Italy).* Geophys. J. Int., **161**, 739-762, DOI 10.1111/j.1365-246X.2005.02571.x.

Galli P.; 2000: New empirical relationships between magnitude and distance for liquefaction. Tectonophysics, 324, 169-187.

GEO-CGT; 2008: *Carta di sintesi geologica alla scala 1:10.000* and *Rapporto finale -* Progetto GEO-CGT. Foglio 067-"Cividale del Friuli". Regione Autonoma Friuli Venezia Giulia.

Ghielmi M., Minervini M., Nini C., Rogledi S., Rossi M. and Vignolo A.; 2010. *Sedimentary and tectonic evolution in the Po-Plain and northern Adriatic Sea area from Messinian to Middle Pleistocene (Italy).* Rend. Fis. Acc., Lincei, suppl., **21**, 131-166.

Grützner C., Aschenbrenner S., Rupnik P.J., Reicherter K., Saifelislam N., Včič B., Vrabec M., Welte J. & Ustaszewski K. 2021. *Holocene surface rupturing earthquakes on the Dinaric Fault System, western Slovenia.* Solid Earth Discussion, [preprint], http://doi.org/10.5194/se-2021-7.

Gulick S.P.S., Reece R.S., Christeson G.L., van Avendonk H., Worthington L.L. and Pavlis T.L.; 2013: *Seismic images of the Transition fault and the unstable Yakutat-Pacific-North American triple junction.* Geology, **41 (5)**, 571-574, doi: 10.1130/G33900.1.

Gutenberg B. and Richter C.F; 1942: *Earthquake magnitude, intensity, energy, and acceleration.* Bull. Seismol. Soc. Am., **32(3)**, 163-191.

Kastelic V., Vrabec M., Cunningham D. and Gosar A.; 2008: *Neoalpine structural evolution and present day tectonic activity of the eastern Southern Alps: the case of the Raune fault, NW Slovenia.* J. Structural Geol., **30**, 963-965, DOI 10.1016/j.jsg.2008.03.009.

King G., Klinger Y., Bowman D. and Tapponnier P.; 2005: *Slip-partitioned surface breaks for the Mw 7.8 2001 Kokoxili earthquake, China.* Bull. Seism. Soc. Am., **95 (2)**, 731-738, doi: 10.1785/0120040101.

Koehler R.D., Carver G.A. and Alaska Seismic Hazard Safety Commission; 2018: *Active faults and seismic hazards in Alaska.* Alaska Division of Geological and Geophysical Surveys Miscellaneous Publication 160, 59 pp, http://doi.otg/10.14509/29705.

Kuribayashi E., Tatsuoka F.; 1975: *Bried review of liquefaction during earthquakes in Japan.* Soil and Foundations, **15**, 81-92.

Mancin N., Barbieri C., Di Giulio A., Fantoni R., Marchesini A., Toscani G. and Zanferrari A., 2016: *The Friulian-Venetian Basin II: paleogeographic evolution and subsidence analysis from micropaleontological constraints.* Ital. J., Geosci., **135 (3)**, 460-473, DOI 10.3301/IJG.2015.35.

Martinis B.; 1977: *Studio geologico dell'area maggiormente colpita dal terremoto friulano del 1976.*

Márton, E., Cosovic, V., Drobne, K. and Moro, A.; 2003. *Palaeomagnetic evidence for Tertiary counterclockwise rotation of Adria*. Tectonophysics, **377**, 143-156.

Masetti D., Fantoni R., Romano R., Sartorio D. and Trevisani E.; 2012: *Tectonostratigraphic evolution of the Jurassic extensional basins of the eastern southern Alps and Adriatic foreland based on an integrated study of surface and subsurface data.* Am. Assoc. Pet. Geol. Bull., **96 (11)**, 2065-2089.

Massari F., Grandesso P., Stefani C. and Jobstraibizer PG.; 1986: *A small polyhistory basin evolving in a context of oblique convergence: the Venetian basin (Chattian to Recent, Southern Alps, Italy).* In: Foreland Basins (P.A. Allen and P. Homewood Eds.), Spec. Publ. Int. Assoc. Sedimentol., **8**, Blackwell Scientific Oxford, 141-168.

Merlini S., Doglioni C., Fantoni R., and Ponton M.; 2002: *Analisi strutturale lungo un profilo geologico fra la linea Fella-Sava e l'avampaese adriatico (Friuli - Venezia Giulia - Italia).* Mem. Soc. Geol. It., **57**, 293-300.

Monegato G.; 2006: *Le successioni conglomeratiche messiniano-pleistoceniche nel bacino del fiume Tagliamento.* Ph.D. thesis, University of Udine, 160 pp.

Monegato G., Ravazzi C., Donegana M., Pini R., Calderoni G. and Wick L.; 2007: *Evidence of a two-fold glacial advance during the last glacial maximum in the Tagliamento end moraine system (eastern Alps).* Quaternary Research, **68**, 284-302.

Monegato G., Stefani C. and Zattin M.; 2010: *From present rivers to old terrigenous sediments: the evolution of the drainage system in the eastern Southern Alps.* Terra Nova, **22(3)**, 218-226, DOI 10.1111/j.1365-3121.2010.00937x.

Monegato G. and Poli M.E.: 2015: *Tectonic and climatic inferences from the terrace staircase in the Meduna valley, eastern Southern Alps, NE Italy*. Quaternary Research, **83**, 229–242.

Monegato G. and Stefani C.; 2011: *Preservation of a long-lived fluvial system in a mountain chain: the Tagliamento Valley (southeastern Italian Alps).* In: Davidson S.K., Leleu S. and North C.P. (eds), From River to Rock Record: The Preservation of Fluvial Sediments and their Subsequent Interpretation, SEPM Spec. Publ., **97**, 359-374.

Monegato G. and Vezzoli G.; 2011: *Post-Messinian drainage changes triggered by tectonic and climatic events (eastern Southern Alps, Italy.* Sediment. Geol., **239 (3-4)**, 188-198, doi:10.1016/j.sedgeo.2011.06.012.

Moulin A., Benedetti L., Gosar A., Rupnik P.J., Rizza M., Bourlès D. and Ritz J.; 2014: *Determining the present-day kinematics of the Idrija fault (Slovenia) from aiborne LiDAR topography.* Tectonophysics, **628**, 188-205, DOI http://dx.doi.org/10.1016/j.tecto.2014.04.043.

Moulin A., Benedetti L., Rizza M., Rupnik P.J., Gosar A., Bourlès D., Keddadouche K., Aumaitre G., Arnold M., Guillou V. and Ritz J.-F.; 2016: *The Dinaric fault system: large-scale structure, rates of slip, and Plio-Pleistocene evolution of the transpressive northeastern boundary of the Adria microplate*. Tectonics, **35**, DOI 10.1002/2016TC004188.

Moulin, A., & Benedetti, L.; 2018: *Fragmentation of the Adriatic promontory: New chronological constraints from Neogene shortening rates across the Southern Alps (NE Italy).* Tectonics, **37(9)**, 3328-3348.

Neri C., Gianolla P., Furlanis S., Caputo R and Bosellini A.; 2007: *Geological map and explanatory notes of the Geological Map of Italy at the scale 1:50.000: sheet 029 "Cortina d'Ampezzo".* APAT – Regione Veneto, http://www.isprambiente.gov.it/Media/carg/29_CORTINA_DAMPEZZO/Foglio.html.

Nicolich R., Della Vedova B., Giustiniani M. and Fantoni R.; 2004: *Carta del sottosuolo della Pianura Friulana (Map of subsurface of the Friuli Plain).* Regione Autonoma Friuli Venezia Giulia, Direzione Centrale Ambiente e Lavori Pubblici, Servizio Geologico, 32 pp.

OGS-CRS: *Friuli Venezia Giulia Seismometric Network Bulletin*. http://www.crs.inogs.it/bollettino/RSFVG/RSFVG.en.html.

Papadopoulos G.A. and Lefkopulos G.; 1993: *Magnitude-distance relations for liquefaction in soil from earthquakes.* Bull. Seism. Soc. Am., **83**, 925-938.

Patricelli, G. and Poli, M. E.; 2020: *Quaternary tectonic activity in the north-eastern Friuli Plain (NE Italy)*. Boll. Geof. Teor. Appl., **61(3)**, 309-332, DOI 10.4430/bgta0319.

Peruzza L., Poli M.E., Rebez A., Renner G., Rogledi S., Slejko D. and Zanferrari A.; 2002: *The 1976-1977 seismic sequence in Friuli: new seismotectonic aspects.* Mem. Soc. Geol. It., **57**, 391-400.

Placer L., Vrabec M. and Celarc B.; 2010: *The bases for understanding of the NW Dinarides and Istria Peninsula tectonics*. Geologija, **53/1**, 55-86, DOI 10.5474/geologija.2010.005.

Podda F. and Ponton M.; 1997: *Evoluzione paleogeografica e paleostrutturale delle Prealpi Carniche settentrionali al passaggio Trias-Giura.* Atti Ticinensi Sci. Terra, **39**, 269-280.

Poli M.E., Peruzza L., Rebez A., Renner G., Slejko D. and Zanferrari A.; 2002: *New seismotectonic evidence from the analysis of the 1976-1977 and 1977-1999 seismicity in Friuli (NE Italy).* Boll. Geof. Teor. Appl., **43**, 53-78.

Poli M.E. and Renner G.; 2004: *Normal focal mechanisms in the Julian Alps and Prealps: seismotectonic implications for the Italian-Slovenian border region*. Boll. Geof. Teorica Appl., 45 (1-2), 51-69.

Poli M.E., Zanferrari A. and Monegato G.; 2009: *Geometria, cinematica e attività pliocenico-quaternaria del sistema di sovrascorrimenti Arba-Ragogna (Alpi meridionali orientali, Italia NE)*. Rendiconti online Soc. Geol. It., **5**, 172-175.

Poli, M.E., Monegato, G., Zanferrari, A., Falcucci, E., Marchesini, A., Grimaz, S., Malisan, P. and Del Pin, E.: 2015. D6/a2.1 - *Seismotectonic characterization of the western Carnic pre-alpine area between Caneva and Meduno (NE Italy, Friuli).* In "Base-knowledge improvement for assessing the seismogenic potential of Italy". DPC-INGV-S1 Project 2014-2015 – Internal report, 22 pp.

Poli M.E. and Zanferrari A.; 2018: *The seismogenic sources of the 1976 Friuli earthquakes: a new seismotectonic model for the Friuli area.* Boll. Geof. Teor. Appl., **59**, 463-480, DOI 10.4430/bgta0209.

Poljak, M., Živčić, M., and Zupančič, P.; 2000: *The seismotectonic characteristics of Slovenia.* In Seismic Hazard of the Circum-Pannonian Region (pp. 37-55). Birkhäuser, Basel.

Pondrelli S., Ekström G. and Morelli A.; 2001: *Seismotectonic re-evaluation of the 1976 Friuli, Italy, seismic sequence.* J. Seismol., **5**, 73-83.

Rebez A., Cecić I., Renner G., Sandron D. and Slejko D.; 2018: *Misunderstood "forecasts": two case histories from former Yugoslavia and Italy.* Boll. Geof. Teor. Appl., 59, 481-504, doi: 10.4430/bgta0244.

Richter C.F.; 1958: *Elementary Seismology.* W.H. Freeman and Company, San Francisco, and Bailey Bros. & Swinfen Ltd., London, 768 pp.

Rollins, K. M., Amoroso, S., Milana, G., Minarelli, L., Vassallo, M., & Di Giulio, G.; 2020: *Gravel Liquefaction Assessment Using the Dynamic Cone Penetration Test Based on Field Performance from the 1976 Friuli Earthquake*. J. Geotech. Geoenviron., **146(6)**, 04020038.

Rovida A., Locati M., Camassi R., Lolli B., Gasperini P. and Antonucci A.: 2021. *Catalogo Parametrico dei Terremoti Italiani (CPTI15), versione 3.0*. Istituto Nazionale di Geofisica e Vulcanologia, DOI https://doi.org/10.13127/CPTI/CPTI15.3 .

Sandron D., Renner G., Rebez A. and Slejko D.; 2014: *Early instrumental seismicity recorded in the eastern Alps.* Boll. Geofis. Teor. Appl., **55(4)**, 755-788, doi: 10.4430/bgta0118.

Saraò, A., Sugan, M., Bressan, G., Renner, G., & Restivo, A. 2021. *A focal mechanism catalogue of earthquakes that occurred in the southeastern Alps and surrounding areas from 1928–2019*. Earth System Science Data, **13**, 2245-2258, https://doi.org/10.5194/essd-13-2245-2021.

Sartorio D., Tunis G. and Venturini S.; 1987: *Nuovi contributi per l'interpretazione geologica e paleogeografica delle Prealpi Giulie (Friuli orientale): il pozzo SPAN1.* Riv. It. Paleont. Strat., **93 (2)**, 181-200.

Sartorio D., Tunis G. and Venturini S.; 1997: *The Iudrio valley section and the evolution of the northeastern margin of the Friuli Platform (Julian Prealps, NE Italy-W Slovenia)*. Mem. Soc. Geol. It., **49**, 163-193.

Serpelloni E., Vannucci G., Anderlini L. and Bennet R.A.; 2016: *Kinematics, seismotectonics and seismic potential of the eastern sector of the European Alps from GPS and seismic deformation data*. Tectonophysics, **688**, 157-181, DOI https://doi.org/10.1016/j.tecto.2016.09.026.

Sitaram M.V.D. and Borah P.K.; 2007: *Signal durations and local Richter magnitudes in northeast India: an empirical approach.* J. Geol. Soc. India, **70(2)**, 323-338.

Slejko D., Neri G., Orozova I., Renner G. and Wyss M.; 1999: *Stress field in Friuli (NE Italy) from fault plane solutions of activity following the 1976 main shock.* Bull. Seismol. Soc. Am., **89**, 1037-1052.

Slejko D.; 2018: *What science remains of the 1976 Friuli earthquake?* Boll. Geof. Teor. Appl., **59**, 327-350, doi: 10.4430/bgta0224.

Steinhauser P. and Lenhardt W.; 1986: *Interpretation of crustal deformations in the Friuli area for the earthquake of 1976.* Gerlands Beitr. Geophys., **95**, 459-467.

Stefani C.; 1987: *Composition and provenance of arenites from the Chattian to Messinian clastic wedges of the Venetian foreland basin (Southern Alps, Italy).* Giorn. Geol., **49**, 155-166.

Talamo R., Pampaloni M. and Grassi S.; 1978: *Risultati delle misure di livellazione di alta precisione eseguite dall'Istituto Geografico Militare nelle zone del Friuli interessate dalle recenti attività sismiche*. Boll. Geod. Sci. Aff., **1**, 6-75.

Tentor M., Tunis G. and Venturini S.; 1994: *Schema stratigrafico e tettonico del Carso Isontino.* Natura Nascosta, **9**, 1-32.

Toscani G., Marchesini A., Barbieri C., Di Giulio A., Fantoni R., Mancin N. and Zanferrari A.; 2016: *The Friulian-Venetian Basin I: architecture and sediment flux into a shared foreland basin.* Ital. J. Geosci., **135** (3), 444-459, DOI 10.3301/IJG.2015.35.

Tunis G. and Venturini S.; 1992: *Evolution of the Southern margin of the Julian Basin with emphasis on the megabeds and turbidites sequence of the Southern Julian Prealps (NE Italy).* Geologia Croatica, **45**, 127-150.

Tuttle M.P., Hartleb R., Wolf L. and Mayne P.W.; 2019: Paleoliquefaction studies and the evaluation of seismic hazard. Geosci., 9, 311-372, doi:10.3390/geosciences9070311.

Tsuchida, H. & Hayashi, S.; 1971: *Estimation of liquefaction potential of sandy soils. Estimation of liquefaction.* In Proceedings of the Third Joint Meeting, US-Japan Panel on Wind and Seismic Effects, UJNR, Tokyo, May 1971, pp. 91-109.

Vallage A., Devès M.H., Klinger Y., King G.C.P. and Rupper N.A.; 2014: *Localized slip and distributed deformation in oblique settings: the example of the Denali fault system, Alaska.* Geophys. J. Int., **197**, 1284-1298, doi: 10.1093/gji/ggu100.

Vecchia O. and De Wrachen D.; 1969: *Le acque sotterranee nella pianura friulana tra Buttrio e Manzano – Studio Geoelettrico.* In: *Le acque sotterranee nella pianura friulana orientale.* D. Ambrosini – Penne Typography.

Venturini S.; 1987: *Nuovi dati sul Tortoniano del sottosuolo della Pianura Friulana.* Gortania-Atti Mus. Friulano St. Nat., **9**, 5-16.

Venturini S.; 2002: *Il pozzo Cargnacco 1: un punto di taratura stratigrafica nella pianura friulana.* Mem. Soc. Geol. It., **57**, 11-18.

Viscolani, A., Grützner, C., Diercks, M., Reicherter, K., & Ustaszewski, K.; 2020: *Late Quaternary Tectonic Activity of the Udine-Buttrio Thrust, Friulian Plain, NE Italy*. Geosci., **10 (2)**, 84.

Vrabec M. and Fodor L.; 2006: *Late Cenozoic tectonics of Slovenia: structural styles at the northeastern corner of the Adriatic microplate.* In: N. Pinter *et al (eds.): The Adria microplate: GPS, Geodesy, Tectonics and Hazards.* NATO Sci. Series, ser. IV, **61**, 151-168, Springer.

Walker R., Jackson J. and Baker C.; 2003: *Surface expression of thrust faulting in eastern Iran: source parameters and surface deformation of the 1978 Tabas and 1968 Ferdows earthquake sequences.* Geophys. J. Int., **152**, 749-765.

Wells, D. L., and Coppersmith, K. J.; 1994: *New empirical relationships among magnitude, rupture length, rupture width, rupture area, and surface displacement*. Bull. Seism. Soc. Am., **84 (4)**, 974-1002.

Wesnousky, S. G., and Jones, C. H.; 1994: *Oblique slip, slip partitioning, spatial and temporal changes in the regional stress field, and the relative strength of active faults in the Basin and Range, western United States.* Geology, **22 (11)**, 1031-1034.

Wittlinger G., Haessler H. and Hoang Trong P.; 1978: *Contribution to the near field study of the aftershocks of the earthquakes on May 6th and September 15th 1976 in Friuli (Italy).* In: Proc. Spec. Meet. On the 1976 Friuli earthquake and the antiseismic design of nuclear installation, CNEN, Roma, Italy, pp. 148-164.

Zanferrari A., Avigliano R., Monegato G., Paiero G., Poli M.E. and Stefani C.; 2008a: *Geological map and explanatory notes of the Geological Map of Italy at the scale 1:50.000: sheet 066 "Udine".* APAT – Servizio Geologico d'Italia – Regione Autonoma Friuli Venezia Giulia, 176 pp., www.isprambiente.gov.it/Media/carg/friuli.html.

Zanferrari A., Avigliano R., Grandesso P., Monegato G., Paiero G., Poli M.E. and Stefani C.; 2008b. *Geological map and explanatory notes of the Geological Map of Italy at the scale 1:50.000: sheet 065 "Maniago".* APAT – Servizio Geologico d'Italia – Regione Autonoma Friuli Venezia Giulia, 224 pp., www.isprambiente.gov.it/Media/carg/friuli.html.

Zanferrari A., Masetti D., Monegato G. and Poli M.E.; 2013: *Geological map and explanatory notes of the Geological Map of Italy at the scale 1:50.000: sheet 049 "Gemona del Friuli".* ISPRA – Servizio Geologico d'Italia – Regione Autonoma Friuli Venezia Giulia, 262 pp., www.isprambiente.gov.it/Media/carg/friuli.html.

Zhang, M., Karathanasis, A.D.; 1997: *Characterization of Iron-Manganese Concretions in Kentucky Alfisols with Perched Water Tables.* Clays Clay Miner., **45**, 428–439, https://doi.org/10.1346/CCMN.1997.0450312.

Živčić M., Suhadolc P. and Vaccari F.; 2000: *Seismic zoning of Slovenia based on deterministic hazard computations.* Pure Appl. Geophys., **157**, 171-184.

Zupancîč P., Cecić I., Gosar A., Placer L., Poljak M. and Živčić M.; 2001: *The earthquake of 12 April 1998 in the Krn Mountains (Upper Soča valley, Slovenia) and its seismotectonic charcteristics.* Geologija, **44**, 169-192.

SITOGRAPHY

http://www.crs.inogs.it/bollettino/RSFVG/RSFVG.en.html), visited in January 2021.

https://egp.gu.gov.si/egp/?lang=en, visited in January 2021.

https://essd.copernicus.org/preprints/essd-2020-369/, visited in April 2021.

http://diss.rm.ingv.it/diss/, visited in May 2021.

http://rcmt2.bo.ingv.it/, visited in May 2021.

https://irdat.regione.fvg.it/CTRN/ricerca-cartografia/, visited in June 2021.

http://www.pcn.minambiente.it/mattm/, visited in June 2021.

https://emidius.mi.ingv.it/DBMI/, visited in June 2021.

http://cnt.rm.ingv.it/, visited in June 2021.

https://egeologija.si/geonetwork/srv/eng/catalog.search#/metadata/0a02f07a-b0a4-46df-b4e3-2276f9aa5d9c, visited in August 2021.

http://diss.rm.ingv.it/dissmap/dissmap.phtml, visited in August 2021.
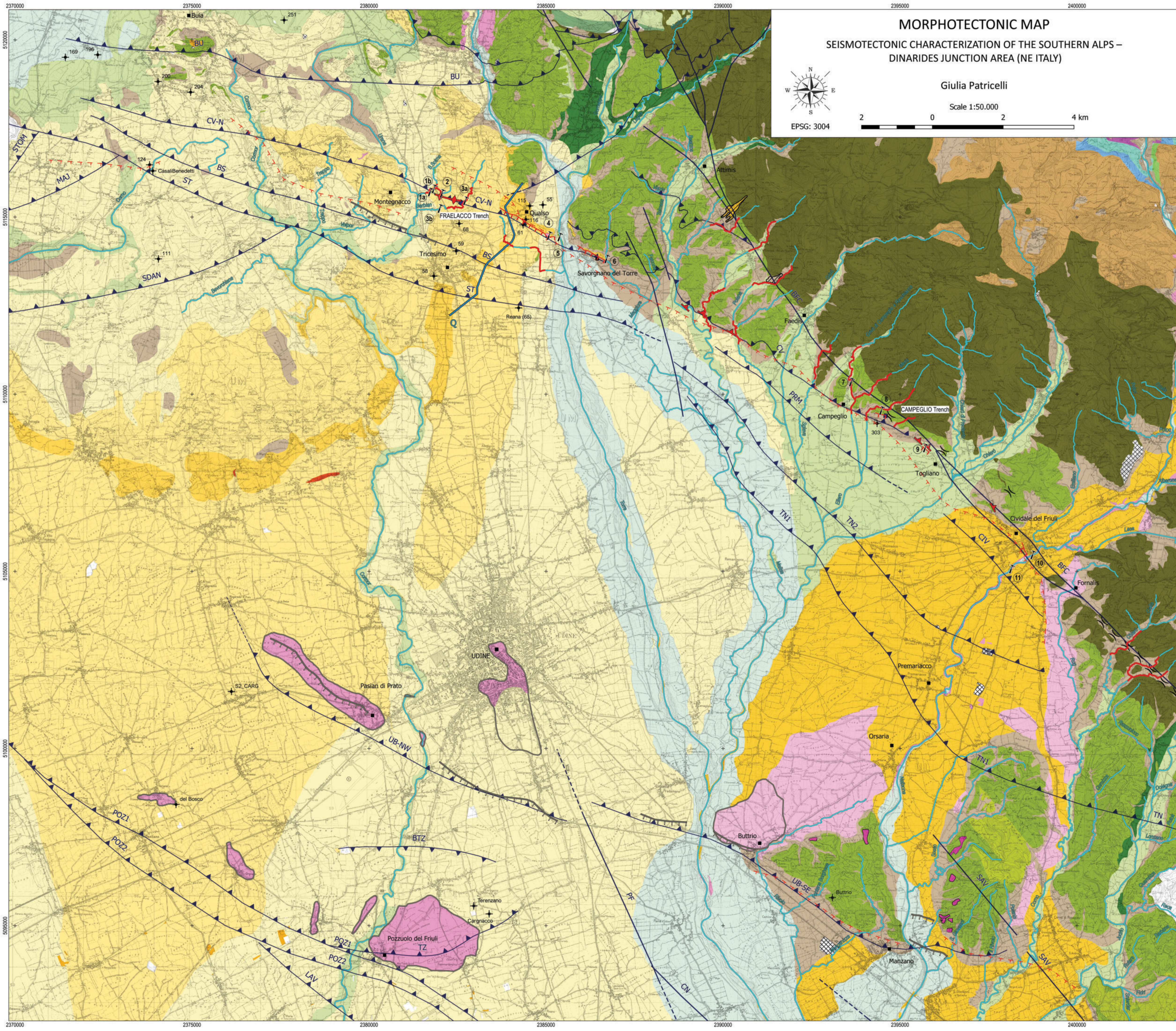
MORPHOTECTONIC MAP

SEISMOTECTONIC CHARACTERIZATION OF THE SOUTHERN ALPS – DINARIDES JUNCTION AREA (NE ITALY)

Giulia Patricelli

Scale 1:50.000

EPSG: 3004

2   0   2   4 km

LEGEND

♪ field stop
✛ geognostic well
▬ trench
▬ section trace

MORPHOTECTONIC ELEMENTS

⟩ counterslope
✕ ✕ saddle
◆ upwarped surface
▬ anomalous drainage
▨ glacis
⊥ scarp
⊥ scarp from bibliography
⊥ buried scarp
▬ pre-LGM unit relief
▬ FS unit outcrop

TECTONIC ELEMENTS

▲ thrust fault
— strike-slip fault

GEOLOGICAL UNITS

Quaternary succession

▨ ANT Anthropic deposit (Present)
■ UIN Ubiquitous Units (Upper Pleistocen-Present)
■ USG Partistagno Unit (Middle-Upper Pleistocene)
■ BTR Secondary drainage basins upper unit (Upper Pleistocene-Present)
■ BTN Secondary drainage basins lower unit (Middle-Upper Pleistocene)
■ GRA Grado Unit (Holocene)
■ GOR Gorizia Unit (Upper Pleistocene)
■ CIV Cividale Unit (Upper Pleistocene)
■ SPB Spilimbergo indifferentiated Unit (Upper Pleistocene)
■ SPB3 Remanzacco Subunit (Upper Pleistocene)
■ SPB2 Canodusso Subunit (Upper Pleistocene)
■ SPB1 Santa Margherita Subunit (Upper Pleistocene)
■ FS Friuli indifferentiated Superunit (Plio?-Middle? Pleistocene)
■ BUT Buttrio Unit (Middle-Upper Pleistocene)
■ PLI Plaino Unit (Middle Pleistocene)
■ PGB Poggiobello Unit (lower-Middle Pleistocene)

Meso-Cenozoic foredeep succession

■ QRN Monte Quarin sandstones and conglomerates (Lutethian p.p.)
■ SVO Savorgnano marls and sandstones (Ypresian p.p.)
■ GRI Grivò Flysch (upper Selandian-Ypresian p.p.)
■ FLY Masarolis, Calla, Monte Brieka, Judrio, Cras Flysch (Campanian/Maastrichtian - middle/upper Thanetian)

Mesozoic basinal succession

■ SOK Soccer Limestone (Albian-Upper Cretaceous)
■ OOV Vajont Limestone (Bathonian p.p.)

Mesozoic carbonatic platform succession

■ CMC Monte Cavallo Limestone (Albian-Upper Cretaceous)
■ CEL Cellina Limestone (Kimmeridgian-Albian p.p.)
■ CG Grey Limestone (lower Hettangian-lower Sinemurian)
■ DAH Dachstein Limestone (Rhaetian)

ACKNOWLEDGMENTS